ISOTOPE TRACING OF ATMOSPHERIC AEROSOLS IN THE SUB ARCTIC PACIFIC

CAROLYN CYNTHIA BURRIDGE

Isotope Tracing of Atmospheric Aerosols in the Sub Arctic Pacific

by

a thesis submitted to the

School of Graduate Studies

in partial fulfillment of the

requirements for the degree of

Master of Science

Earth Science Department

Memorial University of Newfoundland

St. John's Newfoundland, Canada

September 2009

ABSTRACT

The Sub Arctic Pacific Ocean near Ocean Station Papa is characterized as an iron limiting area that affects phytoplankton growth and hence the production of dimethyl sulphide. Dimethyl sulphide is believed to counteract global warming by producing or being converted into other gases or atmospheric aerosols. During the Sub Arctic Ecosystem Response to Iron Enhancement Study in the summer of 2002, various sulphur containing aerosols and gases including dimethyl sulphide, sea salt, biogenic non sea salt, anthropogenic non sea salt, methane sulphonic acid, biogenic sulphur dioxide and anthropogenic sulphur dioxide were collected. The objectives were to determine:

1) The source of SO_2 throughout SERIES

2) The source of NSS SO_4 throughout SERIES

3) The preferred pathway of DMS oxidation during SERIES and

4) The compare results of fertilized area to an unfertilized area to evaluate whether SERIES iron fertilization affected atmospheric DMS oxidation products.

ACKNOWLEDGEMENTS:

A most sincere thank-you to:

- My supervisor Ann-Lise Norman. Her guidance and time has been much appreciated. She is a very intelligent lady and a great mentor… taught me so much. I can never express how thankful I am for all of her help!

- My supervisor Mark Wilson. He's been the helping hand in St John's, NF and was always there when I needed him for an opinion. Thanks again Mark!

- The C-SOLAS group for allowing me to be part of such an interesting experiment. I will always cherish the memories created and friendships formed during SERIES.

- The crews of the research ships involved in SERIES, especially to the crew onboard El Puma… Muchos gracias amigos!

- The Memorial University Stable Isotope group: Robyn, Vanessa, Melanie, Sarah, Misuk, Alison, Pam for all their help and assistance. Always there, through the good and the bad…

- The University of Calgary Stable Isotope group: Steve, Nenita, Jesusa, Wing, Astrid, and Misuk for helping me prepare and analyze my samples while making me feel at home.

- My parents, Carson and Sheila Burridge, and my husband, David Harper, who have supported and encouraged me… Loves ya!

Dedicated to Moire Wadleigh

...whose love of science was contagious.
I will always treasure her wisdom and every giggle we shared...

TABLE OF CONTENTS

LIST OF FIGURES

LIST OF TABLES

CHAPTER 1: INTRODUCTION

1.1 INTRODUCTION

Numerous researchers suggest that marine phytoplankton play a role in regulating climate. Phytoplankton can do this in two main ways: first, marine phytoplankton are responsible for the release of trace gases that can be converted into aerosols that can reflect incoming solar radiation; second, marine phytoplankton cool Earth by decreasing the amount of carbon dioxide (CO_2) in the atmosphere.

Marine phytoplankton produce dimethylsulfoniopropinate (DMSP) that can be converted into dimethyl sulphide (DMS) via bacterial or algal enzyme breakdown of chemical bonds (***Figure 1.1***). DMS is released from the surface ocean to the atmosphere where it is oxidized to sulphur containing aerosols/gases such as methane sulphonic acid (MSA, CH_3SO_3H), sulphur dioxide (SO_2) and/or non sea salt sulphate (NSS SO_4) (***Figure 1.1***). These aerosols may then increase cloud formation and/or increase the amount of radiative backscattering, consequently cooling the surface of the Earth (***Figure 1.1***). As ***Figure 1.2*** shows, phytoplankton can reduce the amount of CO_2 in the atmosphere by using dissolved CO_2 in the ocean for photosynthesis. Also, if phytoplankton are consumed during zooplankton grazing, the zooplankton remains may be deposited in the deep ocean thereby reducing the CO_2 atmospheric reservoir (***Figure 1.2***).

In particular areas, marine phytoplankton growth is limited by certain micronutrients (e.g. iron). During the Sub-Arctic Ecosystem Response to Iron Enrichment Study (SERIES), a

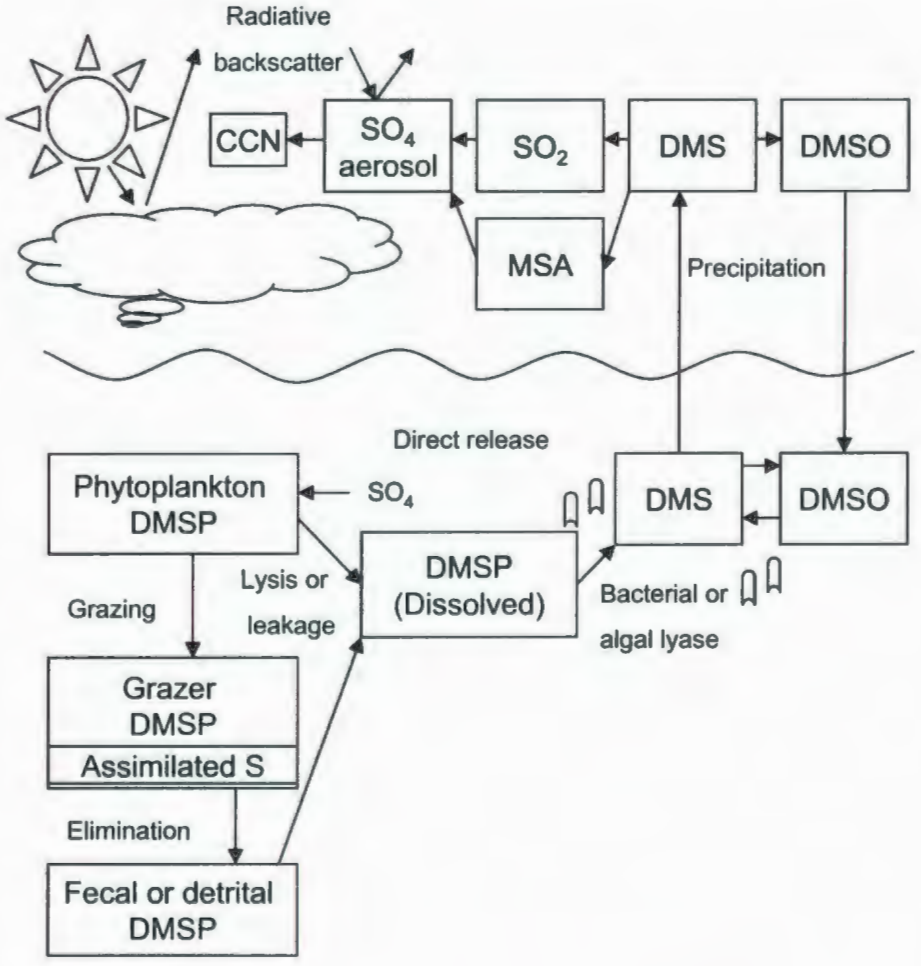

Figure 1.1: The production of atmospheric DMS from DMSP and its oxidation to SO_4 and MSA (DMSP = Dimethylsulfoniopropinate, DMS = Dimethyl Sulphide, DMSO = Dimethylsulphoxide, MSA = Methanesulphonic acid, SO_2 = Sulphur Dioxide, SO_4 = Sulphate and CCN = Cloud Condensation Nuclei, Kiene et al., 2000).

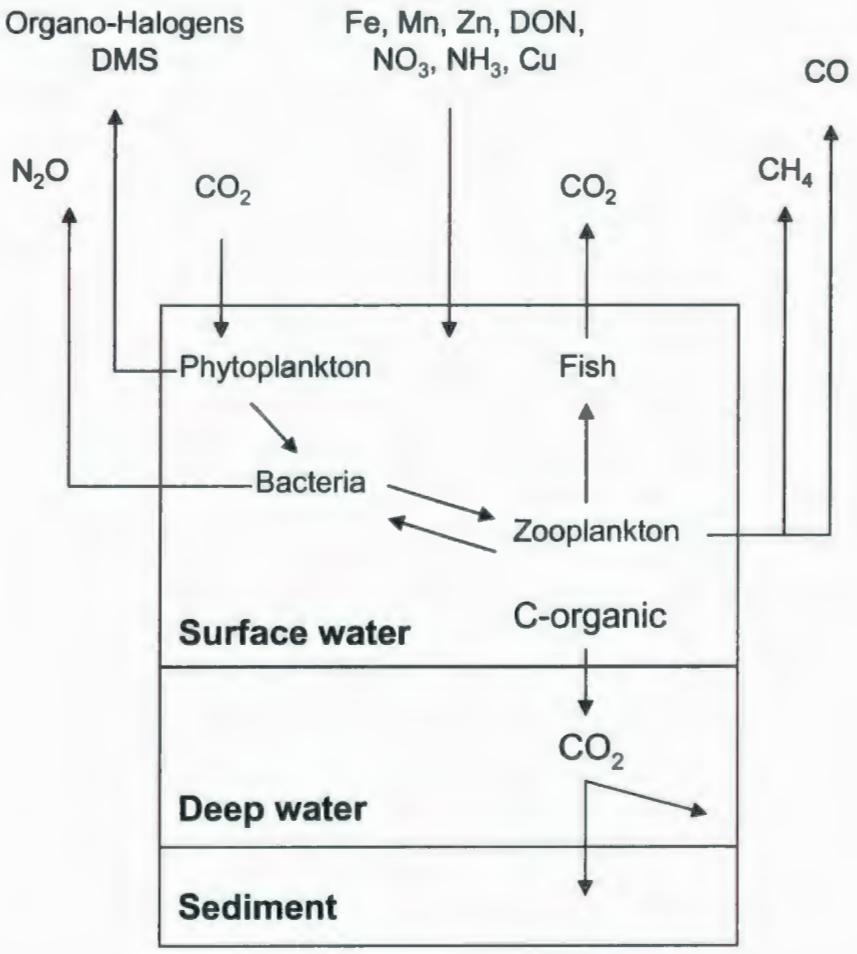

Figure 1.2: The role phytoplankton play in the carbon cycle (CO_2 = Carbon dioxide, C-organic = organic carbon, N_2O = nitrous oxide, DMS = dimethyl sulphide, Fe = Iron, Mn = Manganese, Zn = Zinc, DON = Dissolved organic nitrogen, NO_3 = nitrate, NH_3 = ammonia, Cu = Copper, CH_4 = methane and CO = carbon monoxide).

portion of the Gulf of Alaska was fertilized with iron. It was thought that where iron was not a limiting factor, phytoplankton would bloom and the DMS produced by the bloom would be oxidized to sulphate-containing aerosols in the marine atmosphere. In July 2002, SERIES was the first iron fertilization experiment involving both oceanographers and atmospheric scientists.

Previous studies have separately characterized the physical, chemical and isotopic characteristics of sulphur-bearing aerosols, however the physical, chemical and isotopic characterization of aerosols produced during an iron fertilization experiment have not been previously reported. Therefore the main objectives of this thesis were to determine:

1) The source of SO_2 throughout SERIES

2) The source of NSS SO_4 throughout SERIES

3) The preferred pathway of DMS oxidation during SERIES and

4) The compare results of fertilized area to an unfertilized area to evaluate whether SERIES iron fertilization affected atmospheric DMS oxidation products.

1.2 BIOLOGICAL CONTROL OF CLIMATE

In 1974, Lovelock and Margulis proposed the Gaia Hypothesis. It suggested that biological life controlled climate enabling it to flourish once optimal conditions were obtained. However, if biology, as the sentient being Gaia, were to control climate it would have to be aware of when to create either positive or negative feedbacks and have

a mechanism to regulate climate by altering the atmospheric composition and/or surface albedo (radiation reflected by a surface). In 1983, Watson and Lovelock developed a theory in which life on Earth did not require awareness to control climate and called it Daisyworld. In Daisyworld, two species of daisies existed, one white species and one black species. The daisies could affect climate by altering the surface albedo since a higher proportion of white daisies would increase albedo (thus cooling the Earth) while a higher proportion of black daisies would decrease albedo (thus warming the Earth). For instance, if there was low solar energy and Earth began to cool, more black daisies would grow in an attempt to increase temperature. However if there was high solar energy, Earth would be warm. In order to decrease the Earth's temperature to maintain optimal growing conditions, the white daisies would dominate.

In 1982, Lovelock and Whitfield concluded that climate may be regulated through the carbon cycle, mainly by carbon dioxide (CO_2). Atmospheric CO_2 traps infrared waves of the Earth resulting in greenhouse warming therefore Earth is warmer when atmospheric CO_2 is high and Earth is cooler when atmospheric CO_2 is low. This theory was referred to as the "greenhouse gas hypothesis".

The DMS-cloud-climate hypothesis was proposed independently by both Nguyen et al. (1983) and Shaw (1983). This theory stated that the Earth's climate was actually controlled by organisms through the sulphur cycle: "The mechanism would operate by altering planetary albedo through the selective creation of biospheric organic sulphide

gases which go on to metamorphize into submicron particles and introduce cooling" (Shaw, 1983). Biogenic gases such as DMS, eventually become converted into sulphate aerosols. A small flux of sulphate particles with radii of 0.1 μm would lead to a relatively strong negative feedback because these particles remain in the atmosphere for long periods of time and are non-colored, thereby providing reflection of sunlight (Shaw, 1983). This is an important idea that remains to be quantified. There is no evidence that the biosphere is controlling climate by particle-albedo change through the sulphur cycle, however the sulphur particles are distributed uniformly, the ~0.1 μm radii sulphur particles are the right size to interact efficiently with incoming solar energy and the sulphur particles are derived from long-lived, biologically-produced precursor gases (Shaw, 1983).

Charlson et al. (1987) elaborated on the DMS-cloud-climate hypothesis and it soon became known as the CLAW hypothesis (an acronym from the authors' surnames: Charlson, Lovelock, Andreae and Warren). The CLAW hypothesis stated that a change in oceanic DMS concentration would cause a shift in the NSS SO_4 aerosol concentration which would in turn change the number of cloud condensation nuclei (CCN) and ultimately climate. Once DMS enters the atmosphere, it can be converted to MSA or SO_2 and subsequently biogenic NSS SO_4. According to Charlson et al. (1987), NSS SO_4 was believed to be the main contributor to CCN because:

1) CCN are composed of water soluble materials and NSS SO_4 is water soluble

2) The size distribution of sub-micrometer NSS SO_4 is appropriate for CCN activation

3) The mass concentration of NSS SO_4 and mean radius can be used to estimate a total number population that is in agreement with measured CCN populations

4) The concentration of NSS SO_4 in remote marine rain water agrees with a simple nucleation scavenging calculation

5) Much of the light scattering aerosols in the marine environment are volatile at elevated temperatures and evaporate in the same way that NSS SO_4 would

6) The residence time of CCN is approximately one day which is the same as the residence time of NSS SO_4.

The mechanisms of biologically controlled thermostats for Earth have been the center of criticism and debate.

1.3 OCEANS

Approximately 70% of the Earth's surface is covered by five oceans: Southern (also known as Antarctic), Arctic, Indian, Atlantic and Pacific. Of these, the Pacific Ocean is the largest covering 180 000 000 km^2 of Earth's surface and containing 53% of the Earth's water (Monroe and Wicander, 1997). The Pacific Ocean contains three major gyre systems (large circular oceanic current systems caused by high pressure systems in the atmosphere): the counter-clockwise Sub-Arctic Pacific Gyre involves the North Pacific, Alaska, Kamchatka and Oya Siwa Currents, the clockwise Northern Pacific Gyre includes the North Pacific, California, North Equatorial and Kuro Siwa Currents and the

counter-clockwise Southern Pacific Gyre includes the South Equatorial, East Australian, West Wind Drift and Humboldt (also known as Peru) Currents (***Figure 1.3***).

Because of the size of the Pacific Ocean and its various gyres, areas within it have different physical and chemical properties. For example, the Gulf of Alaska, in the sub-Arctic Pacific Ocean is considered to be a high-nutrient, low-chlorophyll (HNLC) area. Three HNLC areas (the Equatorial Pacific Ocean, Southern Ocean and the Gulf of Alaska in the northeast Pacific Ocean, ***Figure 1.3***) occupy 20% of the world's oceans and are characterized by elevated amounts of nutrients (such as nitrate = NO_3 and phosphate = PO_4) but low chlorophyll production. The micronutrient iron (Fe) was thought to be responsible in limiting the chlorophyll production in HNLC areas as early as the 1930's (Gran, 1931; Hart, 1934; Harvey, 1938). Scientists realized that oceanic iron was not being replenished by physical processes such as river discharge, continental wind blown dust or oceanic upwelling. In the 1980's the most widely accepted cause of HNLC areas was overgrazing of phytoplankton by zooplankton. At that time, iron fertilization experiments were designed to test both the iron limitation and overgrazing hypotheses.

1.4 IRON FERTILIZATION EXPERIMENTS

Prior to 1988, it was thought that iron concentrations in the ocean were relatively high. However in 1988, Martin and Gordon demonstrated that dissolved iron concentrations in the open ocean were two orders of magnitude lower than previously estimated (Martin, 1992). Martin became curious as to whether or not iron played a role in phytoplankton

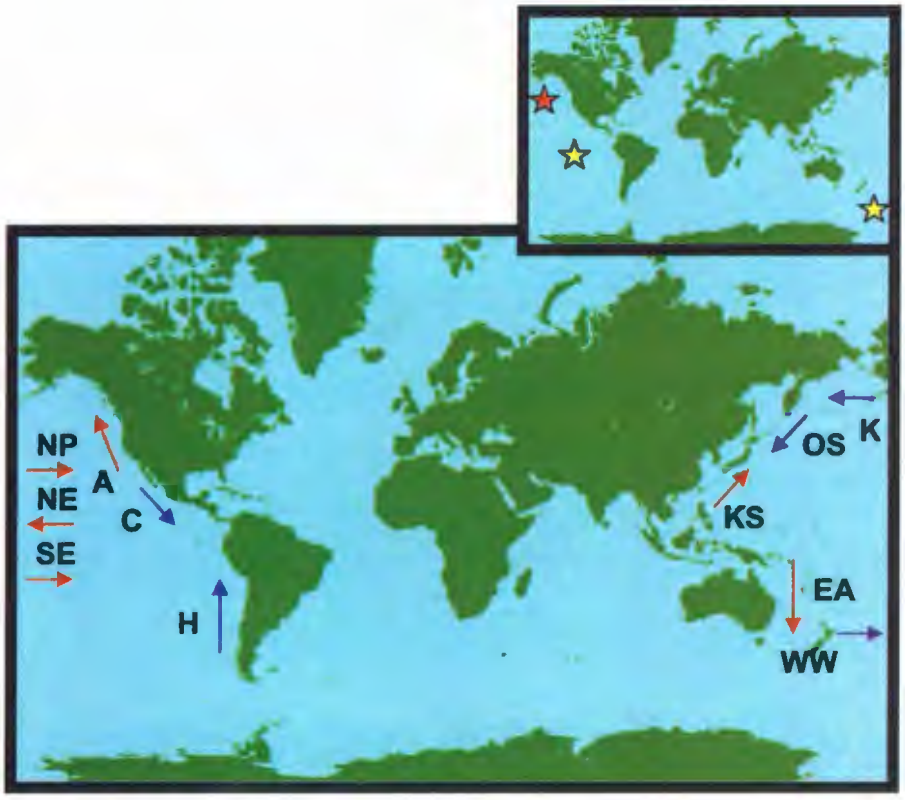

Figure 1.3: Pacific Ocean gyres and worldwide high nutrient low chlorophyll (HNLC) areas. Red arrows are warm water currents (NP = North Pacific, NE = North Equatorial, SE = South Equatorial, A = Alaska, KS = Kuro Siwa, EA = East Australia) and blue arrows are cold water currents (C = California, H = Humboldt, OS = Oya Siwa, K = Kamchatka, WW = Westwind Drift). Inset shows worldwide HNLC areas by stars. The red star shows the location of SERIES.

productivity. Martin retested this theory by collecting surface water from HNLC areas to which he fertilized half the sample with iron (the unfertilized sample acted as a control) and incubating the samples for a week at light and temperature conditions similar to the area from which they were collected (Chisolm, 1995). As expected, the total chlorophyll concentration increased, nitrate concentration decreased and the number of pennate diatoms increased (Chisolm, 1995). However Martin's results were not convincing to all, as some questioned the idea that sample bottles limited the zooplankton grazing (Chisolm, 1995). After discussion at the American Society of Limnology and Oceanography (ASLO) meeting, it was agreed that an in-situ ocean fertilization experiment must be conducted (Cullen, 1995). Since 1988, a number of iron fertilization experiments have taken place: IronEx (Iron Experiment in the equatorial Pacific Ocean), SOIREE (Southern Ocean Iron Release Experiment in the Southern Ocean), SEEDS (Subarctic Pacific Iron Experiment for Ecosystem Dynamics Study in the northern Pacific Ocean) and SERIES (Subarctic Ecosystem Response to Iron Enrichment Study in the Gulf of Alaska, northeast Pacific Ocean).

In mid-October 1993, IronEx I began as a 64 km^2 patch approximately 500 km south of the Galapagos Islands in the equatorial Pacific Ocean (Martin et al., 1994). Prior to enrichment, the ambient iron concentration was 0.06 nM (Gordon et al., 1994). It was increased to ~ 4 nM by releasing an iron solution in the propeller wash of the research vessel (*R/V) Columbus Iselin* (Martin et al., 1994). According to Martin et al. (1994), the patch was then tracked using:

1) biologically inert sulphur hexaflouride (SF_6) that was also released in the propeller wash
2) Four corner buoys and one central buoy equipped with a global positioning system (GPS) receiver as well as a Very High Frequency (VHF) packet radio transmitter and receiver and
3) National Acronautics and Space Administration (NASA) airborne oceanographic lidar (AOL) flights that could detect chlorophyll conditions.

Samples were taken daily from an "in patch" and an "out patch" station to measure the effect of iron on the phytoplankton and its ecosystem. The "in patch" showed the addition of iron resulted in increased phytoplankton biomass (2X), increased chlorophyll (3X) and increased plant production (4X). Unfortunately, the iron-rich patch subducted beneath a low-salinity front, introducing extra variables such as light and salinity, and so the experiment was terminated (Martin et al., 1994).

With the unfortunate subduction of the fertilized patch, IronEx I proved neither the iron limitation theory nor the overgrazing theory (Martin et al., 1994). A second iron fertilization experiment (IronEx II) was therefore planned. In May 1995, IronEx II took place in the eastern Pacific Ocean near 3.5°S, 104°W (Coale et al., 1996). Injections were performed from the *R/V Melville* in the 72 km^2 study area in a rectangular pattern (Coale et al., 1996). In order to sustain iron concentrations, the area was fertilized three times: May 29th (2 nM), June 2nd (1 nM) and June 6th (1 nM) (Coale et al., 1996). As in IronEx I, the fertilized patch was tracked using buoys and SF_6 and an untreated "out patch" area

served as a control. Increases in the phytoplankton growth rate (2X), phytoplankton abundance (20X) and oceanic DMS concentrations (3X) were accompanied by decreases in pCO_2 and NO_3 concentrations (Frost, 1996). The combination of these observations with zooplankton grazing and concentrations of possible secondary limiting nutrients (e.g. zinc and silicate) throughout the experiment showed that the phytoplankton bloom was iron limited and zooplankton grazing and secondary nutrient limitation were not restrictive factors (Coale et al., 1996). In addition, two sub-experiments took place: Patch 2 with acidified water and SF_6 tracer (to test effects of acidification and ship contamination) and Patch 3 with a single infusion of low-concentration iron and SF_6 (to mimic iron in equatorial undercurrents found west of study area) (Coale et al., 1996). It was concluded that the observed biological shift in both Patch 2 and 3 was not caused by the additional chemicals or the presence of the ship but rather by the iron addition (Coale et al., 1996).

Results from IronEx II together with results from other studies (e.g. Price et al., 1991; Dugdale and Wilkerson, 1990; Bruland et al., 1991; Coale et al., 1996) supported the idea that iron transport could influence pCO_2 and prompted scientists to conduct an iron fertilization experiment in another HNLC area (Coale et al., 1996). In February 1999 (Austral summer), the Southern Ocean Iron Release Experiment (SOIREE) took place at 61°S and 140°E, an area characterized by iron and light co-limitation. A portion of the Southern Ocean, with initial iron concentrations of 0.08 nM (Boyd et al., 2000), was fertilized and tracked using methods exercised in IronEx I and IronEx II. The *R/V*

Tangaroo released dissolved iron in a hexagonal pattern over 50 km^2 to produce concentrations of ~ 3 nM of iron in surface waters. On Day 3, 5 and 7 of the experiment the iron fertilization was repeated when iron concentrations in the patch became similar to those in the control area. After 13 days, the fertilization of the area resulted in elevated growth rates (2.5X), increased chlorophyll (6X), enhanced bacterial production (3X) and increased oceanic DMS (3X) (Boyd et al., 2000).

SEEDS (Subarctic Pacific Iron Experiment for Ecosystem Dynamics Study) took place in the summer of 2001 in the northwestern Pacific Ocean (Tsuda et al., 2003). A single injection of iron solution (as $FeSO_4$) was added to an 8 km by 10 km square patch on July 18, 2001 (Tsuda et al., 2003). As in previous experiments, the fertilized area was tracked and compared to an unfertilized area. Initial iron concentrations were 1.88 nM and these concentrations decreased rapidly to 0.15 nM where they remained relatively constant even after the phytoplankton bloom (Tsuda et al., 2003). Phytoplankton biomass rose significantly between Day 6 to Day 10 and remained at approximately 20 mg/m^3 until Day 13, the last day of the study (Tsuda et al., 2003). Large centric diatoms dominated the bloom (Tsuda et al., 2003). There was a large drawdown of pCO_2 and dissolved inorganic carbon with the pCO_2 changing after Day 5 and having its largest change on Day 12 (Tsuda et al., 2003). It was unknown if the organic carbon produced during the iron enrichment caused a decrease in CO_2 in the surface ocean however the SEEDS results suggested the northwestern Pacific was more sensitive to iron fertilizations than the equatorial Pacific and Southern Oceans (Tsuda et al., 2003).

SEEDS II began on July 20, 2004 in the western Subarctic Pacific near the SEEDS I location (approximately 93 km south where there was a broad area of HNLC waters, <0.02 nM Fe) (Tsuda et al., 2007). The *R/V Hakuho Maru* injected an iron solution and SF_6 (used to track the patch) in an 8 km by 8 km grid pattern on Day 1 and injected more iron solution on Day 6. Observations of the patch were done by the *R/V Hakuho Maru* from Day 1 to Day 14, by the *R/V Kiro Moana* from Day 14 to Day 22 and again by the *R/V Hakuho Maru* from Day 23 to Day 26. The patch could not be found when the *R/V Hakuho Maru* arrived to the area on Day 31 so the in patch results were obtained for a total of 26 days. SEEDS II results were unlike the results of SEEDS I for two main reasons: first, the chlorophyll levels were much lower (2.48 mg/m^3 in SEEDS II compared to 18 mg/m^3 in SEEDS I) suggesting the phytoplankton biomass was unaffected by the addition of iron (Tsuda et al., 2007). Secondly, a diatom bloom was not observed in SEEDS II as seen in SEEDS I (Tsuda et al., 2007). In SEEDS II, the copepod biomass increased exponentially and was five times higher than SEEDS I, and it appeared that copepod grazing may have prevented a diatom bloom from developing in SEEDS II (Tsuda et al., 2007). Therefore SEEDS II appeared to be unsuccessful due to grazing rather than iron limitation (Tsuda et al., 2007).

SERIES took place in the Gulf of Alaska at Ocean Station Papa (50°N and 145°W) during July 2002 (***Figure 1.3***). The location for the iron fertilization was an area near Ocean Station Papa with uniform physical characteristics where the patch would unlikely

subduct. This 8 km by 8 km area was fertilized on July 9, 2002 by the propeller wash of the Canadian *JP Tully* in an expanding square pattern. Methods exercised in previous iron enrichment experiments were used to map the patch (e.g. SF_6, buoys, chlorophyll and fluorescence). With atmospheric measurements an integral part of SERIES, measurements inside and downwind of the fertilized patch were compared to measurements taken outside and upwind of the fertilized patch. Following fertilization, the seawater iron concentration had increased to the target concentration of approximately 4 nM. Due to strong winds and rough seas, the patch was re-injected on July 16, 2002 to obtain a concentration of approximately 2 nM. Only a few hours after the initial fertilization, there was a small, rapid increase in bacterial abundance and production. During the first days of the iron enrichment experiment, bacteria were found to be limited by iron as well as limited by dissolved organic matter. Nanophytoplankton growth rates increased however growth rates were later slowed down by grazing. The community structure shifted from nanophytoplankton to diatoms (Boyd et al., 2004) and was accompanied by high DMS production during the nanophytoplankton bloom to low DMS production during the diatom bloom. The "bloom" ended on July 31 with iron and then silicic acid exhaustion (Boyd et al., 2004) and the silicate-limiting induced sinking of diatoms was unique (Boyd et al., 2004). The bacterial response in SERIES was larger than in previous iron fertilization experiments: over 50% of the carbon that was fixed by the phytoplankton bloom was grazed or remineralized by bacteria resulting in only approximately 18% of the particulate carbon being exported to the deep ocean. The patch was monitored for 26 days by three ships (Canadian *JP Tully* – fertilized the patch on

July 9 and left July 23, Mexican *El Puma* – present July 9 to July 28 and Japanese *Kaiyo Maru* – present July 23 to August 4), the longest continuous monitoring of an iron enriched patch at that time (Boyd et al., 2004).

1.5 ATMOSPHERE

The atmosphere is a layer surrounding the Earth composed of a mixture of gases, water, ice and minute solids. The atmosphere can be divided into two large layers known as the homosphere (a well-mixed zone which is 0 to 110 km above Earth's surface) and the heterosphere (a stratified zone which is >110 km above Earth's surface). The atmosphere can be sub-divided vertically into the troposphere (0 to 15 km), stratosphere (15 to 50 km), mesosphere (50 to 84 km), thermosphere (84 to 500 km) and exosphere (>500 km). Due to the ability of different gases to absorb light of different wavelengths, the atmosphere has a layered temperature structure.

Presently, the atmosphere is strongly oxidizing and is composed of approximately 78% nitrogen, 21% oxygen, <1% argon and carbon dioxide and 0 to 4% water vapour (Curry and Webster, 1999). Numerous trace gases, gases having concentrations less than 1 part per million by volume (i.e. < 1 ppmv), exist in the atmosphere. The abundances of trace gases have changed as a result of geological, biological, chemical and anthropogenic processes (e.g. deforestation, biomass burning, industrial activities) (Seinfeld and Pandis, 2006).

Atmospheric trace constituents have become increasingly important because they are known to affect Earth's radiation. Greenhouse gases such as carbon dioxide (CO_2), ozone (O_3), methane (CH_4), nitrous dioxide (NO_2) and halogen-containing compounds absorb infrared radiation from Earth's surface and re-radiate a portion back to the surface thereby acting as a thermal insulator for Earth's atmosphere. These gases have the ability to increase Earth's temperature by several degrees Celsius. Aerosols, particularly sulphate aerosols, decrease Earth's temperature by reflecting incoming solar radiation either directly by interactions with the particles or indirectly by interactions with clouds they produce (***Figure 1.4***).

1.6 AEROSOLS

Aerosols are mixtures of particles and gases that are present within the Earth's atmosphere. The aerosol load of the atmosphere is usually smaller (by one or two orders of magnitude) than the load of atmospheric trace gases (Jaenicke, 1980). Over the oceans, rural areas and cities, the concentrations of aerosols are in the $10^3/cm^3$, $10^4/cm^3$ and $10^5/cm^3$ range respectively (Curry and Webster, 1999).

Aerosol diameters can range between 0.001 and 100 μm. There are several ways of classifying aerosols according to size: Junge (1963) used location (marine, continental and background) and particle size (0.001-0.1 μm radius, 0.1-1 μm radius and >1 μm radius) to divide aerosols into Aitken aerosols, Large aerosols and Giant aerosols; Whitby (1973) used production mechanism (gas-to-particle conversion (GPC), coagulation and/or

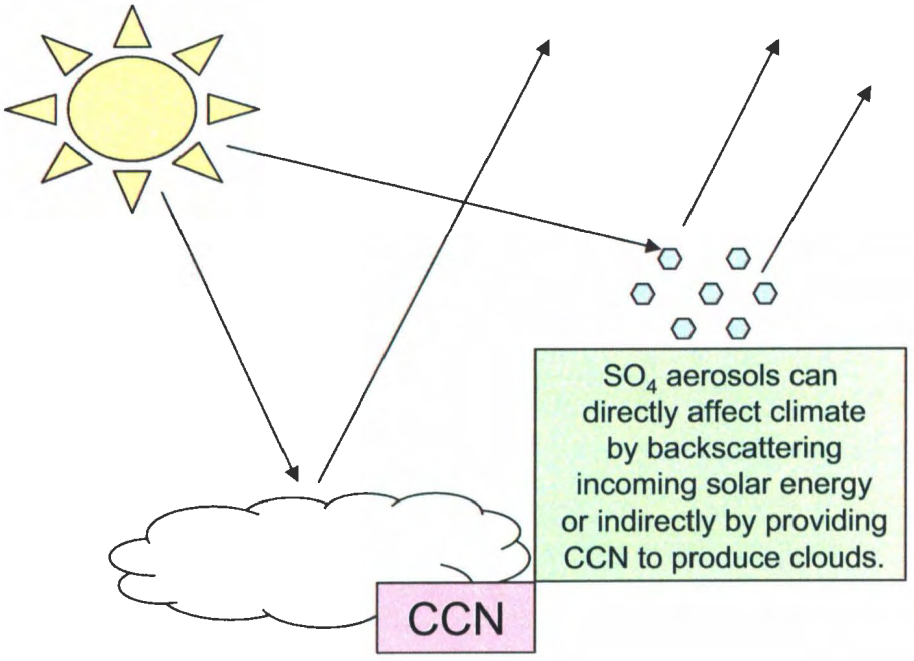

Figure 1.4: Sulphate aerosols affect climate (CCN = Cloud Condensation Nuclei and SO_4 = Sulphate).

heterogeneous condensation and mechanical production) and particle size (0.001-0.1 μm radius, 0.1-1 μm radius and >1 μm radius) to classify aerosols as Nucleation mode, Accumulation mode and Coarse mode (Jaenicke, 1993). ***Figure 1.5*** shows the size of the particles relates to their sources, their processes and their transport (Krouse and Grinenko, 1991).

Tropospheric aerosols have a variety of sources and accordingly many classification schemes were developed:

1. Area, Volume and Point Sources (Jaenicke, 1980): Area sources, also known as "surface sources", produce aerosols at the base of the atmospheric volume (e.g. the production of aerosols from desert or ocean surfaces) while volume sources, also known as "spatial sources", produce aerosols within the atmospheric volume (e.g. the production of aerosols by gas-to-particle conversion). Point sources are sources that produce aerosols on a local or regional scale (e.g. the production of aerosols by volcanoes). Typically particles from area sources are larger than particles from volume sources (Jaenicke, 1980).

2. *Stratosphere, Oceanic and Continental Sources* (Jaenicke, 1980): Stratospheric aerosols, oceanic aerosols and continental aerosols are aerosols with a stratospheric, oceanic and continental origin respectively. For example, tropospheric sulphur may be derived from stratospheric carbonyl sulphide, COS (stratospheric source), from sea spray (oceanic source) or by soil dust (continental source). The stratospheric source does not

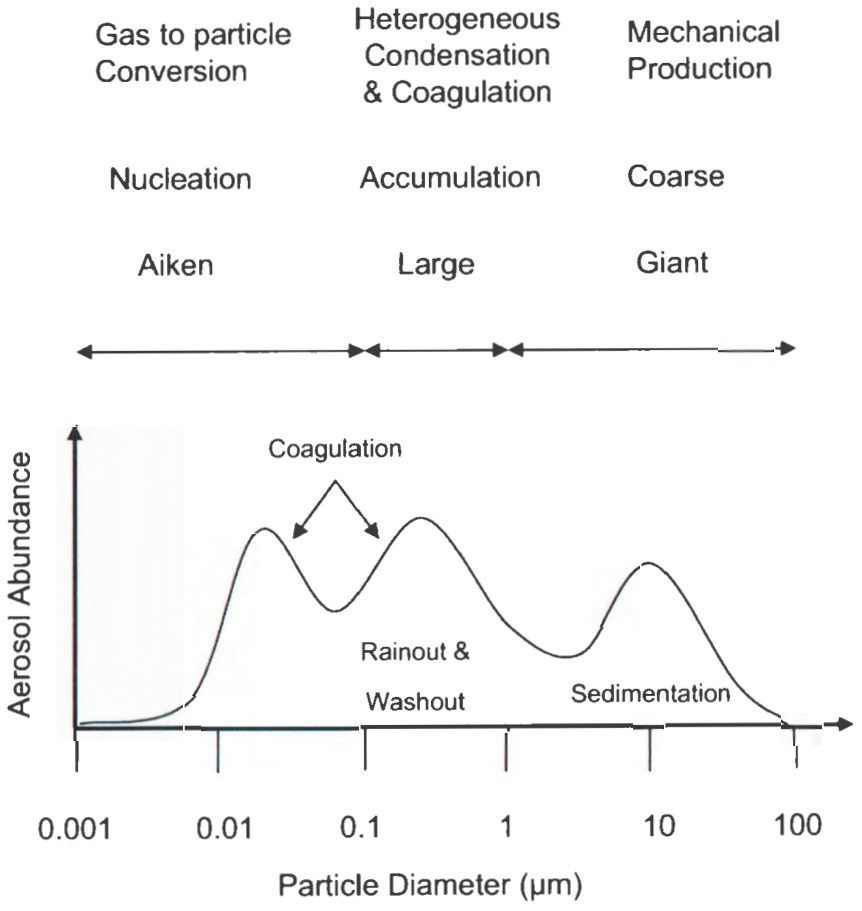

Figure 1.5: Aerosol abundance (change in number concentration) and size classifications (Junge, 1963; Whitby, 1973; Jaenicke, 1993).

seem to play as much of an important role in providing aerosols to the troposphere as the oceanic or continental sources.

3. *Natural and Anthropogenic Sources*: Aerosols may be produced naturally by soil dust, combustion, sea spray, vegetation and volcanoes (National Research Council of Canada, 1982). In contrast, aerosols may be produced by the activities of humans: industrial processes, fuel combustion, transportation, solid waste incineration, slash burning, fertilizer application, etc. (National Research Council of Canada, 1982). Anthropogenic particle emissions account for 7 to 19% of the global total while natural particle emissions account for 81 to 93% (Hidy and Brock, 1971; Peterson and Junge, 1971). The magnitude of natural and anthropogenic sources is dependent on factors such as location, type of activity and season. For instance, roughly about $^{2}/_{3}$ of the oceanic particles are natural and $^{1}/_{3}$ are anthropogenic (Berner and Berner, 1996) however, the proportion of the anthropogenic source may increase if there was an increase in shipping activities or the proportion of the natural source may increase if there was a dry period that would cause more soil dust to blow from the continents to the oceans.

The two ways aerosols are produced are: 1) production of aerosols by disintegration of material and release into the atmosphere 2) production of aerosols by modification of gases and existing aerosols in the atmosphere. These production mechanisms can respectively categorize aerosols as primary aerosols or secondary aerosols. The size of the particle is generally indicative of the type of production with primary aerosols (such as sea spray formed by the bursting of bubbles in breaking waves) being larger than

secondary aerosols (such as sulphate formed by the photochemical oxidation of sulphur dioxide).

The production mechanism and source can be combined so that aerosols can be categorized as:

1) primary natural aerosols (e.g. windblown dust, forest fires, sea spray, volcanoes, organics like pollen, spores, bacteria, algae, hair, plant debris, fragments of insects, etc.)
2) secondary natural aerosols (e.g. gas-to-particle conversion of dimethyl sulphide (DMS), hydrogen sulphide (H_2S), volcanic sulphur dioxide (SO_2), biogenic nitrogen oxides (NO_x), volatile organic compounds (VOC's), etc.)
3) primary anthropogenic aerosols (e.g. industrial dust, soot, biomass burning, windblown dust produced by construction and mining, etc.) and
4) secondary anthropogenic aerosols (e.g. gas-to-particle conversion of sulphur dioxide (SO_2) from smelters, power plants, nitrogen oxides (NO_x) from vehicles and power plants, etc.).

The primary biogenic sources account for 48 to 73%, secondary biogenic sources account for 27 to 52%, primary anthropogenic sources account for 5 to 41% and secondary anthropogenic sources account for 59 to 95% of the aerosols in the atmosphere (National Research Council of Canada, 1982).

The processes that an aerosol undergoes in the atmosphere are known as "aging". Aging includes gas-to-particle conversion, heterogeneous or homogeneous nucleation, coagulation, dilution, scavenging and sedimentation. Aging may have different effects. For instance it may cause new aerosols to form (e.g. gas-to-particle conversion), cause existing aerosols to grow (e.g. coagulation) or cause aerosols to be removed (e.g. sedimentation).

New aerosols can form from gas-to-particle conversion, whereby a gaseous precursor is converted into a solid and/or liquid particle by either heterogeneous nucleation (formation of a new particle in the presence of a substance/phase that is different from itself) or homogeneous nucleation (formation of a new particle in the presence of a substance/phase that is similar to itself) (Jaenicke, 1993).

Aerosols can "grow" by colliding with each other and combining. This process, known as coagulation, is most rapid where there are high concentrations of aerosols (Jaenicke, 1980). On the other hand, if aerosols are mixed with clean air or aerosols of a lower concentration, dilution can occur (Jaenicke, 1980).

Aerosols can be removed from the atmosphere by scavenging or sedimentation. There are many types of scavenging and the type depends upon location (in-cloud or below cloud scavenging), type of precipitation (snow or rain scavenging), type of pollutant (particle or gas scavenging) or the mechanism (electrostatic or nucleation scavenging) (National

Research Council of Canada, 1982). Aerosols are removed by sedimentation when their mass causes them to eventually be deposited from the atmosphere.

Aging determines the residence time of aerosols (Jaenicke, 1980). The residence time is the ratio of aerosol concentration ([Aerosol]) to the change in concentration with time (Δ) (Jaenicke, 1980):

Equation 1.1

$$\text{ResidenceTime} = \frac{[\text{Aerosol}]}{\Delta[\text{Aerosol}]}$$

The residence time among aerosols varies: large aerosols have residence times <1 day (Bonsang et al., 1980) while fine aerosols have residence times <1 week (Prospero et al., 1983).

The distance an aerosol is transported is related to the size of the particle. For example, fine particles may be transported over large distances (National Research Council of Canada, 1982). The transport of fine aerosols is limited by Brownian motion (random motion of particles in response to their thermal motion and collision with gas particles) and coagulation (when aerosols collide and combine to produce larger aerosols) (Jaenicke, 1993). Coarse aerosols are larger and heavier, therefore coarse aerosols settle out of the atmosphere before being transported over long distances (National Research Council of Canada, 1982; Berner and Berner, 1996).

The chemical composition of an aerosol is related to its size, source and aging processes. In terms of size, generally fine particles (<1 μm) contain sulphates, nitrates, ammonium, lead, bromine, elemental carbon and condensed organic matter (National Research Council of Canada, 1982) while coarse particles (>1 μm) contain mostly crustal elements such as calcium, aluminum, silica, iron, and vegetation derived components, as well as sea spray (Miller et al., 1972). The chemical composition of aerosols may consist of: 1) a water soluble portion (e.g. sulphate, nitrate, ammonium, etc.) 2) an insoluble inorganic portion (e.g. silicates, oxides, etc.) and 3) a carbonaceous portion (soluble and insoluble organic matter) (Berner and Berner, 1996; Rahn, 1976). While most oceanic aerosols are composed of soluble materials, most continental aerosols are mixtures of soluble and insoluble components (Junge 1963, Fitgerald, 1991). For example, a continental aerosol is composed of approximately 30% insoluble inorganic material, 10% insoluble organic material, 20% soluble organic material and 40% water soluble material (Jaenicke, 1980). The average chemical composition of fine aerosols in both rural and urban areas is shown in ***Table 1.1.***

Sea spray particles will be composed primarily of compounds found in seawater, primarily sodium chloride (NaCl) with trace amounts of potassium (K), magnesium (Mg), calcium (Ca), sulphates (SO_4), carbonates (CO_3) and organics. The composition of anthropogenic aerosols will depend on the type of activity and the materials used (National Research Council of Canada, 1982) with aerosols from a coal-fired power plant, for example, primarily composed of silicates, aluminum oxides, sulphates and

Table 1.1: Average chemical composition of fine rural and urban aerosols (Brasseur et al., 2003).

Compound	Average composition of fine urban aerosols (in %)	Average composition of fine rural aerosols (in %)
Organic Carbon	31	11
Inorganic Carbon	9	0.3
NH_4	8	7
NO_3	6	3
SO_4	28	22
Not detectable	18	57

carbon. The composition of aerosols will change during aging processes because aerosols provide sites for chemical reactions to take place within the atmosphere.

The effect of aerosols on climate has become a popular topic of scientific discussion as the global warming versus global cooling debate continues. Scientists are trying to understand whether aerosols warm or cool the earth and have determined that the composition of the aerosols and their absorbing abilities will determine the positive or negative climatic feedback. For example, if the aerosol is composed of dark colored, carbonaceous material, there will tend to be absorption of solar energy and hence warming. However, if the aerosol is composed of light colored, sulphate material, there will tend to be scattering of solar energy and hence cooling. Sulphate aerosols are the focus of this thesis and can affect the climate in two main ways: 1) they can directly cool Earth by scattering incoming solar radiation in a clear sky and 2) they can indirectly cool Earth by producing cloud condensation nuclei (CCN) (***Figure 1.4***).

Aerosols in the accumulation mode will be efficient scatterers because their size is the same as the wavelength of incoming solar radiation (Curry and Webster, 1999) hence causing a negative climate feedback through the direct effect. Sulphate aerosols have the potential of reflecting the incoming solar energy over the open ocean since they are usually in the accumulation mode. In addition, the size of sulphate aerosols makes them good candidates for CCN. If there is an increase in the CCN, there is an increase in smaller cloud droplets, an increase in albedo and lifetime of clouds (Berner and Berner

1996) hence a negative climate feedback through the indirect effect. In the remote atmosphere the radiative properties of clouds are sensitive to the number of CCN present (Calhoun and Bates, 1989) and approximately 20% of the total atmospheric aerosol population over oceans serve as CCN in clouds (Curry and Webster, 1999).

Scientists are trying to measure both the direct effect and indirect effect of sulphate aerosols on climate. Recently the direct effect has been estimated to cause a cooling of 1 W/m^2 averaged over the northern hemisphere (Charlson et al. 1987; Charlson et al., 1990) whereas the magnitude of the indirect effect is not well known because there is no accepted relationship between the sulphate mass concentration and the number of CCN and cloud droplets (Charlson and Wigley, 1994).

1.7 SULPHUR CYCLE

Sulphur is widespread throughout the lithosphere, hydrosphere, atmosphere and biosphere and can exist in a variety of free and/or combined forms. It is a non-metal (atomic number = 16, atomic weight = 32.065 g/mol) that can occur in a range of valence states, from -2 in reduced sulphides to +6 in oxidized sulphates (***Table 1.2***, Charlson et al., 1992). Sulphur may exist in solid, liquid or gaseous states (Krouse and Grinenko, 1991).

Table 1.2: Oxidation states of sulphur gases and the aerosol each gas produces where H_2S = Hydrogen Sulphide, (R) is a hydrocarbon chain, S = Sulphur, H = Hydrogen, OCS = Carbonyl Sulphide, CS_2 = Carbon Disulphide, CH_3SOCH_3 = Methyl Sulphoxide, SO_2 = Sulphur Dioxide, $SO_2 \cdot H_20$ = SO_2-H_2O complex, HSO_3 = Hydrogen Sulphite, SO_3 = Sulphur Trioxide, H_2SO_4 = Sulphuric Acid, HSO_4 = Hydrogen Sulphate, SO_4 = Sulphate, $(NH_4)_2SO_4$ = Ammonium Sulphate, Na_2SO_4 = Sodium Sulphate and CH_3SO_3H = Methane Sulphonic Acid (Charlson et al., 1992).

Oxidation State	Gas	Aerosol
-II	H_2S, (R)SH	-
	(R)S(R)	-
	OCS	-
	CS_2	-
-I	(R)SS(R)	-
0	CH_3SOCH_3	-
IV	SO_2	$SO_2 \cdot H_20$
	SO_2	HSO_3
VI	SO_3	H_2SO_4, HSO_4
	SO_3	SO_4
	SO_3	$(NH_4)_2SO_4$, etc.
	SO_3	Na_2SO_4
	SO_3	CH_3SO_3H

The Earth's sulphur cycle includes three major reservoirs: the lithosphere, hydrosphere and atmosphere (***Figure 1.6***). According to Jackson and Jackson (1996), the lithosphere accounts for 2.5 X 10^{20} mol of sulphur, the hydrosphere for 0.4 X 10^{20} mol of sulphur and the atmosphere for 1.25 X 10^{11} mol of sulphur. The size of the atmospheric reservoir may seem small considering that sulphur exists as highly volatile species produced in large quantities by natural processes (41.47 X 10^{11} mol of sulphur per year) and anthropogenic processes (16.2 X 10^{11} mol of sulphur per year) (***Figure 1.6***). However because of the short residence times of atmospheric sulphur species, they are quickly removed from the atmospheric reservoir (***Table 1.3***).

Atmospheric species of sulphur can vary in time and space. For example, some atmospheric sulphur source fluxes are continuous (e.g. global sea spray) while others are episodic (e.g. volcanic eruptions). Anthropogenic sources are dominant in the northern hemisphere whereas natural sources are dominant in the southern hemisphere (Liss et al., 1993; Berresheim et al., 1989). Atmospheric sulphur sources can be:

1) naturally-produced, continentally-derived (e.g. volcanic emissions, biogenic emissions and aeolian emissions)
2) anthropogenically-produced, continentally-derived (e.g. combustion of fossil fuels, refining of fossil fuels, ore smelting and gypsum processing)
3) naturally- produced, marine-derived (e.g. biogenic emissions and sea spray) or

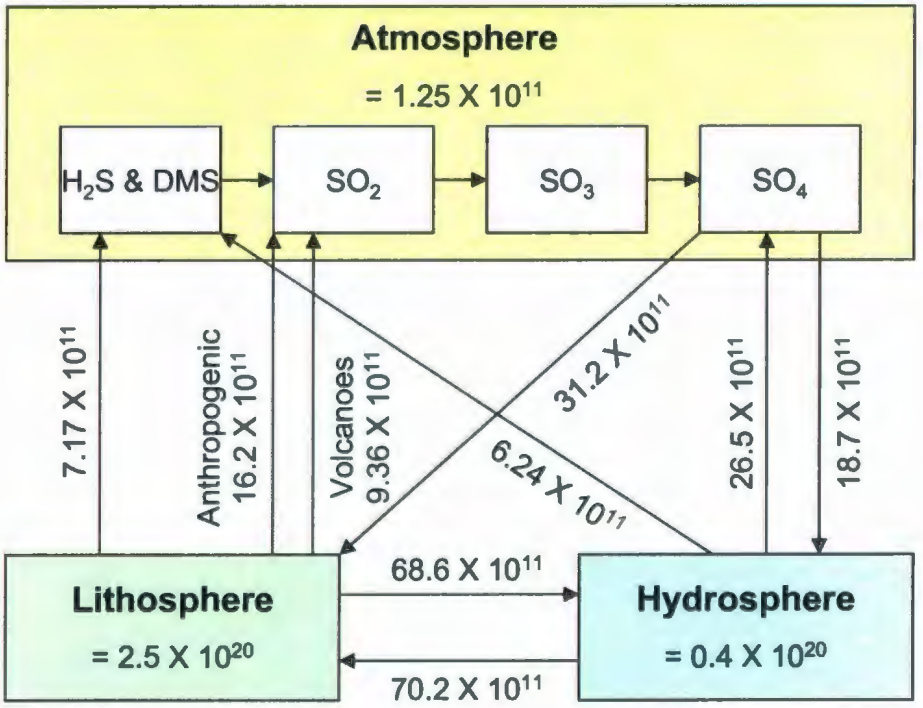

Figure 1.6: The sulphur cycle. Boxes show the amount of sulphur in each reservoir (mol) and arrows show the amount of sulphur transferred from one reservoir to another in one year (mol/yr) (Jackson and Jackson, 1996).

Table 1.3: Residence times of atmospheric sulphur species.

Sulphur Species	Residence Time (in days)
DMS	< 2 days (Charlson et al., 1992)
SO_2	2 to 8 days (Katz, 1977)
MSA	12 days (Millet et al., 2004)
NSS SO_4	< 6 days (Charlson et al., 1990).
SS SO_4	< 2.5 days (Gong et al., 1997)

4) anthropogenically-produced, marine-derived (e.g. ship stack emissions, oil rig stacks and planes).

The dominant sulphur species in the atmosphere of the northern Pacific Ocean (the location of this study) are sea spray sulphate (SS SO_4), dimethyl sulphide (DMS), methane sulphonic acid (MSA), sulphur dioxide (SO_2) and non-sea-salt sulphate (NSS SO_4) (***Figure 1.7***).

Sea spray particles form from bursting bubbles in breaking waves at the ocean-atmosphere interface. There are two kinds of sea spray particles: film drops and jet drops (***Figure 1.8***). Film drops form from the shattering of a bubble film cap while jet drops form from a central jet (***Figure 1.8***). Cipriano and Blanchard (1981) found that sea spray particles <10 μm in diameter originated as film drops from bubbles larger than 1 mm and that sea spray particles >20 μm were produced from jet drops from bubbles >200 μm. The size of the sea spray particle is also dependent on the relative humidity such that an increase in the relative humidity produces sea spray particles of decreasing diameter (Duce et al., 1983). The residence time of sea spray is also dependent on the aerosol size with coarser aerosols having shorter residence times than finer aerosols (0.5 hour and <2.5 days respectively) (Gong et al., 1997).

DMS is produced by assimilatory sulphate reduction, ASR, by phytoplankton in the marine environment. During ASR by phytoplankton, oceanic sulphur is reduced to produce methionine and dimethylsulfoniopropionate (DMSP) (Andreae, 1980). The

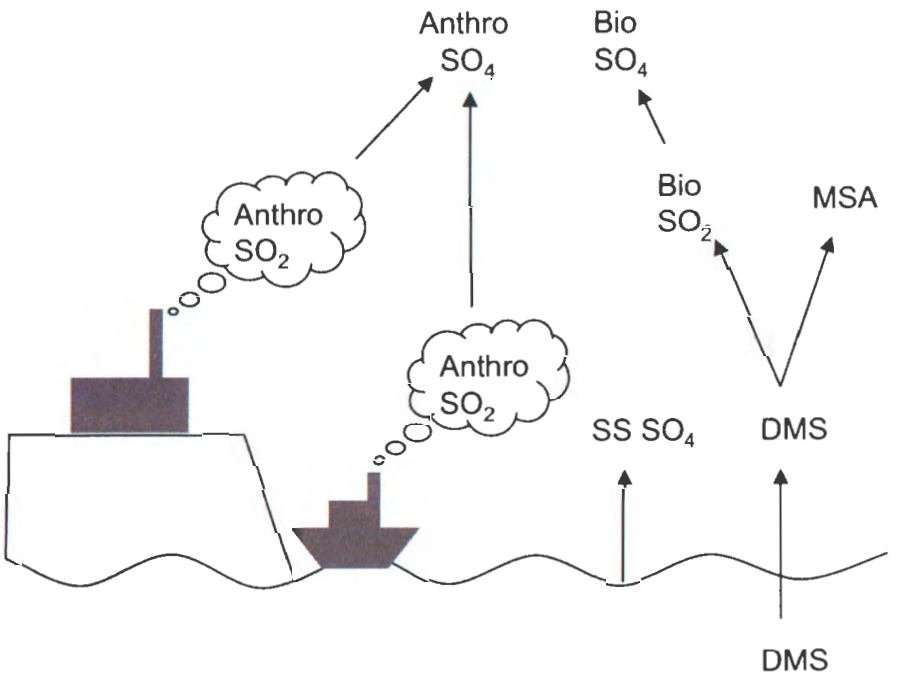

Figure 1.7: Dominant sulphur species in the atmosphere of the northern Pacific Ocean (Anthro SO_2 = anthropogenic sulphur dioxide, Anthro SO_4 = anthropogenic sulphate, SS SO_4 = sea salt sulphate, DMS = dimethyl sulphide, MSA = methane sulphonic acid, Bio SO_2 = biogenic sulphur dioxide and Bio SO_4 = biogenic sulphate).

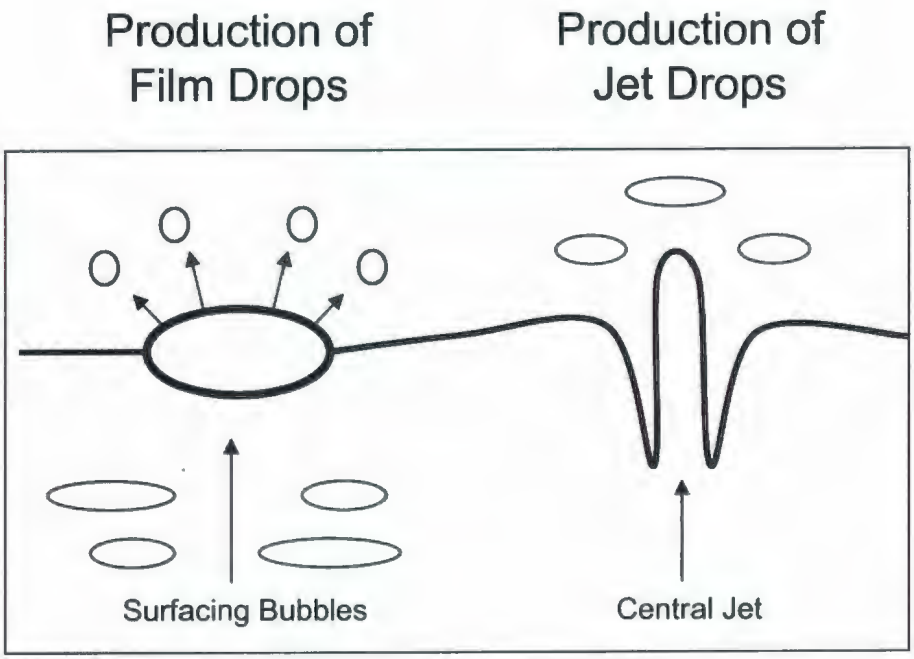

Figure 1.8: Schematic of the formation of sea spray particles: film drops and jet drops (Woolf and Monahan, 1988).

enzymatic breakdown of DMSP produces oceanic DMS and acrylic acid (Challenger and Simpson, 1948). The DMS flux into the atmosphere depends mainly on the oceanic DMS concentration and the wind speed such that stronger winds release more DMS gas. Atmospheric DMS is oxidized by reaction with hydroxyl (OH), nitrate (NO_3), halogens or halogen oxides (e.g. bromate, BrO). OH is an important oxidant in the daytime, NO_3 in the nighttime and BrO in the Arctic (Turnipseed and Ravishankara, 1993). The atmospheric lifetime of DMS is < 2 days and is controlled mainly by the concentrations OH and NO_3 which are in turn controlled by concentrations of nitrous oxides (NO_x) and ozone (O_3) and ambient conditions such as temperature and solar flux.

Oxidation of DMS by OH can occur via two processes: 1) hydrogen abstraction and 2) addition of OH to the sulphur atom to form a weak adduct that will react with oxygen (O_2) (Hynes et al., 1986) (***Figure 1.9***). Hynes et al. (1986) found that 70% of the DMS will oxidize by the abstraction pathway (at room temperature and at one atmosphere of air pressure). This corresponds to the 70% yield of SO_2 discovered by Barnes et al., 1989. Hence it is reasonable to predict that SO_2 is a major product of abstraction and MSA, dimethylsulphoxide (DMSO) and dimethylsulphone ($DMSO_2$) are the dominant products of addition. Hynes et al. (1986) also found that at lower temperatures, the addition and abstraction pathways are equally important in OH oxidation of DMS. However, Plane (1989) reported that the rate of addition increased with decreasing temperature. For example, at 27°C there will be 25% oxidation of DMS by OH via the addition pathway while at -23°C there will be 70% (Hynes et al., 1986). Yin et al. (1990) stated that the

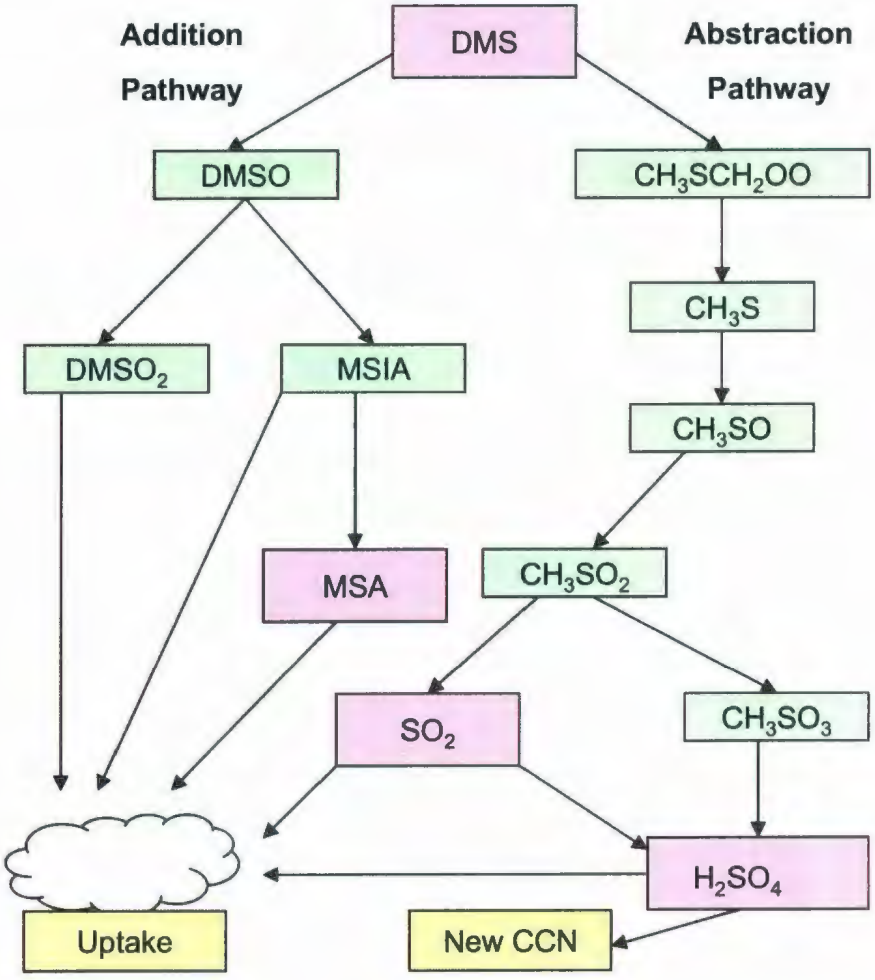

Figure 1.9: A conceptual box model of dimethyl sulphide (DMS) oxidation pathways. The green boxes show intermediate species in the production of methane sulphonic acid (MSA), sulphur dioxide (SO_2) and sulphuric acid (H_2SO_4) from dimethyl sulphide (DMS) (Modified from von Glasow and Crutzen, 2004).

abstraction pathway is limited by light intensities and/or temperatures such that lower light intensities and temperatures can cause a slower decomposition rate of the methylsulphonyl radical (CH_3SO_2), a precursor of SO_2 in the oxidation of DMS (Yin et al., 1990). Thus at low temperatures there will be higher concentrations of MSA and at high temperatures there will be higher concentrations of SO_2 (Bates et al., 1992). The preferred oxidation pathway also seems to depend on the ambient amount of pollution with the addition pathway dominating in polluted environments and abstraction dominating in clean environments (Yin et al., 1990). Laboratory tests revealed that at low NO_x levels, less than 20% MSA was produced (Tyndall et al., 1986; Saltzman et al., 1986).

Oxidation of DMS by NO_3 is rapid and may be a dominant oxidation process for DMS however its products and reactions are not well defined. For instance, Daykin and Wine (1990) and Jensen et al. (1992) measured large yields of species that suggest an intramolecular hydrogen abstraction within a NO_3-DMS complex even though it is generally believed that NO_3 adds to the sulphur atom.

It appears that the role of halogens and halogen oxides are relatively unimportant except in Arctic environments and that OH and NO_3 dominate the oxidation of DMS. In unpolluted environments, daily cycles showing a maximum at night and a minimum in the afternoon are indicative of oxidation by OH (Andreae, 1985). In polluted

environments, Andreae (1985) found the daily cycle was not as pronounced, suggesting a nighttime sink by NO_3.

The oxidation of DMS by OH yields MSA via the addition reaction. There have been no gas-phase studies involving MSA and therefore the oxidants and reactions are highly uncertain. Due to its vapour pressure, MSA is suspected to go into aqueous phases rather than gaseous phases. MSA in the marine environment is formed distinctly from DMS (Bates et al., 1992). MSA is one of the more stable oxidation products of DMS and the mean residence time of MSA is 12 days (Millet et al., 2004).

SO_2 is present in the marine atmosphere from anthropogenic activity, volcanic activity or oxidation of biogenic reduced sulphur gases like DMS. Oxidation can take place by gas phase reactions or by aqueous phase reactions. Gas phase reactions are irreversible while aqueous phase reactions often obtain equilibrium and are therefore reversible. SO_2 will have a mean residence time of 2 days if it was oxidized in the aqueous phase and a minimum of 8 days if oxidized in the gas phase (Katz, 1977). Gaseous SO_2 is oxidized by OH or NO_3, however, oxidation of SO_2 by NO_3 is extremely slow (Plane, 1989). Oxidation in the aqueous phase is by ozone (O_3) or hydrogen peroxide (H_2O_2) (Benkovitz et al., 2006). The SO_2 oxidation rate depends on factors such as relative humidity with more rapid oxidation occurring in humid environments (Jackson and Jackson, 1996).

The majority of anthropogenic SO_2 is produced from the burning of fossil fuels (e.g. coal and oil). Sulphur contaminants (e.g. pyrite in coal and organic sulphur compounds in coal and oil) can be oxidized to SO_2 during combustion. The type of fossil fuel being combusted will affect how much sulphur will be emitted: coal generally has a higher sulphur content (mean 2% sulphur by weight) than oil (mean 0.3 to 0.8% sulphur by weight) and natural gas (mean 0.05% sulphur by weight) (Möller, 1984). Anthropogenic SO_2 found in the oceanic atmosphere can originate from combustion of fossil fuels either on continents or from ships. Ship sulphur emissions are nearly equal to the natural sulphur flux from ocean to atmosphere in many areas (Capaldo et al., 1999). In fact, satellite images show clouds form over shipping lanes (Weart, 2009) possibly because the SO_2 in the ship exhaust can become oxidized to form CCN.

NSS SO_4 can have either a biogenic origin (i.e. from oxidation of DMS) or an anthropogenic origin (i.e. from oxidation of sulphur involved in human activities like combustion of fossil fuels, refining of fossil fuels, ore smelting and gypsum processing). The NSS SO_4 can be involved in nucleation processes, forming new particles, or condensation processes, combining with existing particles. If the NSS SO_4 formed on cloud condensation particles and if the cloud evaporates rather than precipitates, the NSS SO_4 will be released back into the atmosphere in the accumulation mode. The mean residence time of NSS SO_4 aerosols is approximately 6 days (Charlson et al., 1990).

1.8 STABLE ISOTOPES

Stable isotopes are elements having different numbers of neutrons in the nucleus (thus different masses) and are not involved in any radioactive decay process. Sulphur isotopic studies began in the 1940's (Thode et al., 1949) and interest grew quickly due to sulphur's relatively large isotopic mass differences, variety of chemical forms and widespread distribution on Earth (Thode, 1991). The isotopes, their relative atomic masses and natural abundances according to Rosman and Taylor (1998) and Audi and Wapstra (1995) are:

^{32}S	31.972	95.02 %
^{33}S	32.971	0.75 %
^{34}S	33.967	4.21 %
^{36}S	35.967	0.02 %

Isotopic compositions are reported as the ratio of the isotope amount of the two most abundant isotopes for an element in a sample (e.g. $^{34}S/^{32}S_{sample}$) and comparing it to the ratio of the isotope amount of the two of the most abundant isotopes for the same element in an international standard (e.g. $^{34}S/^{32}S_{VCDT}$). This eliminates obtaining an absolute value for an element's isotopic composition as well as allowing comparisons of data from different laboratories. For sulphur, troilite (FeS) from the Canon Diablo iron meteorite was used in the Canon Diablo Troilite standard (CDT) that has a $^{34}S/^{32}S = 1/22.22$ or $^{34}S/^{32}S = 0.0450045$ (Thode, 1991). This standard has become scarce and was found to be

inhomogeneous so a synthetic standard was developed by the International Atomic Energy Agency (IAEA) in Vienna and named Vienna Canon Diablo Troilite (VCDT) (Rollinson, 1993). Standard delta notation (δ) expresses the isotope amount of the sample to the standard in per mil (parts per thousand, ‰):

Equation 1.2

$$\delta = \left(\frac{R_{sample}}{R_{standard}} - 1 \right) \times 100$$

where R_{sample} is the isotope amount of the number of heavy to light isotopes of interest in the sample and $R_{standard}$ is the isotope amount of the number of heavy to light isotopes in the standard. CDT and VCDT are assigned a value of 0‰. ***Figure 1.10*** shows examples of sulphur isotopic compositions ($\delta^{34}S$) in the SERIES area.

Isotope fractionation, or partitioning of isotopes, occurs during chemical reactions and physical processes that discriminate between the isotopes of different elements as a function of mass. According to Rollinson (1993), fractionation provides information on isotope exchange processes and kinetic processes. Isotope exchange processes occur when the isotopes of an element redistribute themselves among different molecules containing that element. For example, the exchange of ^{32}S and ^{34}S between $H_2{}^{32}S$ and $H_2{}^{34}S$:

Equation 1.3

$$H_2{}^{32}S \leftrightarrow H_2{}^{34}S$$

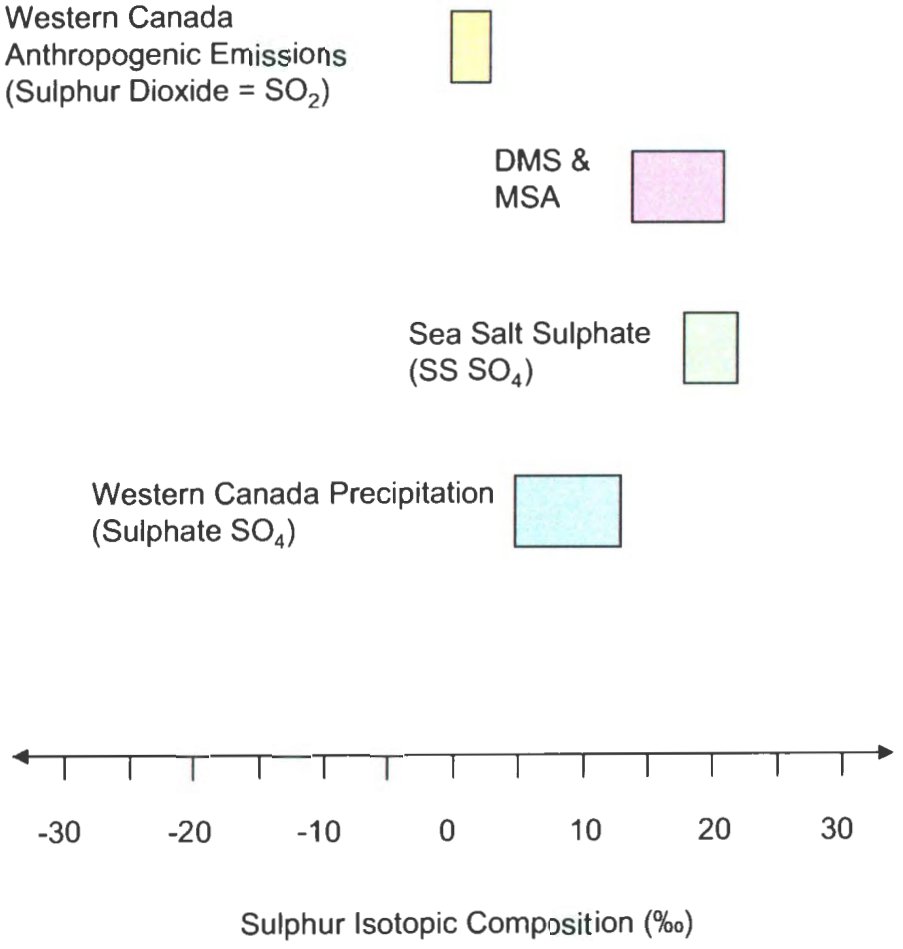

Figure 1.10: Sulphur Isotopic Compositions (Sea Salt Sulphate (SS SO_4) = Rees, 1978; Dimethyl sulphide (DMS) & Methane sulphonic acid (MSA) = Calhoun et al., 1991; Western Canada Precipitation & Western Canada Anthropogenic Emissions = Norman et al., 2004a).

Because the reactants and products of isotope exchange processes are assumed to be in equilibrium, the resulting fractionation is sometimes referred to as equilibrium fractionation. On the other hand, kinetic processes involve unidirectional or incomplete reactions that affect the bonds of the involved species. For example, the reduction of sulphate involving ^{32}S ($^{32}SO_4 \rightarrow H_2{}^{32}S$) takes place at a rate of k_{32} and the reduction of sulphate involving ^{34}S ($^{34}SO_4 \rightarrow H_2{}^{34}S$) takes place at a rate of k_{34} (Thode, 1991).

Equation 1.4 $2^{32}SO_4 + 2H_2O \rightarrow 2H_2{}^{32}S + 5O_2$ $rate=k_{32}$

Equation 1.5 $2^{34}SO_4 + 2H_2O \rightarrow 2H_2{}^{34}S + 5O_2$ $rate=k_{34}$

The ratio of k_{32}/k_{34} is 1.022 at room temperature meaning the reduction involving ^{32}S reacts 1.022 times faster than the reduction involving ^{34}S (Thode, 1991). The nature of isotope fractionation expected during isotope exchange and kinetic processes is described by the fractionation factor, α:

Equation 1.6 $\alpha_{A\ B} = \frac{R_A}{R_B}$ at a specified temperature

where R is the ratio of the heavy isotope to the light isotope in two different molecules or phases (A and B) and the reaction is in equilibrium at a specific temperature (Faure, 1986). When expressed in terms of the delta values, the equation becomes (Nielsen, 1979):

Equation 1.7

$$\alpha_{A-B} = \frac{1+\frac{\delta_A}{1000}}{1+\frac{\delta_B}{1000}} = \frac{1000+\delta_A}{1000+\delta_B}$$ at a specified temperature

Stable isotopes can be used to "fingerprint" the source of a substance so the stable isotopes of sulphur will be used to determine the proportion of sea spray, anthropogenic, and biogenic sources.

1.9 USING %SS SO_4 AND $\delta^{34}S_{SO4}$ TO DETERMINE AEROSOL SOURCE

Sea salt tracers (e.g. magnesium = Mg, sodium = Na, chloride = Cl) can be used to distinguish the sea salt sulphate, SS SO_4, from the non sea salt sulphate, NSS SO_4, (both biogenic or anthropogenic) and estimate the percent sea salt sulphate, %SS SO_4 (Mizutani and Rafter, 1969):

Equation 1.8

$$\%SS\,SO_4 = \left(0.14 \div \frac{SO_{4\,sample}}{Cl_{\,sample}}\right) \times 100$$

Equation 1.9

$$\%SS\,SO_4 = \left(0.25 \div \frac{SO_{4\,sample}}{Na_{\,sample}}\right) \times 100$$

Equation 1.10

$$\%SS\,SO_4 = \left(2.1 \div \frac{SO_{4\,sample}}{Mg_{\,sample}}\right) \times 100$$

where 0.14, 0.25 and 2.10 correspond respectively to the mass ratios of SO_4/Cl, SO_4/Na and SO_4/Mg of seawater. Consequently, the percent of non sea salt sulphate, %NSS SO_4, can be calculated:

Equation 1.11

$$\%\ \mathrm{NSS\ SO_4} = 100 - \%\ \mathrm{SS\ SO_4}$$

The %SS SO_4 and %NSS SO_4 can be used to calculate the fraction of sea salt suphate ($F_{SS\ SO4}$) and the fraction of non sea salt sulphate ($F_{NSS\ SO4}$):

Equation 1.12

$$F_{SS\,SO4} = \%\ \mathrm{SS\ SO_4} \div 100$$

Equation 1.13

$$F_{NSS\,SO4} = \%\ \mathrm{NSS\ SO_4} \div 100$$

The sulphur isotopic compositions ($\delta^{34}S$) have been used in a number of studies (e.g. Nriagu et al., 1991; McArdle et al., 1998; Patris et al., 2000; Turekian et al., 2001) to determine the sources of aerosols, especially fine NSS SO_4 aerosols that can be either anthropogenic or biogenic. The isotopic composition of NSS SO_4 ($\delta^{34}S_{\ NSS\ SO4}$) can be calculated provided the isotopic composition of the total SO_4 ($\delta^{34}S_{\ SO4}$), the isotopic composition of SS SO_4 ($\delta^{34}S_{\ SS\ SO4}$), the fraction of sea salt sulphate ($F_{SS\ SO4}$) and the fraction of non sea salt sulphate ($F_{NSS\ SO4}$) are known using:

Equation 1.14

$$\delta^{34}S_{SO4} = \left(\delta^{34}S_{SS\,SO4}\right)\left(F_{SS\,SO4}\right) + \left(\delta^{34}S_{NSS\,SO4}\right)\left(F_{NSS\,SO4}\right)$$

Subsequently, the fraction of biogenic NSS SO_4 ($F_{Bio\ NSS\ SO4}$) and anthropogenic NSS SO_4 ($F_{Anthro\ NSS\ SO4}$) can be estimated by the equation:

Equation 1.15

$$\delta^{34}S_{SO4}F_{SO4} = (F_{SS\,SO4})(\delta^{34}S_{SS\,SO4}) + (F_{Anthro\ NSS\,SO4})(\delta^{34}S_{Anthro\ NSS\,SO4}) + (F_{Bio\ NSS\,SO4})(\delta^{34}S_{Bio\ NSS\,SO4})$$

where

Equation 1.16

$$F_{SO4} = F_{SS\,SO4} + F_{Anthro\ NSS\,SO4} + F_{Bio\ NSS\,SO4} = 1$$

Solving for $F_{Bio\ NSS\ SO4}$ gives:

Equation 1.17

$$F_{Bio\ NSS\,SO4} = \frac{(\delta^{34}S_{SO4})(F_{SO4}) - (F_{SS\,SO4})(\delta^{34}S_{SS\,SO4}) - (\delta^{34}S_{Anthro\ NSS\,SO4}) + (\delta^{34}S_{Anthro\ NSS\,SO4})(F_{SS\,SO4})}{\delta^{34}S_{Bio\ NSS\,SO4} - \delta^{34}S_{Anthro\ NSS\,SO4}}$$

where $\delta^{34}S_{SO4}$ is the value obtained from the mass spectrometer for that sample, $\delta^{34}S_{SS\ SO4}$ is the isotopic composition of sea salt sulphate (=+21 ± 0.2‰ based on results from Rees et al., 1978), $\delta^{34}S_{Anthro\ NSS\ SO4}$ is the isotopic composition of anthropogenic non sea salt sulphate (=+2.0 ± 1.0‰ based on results from Norman et al., 2004a), $\delta^{34}S_{Bio\ NSS\ SO4}$ is the isotopic composition of biogenic non sea salt sulphate (=+18.6 ± 0.9‰ based on results from Patris et al., 2000), F_{SO4} was the fraction of total sulphate (=1 based on Equation 16) and $F_{SS\ SO4}$ was the fraction of sea salt in the sample (calculated using Equation 12).

Most aerosol studies that use stable isotopes to determine sources over the oceans, utilize a three source mixing model whereby one corner represents sea spray ($\delta^{34}S_{SS\ SO4}$ = +21‰, 100% SS SO_4), another corner represents biogenic sulphur ($\delta^{34}S_{Bio\ NSS\ SO4}$ = +18.6‰, 0% SS SO_4) and the third corner represents anthropogenic sulphur ($\delta^{34}S_{Anthro\ NSS\ SO4}$ = +2‰, 0% SS SO_4) (***Figure 1.11***). Once the % SS SO_4 and isotopic composition ($\delta^{34}S_{SO4}$) are plotted for each sample, the source of the particular sample can be determined.

1.10 OBJECTIVES

The main objectives of this thesis were to determine:

1) The source of SO_2 throughout SERIES

2) The source of NSS SO_4 throughout SERIES

3) The preferred pathway of DMS oxidation during SERIES and

4) The overall effects of the SERIES iron fertilization on the aerosols (by comparing the fertilized area to an unfertilized area).

Chapter 2 will provide a brief review of previous results, Chapter 3 will describe methods used to collect and analyze samples, Chapter 4 will discuss results and interpretations and Chapter 5 will provide a summary and suggestions for future work.

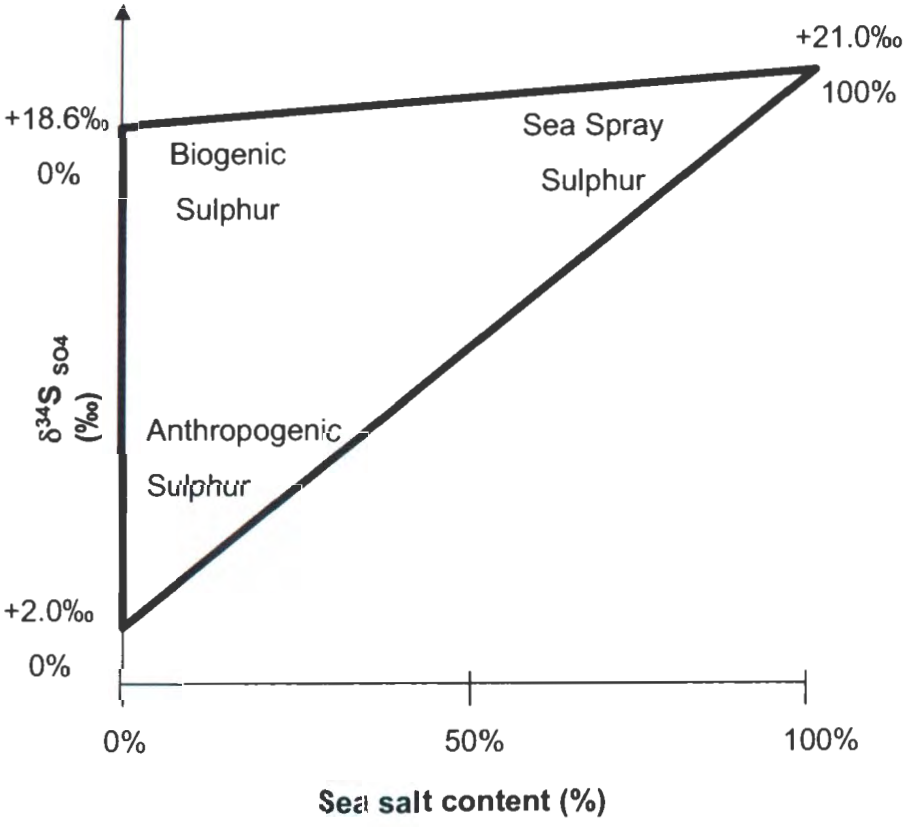

Figure 1.11: A mixing model using sea salt content (%SS SO_4) and isotopic composition ($\delta^{34}S_{SO4}$). Each corner represents a different source, the lines connecting two corners represent mixing between two of the sources. For example, biogenic sulphur is 0% and +18.6 ‰ and anthropogenic sulphur is 0% and +2.0 ‰. The line connecting the biogenic and anthropogenic corners shows mixing of biogenic and anthropogenic sulphate sources.

CHAPTER 2: PREVIOUS RESULTS

SERIES took place in the open ocean, so this chapter includes previous results of sulphur-bearing aerosols and gases expected: SS SO_4 aerosols, biogenic and anthropogenic NSS SO_4 aerosols, MSA aerosols and biogenic and anthropogenic SO_2.

2.1 SS SO_4 AEROSOLS

Sea salt aerosols are naturally produced at the ocean-atmosphere boundary. Wind speeds affect the concentration of sea salt aerosols by influencing wave activity. Wave activity produces aerosols when jet drops or film drops propel sea water into the atmosphere (Woolf and Monahan, 1988). Sea salt concentrations have a seasonal dependence with summer concentrations at a minimum and winter concentration at a maximum (Gong et al., 1997). Data collected from Mace Head (53.19°N, 9.54°W), Heimaey (63.40°N, 20.30°W), Bermuda (32.27°N, 64.87°W) and Oahu (21.33°N, 157.70°W) showed sea spray concentrations are affected by geographic location, with smaller seasonal sea spray concentration changes observed in locations closer to the equator (Gong et al., 1997). ***Table 2.1*** shows mean SS SO_4 concentrations collected in marine locations.

2.2 NSS SO_4 AEROSOLS

NSS SO_4 aerosols have been shown to exhibit a seasonal cycle with a summer maximum (Nriagu et al., 1991; Prospero et al., 1991; Wagenbach et al., 1988; Leck et al., 1996; Ayers et al., 1991; McArdle et al., 1998). Saltzman et al. (1983) recorded a mean NSS

Table 2.1: SS SO_4 aerosol concentrations (in $\mu g/m^3$) from previous studies of marine air

Reference	Location	Mean
Prospero, 1979	Central and Northern Atlantic (22-64°N)	6.71 ± 4.24
Prospero, 1979	Tropical and Equatorial North Atlantic (0-28°N)	11.2 ± 6.92
Prospero, 1979	Tropical and Central South Atlantic (5-35°S)	9.06 ± 5.25
Prospero, 1979	Pacific (28°N – 40°S)	8.44 ± 5.14
Prospero, 1979	Mediterranean	6.98 ± 2.92
Prospero, 1979	Indian (15°S to 7°N)	3.52 ± 1.10
Prospero, 1979	Malacca Straits, South China and Phillipine Seas	6.47 ± 3.32

SO_4 concentration of 0.630 $\mu g/m^3$ in the atmosphere of the Pacific Ocean, which was typical of results from other remote marine areas (Savoie and Prospero, 1982). Bates et al. (1992) stated the northern hemisphere of the Pacific Ocean had NSS SO_4 concentrations between 1.729 and 3.074 $\mu g/m^3$. ***Table 2.2*** shows NSS SO_4 results from other study areas.

Wylie et al. (1993) stated that the size of the NSS SO_4 aerosol depended upon the weather: when there was dry weather there was an increase in the fine aerosols whereas when there was humid weather there was an increase in larger aerosols. Both Krischke et al. (2000) and Scaire et al. (2000) found that approximately 70% of the NSS SO_4 occurred in fine aerosols.

As discussed in ***Section 1.9*** (Using Sea Spray and Isotopes to Calculate Aerosol Source), the isotopic composition of NSS SO_4 ($\delta^{34}S_{NSS\ SO4}$) depends on the source(s) from which it formed. ***Table 2.3*** shows $\delta^{34}S_{NSS\ SO4}$ from previous studies.

Patris et al. (2000) found that 50 to 90% of coarse NSS SO_4 aerosols had a biogenic isotopic signature in both the northern and southern hemispheres of the Atlantic Ocean. However the fine NSS SO_4 aerosols of the southern hemisphere of the Atlantic were shown to have a stronger input of biogenic sources than those of the northern hemisphere of the Atlantic: southern hemisphere fine aerosols having 60% with a biogenic origin and northern hemisphere fine aerosols having 35% with a biogenic origin (Patris et al., 2000).

Table 2.2: NSS SO_4 aerosol concentrations (in $\mu g/m^3$) from previous studies of marine air

Reference	Location	Mean
Berresheim et al., 1991	North Atlantic, Marine air	0.404
Berresheim et al., 1991	North Atlantic, Continental air	1.224
Saltzman et al., 1983	Indian Ocean	0.520

Reference	Location	Maximum	Minimum
Bates et al., 1992	Southern Pacific Ocean	1.537	0.077
Wylie et al., 1993	Ross Island, Antarctica	1.114	0.293
Leck et al., 1996	Arctic Ocean	0.672	0.003
Prospero et al., 1991	Mawson, Antarctica	0.250	0.0065

Table 2.3: $\delta^{34}S_{NSS\ SO4}$ (in ‰) from previous studies of marine air

Reference	Location	$\delta^{34}S_{NSS\ SO4}$
Gravenhorst, 1977	North Atlantic	+7 to +9
Gravenhorst, 1977	Southwest Atlantic	-12 to +10
Patris et al., 2000	African coast	+9.4

2.3 MSA AEROSOLS

MSA aerosols over the marine atmosphere were first measured by Saltzman et al. in 1983. Since then numerous researchers have measured MSA in a variety of locations (***Table 2.4***) and many have found there is also a seasonal pattern (with a summer maximum) in MSA concentrations (Prospero et al., 1991; Ayers et al., 1991; Leck et al., 1996; McArdle et al., 1998). MSA from the Pacific Ocean has been reported by Saltzman et al. (1983) to range between 0.035 to 0.042 $\mu g/m^3$ and by Bates et al. (1992) to range between 0.002 to 0.045 $\mu g/m^3$. Although Pszenny (1992) stated there was no relationship between MSA and size, both Saltzman et al. (1983) and Scaire et al. (2000) showed that MSA occurs in sub-micrometer aerosols but in slightly larger aerosols than NSS SO_4.

2.4 MSA TO NSS SO_4

It has been suggested that the MSA to NSS SO_4 ratio may be indicative of source or oxidation pathway and may be dependent upon temperature and/or latitude. The MSA to NSS SO_4 ratio near the equator is relatively constant (approximately 0.065) (Saltzman et al., 1983, Saltzman et al., 1986). The MSA to NSS SO_4 in oceanic areas affected by anthropogenic sulphur emissions (e.g. North Atlantic Ocean) is typically <0.3 (Savoie et al., 1989; Galloway, 1990) while it is >0.5 in oceanic areas unaffected by anthropogenic sulphur emissions (e.g. mid to high latitudes in the southern hemisphere) (Bates et al., 1990; Berresheim et al., 1990). Ratios close to 1 have been observed near Antarctica

Table 2.4: MSA aerosol concentrations (in $\mu g/m^3$) from previous studies of marine air

Reference	Location		Mean
Saltzman et al., 1983	Indian Ocean		0.020
Berresheim et al., 1991	North Atlantic, Marine air		0.011
Berresheim et al., 1991	North Atlantic, Continental air		0.009
Reference	**Location**	**Maximum**	**Minimum**
Prospero et al., 1991	Mawson, Antarctica	0.060	0.002
Wylie et al., 1993	Ross Island, Antarctica	0.222	0.039
Leck et al., 1996	Arctic Ocean	0.096	0.0001
Ayers et al., 1991	Cape Grim	0.032	0.0013
Scaire et al., 2000	Atlantic Ocean	0.038	0.0009
McArdle et al., 1998	Mace Head	0.173	
McArdle et al., 1998	Plynlimon	0.212	

(Berresheim, 1987; Pszenny et al., 1989). Therefore MSA to NSS SO_4 tends to increase with increasing latitude and/or decreasing temperature and may be due to a preferred oxidation pathway that favors addition (production of MSA) as opposed to abstraction (production of SO_2). If the addition pathway were preferred, more MSA would be produced and there would be higher MSA to NSS SO_4 expected. However as Ayers et al. (1991) pointed out after reporting a winter minimum (mean = 0.06) and a summer maximum (mean = 0.18) at Cape Grim, the sampling techniques can have an influence on the MSA to NSS SO_4 ratio. For example, biogenic NSS SO_4 formed from biogenic SO_2 may be simultaneously collected and included as the NSS SO_4 portion during analysis, causing a reduction in the MSA to NSS SO_4 ratio. Also, if aerosols are collected on one filter as opposed to two filters that separate coarse and fine aerosols, the size sampled will affect the MSA to NSS SO_4 ratio as MSA combines with pre-existing aerosols and is concentrated in slightly larger aerosols than NSS SO_4 (Scaire et al., 2000).

2.5 SO_2 GAS

Gaseous sulphur dioxide (SO_2) in a clean atmosphere shows a seasonal cycle with maximum occurring in summer (from oxidation of DMS). Leek et al. (1996) as well as Berresheim et al. (1991) observed a maximum in winter in an atmosphere heavily influenced by continents, likely from combustion of fossil fuels for heating. Nguyen et al. (1983) reported a latitudinal dependence/primary productivity dependence of SO_2 concentrations: areas that were further from the equator were areas of low productivity

(<36 g/cm^{2}yr) and had low SO_2 concentrations (~0.030 μg/m^3), areas of intermediate productivity (36 to 90 g/cm^{2}yr) had intermediate SO_2 concentrations (~0.100 μg/m^3) and areas near the equator had high productivity (>90 g/cm^{2}yr) and had high SO_2 concentrations (0.200 to 0.300 μg/m^3). Nguyen et al. (1983) stated that the mean background SO_2 concentration over the world's oceans was 0.100 μg/m^3. Bates et al. (1992) reported SO_2 concentrations ranging from 0.122 to 0.833 μg/m^3 in the northern hemisphere of the Pacific Ocean (higher than values previously reported by Quinn et al., 1990). ***Table 2.5*** shows additional SO_2 concentration results.

Assuming no isotope fractionation occurred (Norman et al., 2004a), the $\delta^{34}S_{SO2}$ will be the same as the $\delta^{34}S_{SO4}$ from which it formed (***Table 2.3***).

Table 2.5: SO_2 gas concentrations ($\mu g/m^3$) from previous studies of marine air

Reference	Location	Mean
Berresheim et al., 1991	Atlantic Ocean, Marine air	0.169
Berresheim et al., 1991	Atlantic Ocean, Continental air	1.936
Scaire et al., 2000	Atlantic Ocean	0.053

Reference	Location	Maximum	Minimum
Bates et al., 1992	Southern Pacific Ocean	0.135	0.010
Leck et al., 1996	Arctic Ocean	0.045	0.003

CHAPTER 3: METHODS

3.1 AEROSOLS AND SO_2 GAS

Aerosol and gas samples were collected from July 10 to July 30, 2002 using high volume air samplers when conditions were favorable (i.e. no precipitation and when the ship was heading into the prevailing wind). Analyses of the gas and aerosol samples took place after the cruise at the University of Calgary and Memorial University of Newfoundland. Ship fuel samples were prepared at Memorial University of Newfoundland and were subsequently analyzed at the University of Calgary. The following sections provide detail on the procedures used during sample collection, preparation and analysis.

3.1.1 COLLECTION OF AEROSOLS AND SO_2 GAS

Aerosols and sulphur dioxide gas were collected using two Anderson Sierra and two Sierra Miscu high-volume, mass-flow controlled samplers set at a flow rate of 1.13 m^3/min. Samplers were located at the front of the flying bridge of the Mexican *El Puma*, approximately 10 m above sea level. Two samplers collected aerosols in/downwind of the patch (Samplers 3 and 4) and two samplers collected out/upwind of the patch (Samplers 1 and 2) therefore Samplers 1 and 2 collected background concentrations and Samplers 3 and 4 collected concentrations influenced by the fertilized patch. Two samplers (Samplers 2 and 3) were equipped with Graseby Series 230 five-stage cascade impactors and back-up filters; two samplers (Sampler 1 and 4) were equipped with bulk aerosol filters and sulphur dioxide filters (***Figure 3.1***).

Sampler 2:
Outside/upwind of the patch

Sampler 3:
Inside/downwind of the patch

Sampler 1:
Outside/upwind of the patch

Sampler 4:
Inside/downwind of the patch

Figure 3.1: SERIES High Volume Samplers. Two samplers (Samplers 2 and 3) were equipped with a 5-stage cascade impactor and a back-up filter while the other two samplers (Samplers 1 and 4) were equipped with a total particulate filter and a sulphur dioxide filter.

A cascade impactor (***Figure 3.2***) is a set of staggered slotted plates used to collect aerosols of known diameters on filters positioned between the plates. The staggering of the slots in the various stages of a cascade impactor enables aerosols above a certain cut-off diameter for a particular stage to be collected on the filter for that stage while aerosols smaller pass through the filter and onto the next stage. The cut-off diameter for the aerosols is controlled by the slot width of the plate, where the slot width per stage remains constant but the slot width between stages decreases toward the bottom of the cascade impactor. Therefore aerosols of a similar diameter are collected on the same slotted filter but due to the narrowing of the slot width, smaller aerosols are collected on successively lower stages.

During SERIES, PM_{10} heads were installed on Samplers 2 and 3, the samplers equipped with cascade impactors and back-up filters. This meant only aerosols <10 μm were sampled and sorted according to size where Stage 1, the uppermost stage, collected aerosols between 7.2 μm and 10 μm, Stage 2 between 7.2 μm and 3.0 μm, Stage 3 between 3.0 μm and 1.5 μm, Stage 4 between 1.5 μm and 0.95 μm and Stage 5 between 0.95 μm and 0.45 μm (***Figure 3.2***). The back-up filter collected aerosols <0.45 μm onto a solid 8 x 10 inch quartz filter (***Figure 3.2***).

The other two samplers, one in/downwind of the patch sampler (Sampler 1) and one out/upwind of the patch sampler (Sampler 4), collected bulk aerosols and sulphur dioxide gas (***Figure 3.1***). Untreated quartz filters collected bulk aerosols while a potassium

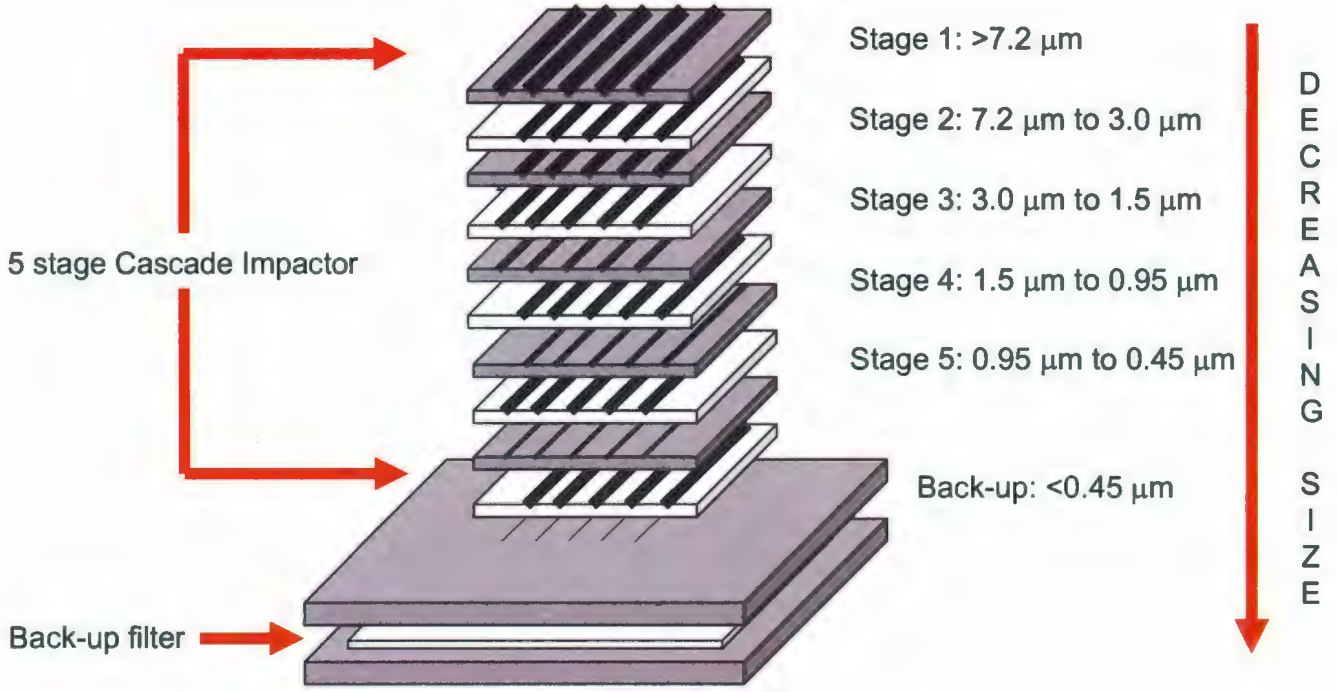

Figure 3.2: A 5-stage cascade impactor. Segregates aerosols of various sizes due to its slots of decreasing width while a back-up filter collects aerosols small enough to pass through the cascade impactor.

carbonate/glycerol-impregnated quartz filter (see ***Appendix 3.1***) absorbed sulphur dioxide gas (***Figure 3.1***).

Throughout the cruise, 23 samples, containing 8 filters per sample, were collected onboard El Puma. Sampling times varied between 4 and 31 hours and depended on sampling conditions (e.g. no precipitation and ship steaming into wind). Usually after approximately 12 hours of sampling, filters were removed from the samplers. The sulphur dioxide filters were immediately folded and placed in a labeled sampling bag. The cascade impactor and the bulk filter and filter holder were placed in a larger bag for transport inside the ship. Wearing powder-free gloves and working in a portable fumehood inside the ship, filters were folded so that the aerosols were contained inside. Folded filters were then wrapped individually with aluminum foil and placed in individually labeled sample bags. The filters were then double bagged (to reduce contamination) and given a sample set name. The sample bags were placed in a sealed, plastic container until sample preparation in the laboratory. The cascade impactor and bulk filter holder were cleaned using isopropyl alcohol, Kim Wipes and/or Q-tips. Filters were then loaded for the following sample and placed in a larger plastic bag that was stored in the clean-ceil until use.

A sample set naming system indicated type of sample (by number) as well as the order of collection (by letter). Samples beginning with the number 1 collected bulk aerosols and SO_2 gas out/upwind of the patch, samples beginning with the number 2 collected size-

segregated aerosols out/upwind of the patch. The number 3 indicated the collection of size-segregated aerosols in/downwind of the patch and any sample beginning with the number 4 collected bulk aerosols and SO_2 gas in/downwind of the patch (with the exception of 4E which was mislabeled and was actually an out/upwind bulk sample). Samples containing the letter A were the first samples collected, samples containing the letter B were the second samples collected and so on. For the size-segregated samples, the sample set name was followed by a dash and a sample stage number. For instance, in Sample 3A, 3A-1 meant Stage 1 (7.2 μm and 10 μm aerosols), 3A-2 meant Stage 2 (7.2 μm and 3.0 μm aerosols), 3A-3 meant Stage 3 (3.0 μm and 1.5 μm aerosols), 3A-4 meant Stage 4 (1.5 μm and 0.95 μm aerosols), 3A-5 meant Stage 5 (0.95 μm and 0.45 μm aerosols) and 3A-6 meant the back-up filter (<0.45 μm aerosols). In addition, SO_2 samples were indicated by the sample set followed by a dash and SO_2. For instance 3A-SO_2 meant the SO_2 filter of Sample 3A. Blanks included 1E & 2E, 1I & 2I, 1J & 2J, 3E & 4G, 3L & 4N and 3M & 4O. Sample 2F was destroyed during shipping. The sampling details are shown in ***Appendix 3.2*** (sampling dates and times given in Pacific Time).

3.1.2 PREPARATION OF AEROSOLS AND SO_2 GAS FOR STABLE ISOTOPIC ANALYSIS

The preparation of methane sulphonic acid aerosols, sulphate aerosols and sulphur dioxide for isotope analysis incorporated a method that was designed and completed in February and March of 2003 in the Isotope Sciences Laboratory at the University of Calgary.

3.2.2.1 PREPARATION OF AEROSOLS

Sulphate from aerosol filters was extracted by sonication and precipitated as barium sulphate ($BaSO_4$). Determining the isotopic composition of sulphate aerosols was an important aspect of this thesis therefore a method was devised to separate the sulphate (as barium sulphate, $BaSO_4$) from the methane sulphonic acid (MSA) in order to prevent false biologically-derived isotopic signatures. The procedure is outlined in ***Appendix 3.3***.

After the MSA and sulphate were separated, the filter paper containing the sulphate was transferred from the vacuum apparatus to a clean, labelled watch glass. The filter was covered with another watch glass and placed in a 110 °C oven for 60 minutes. The filter paper was cooled to room temperature. The filter was placed into a clean labelled crucible and covered with a lid. The crucibles were put in an 800 °C oven for 90 minutes. Once the crucibles had cooled to room temperature, they were tapped gently to loosen the barium sulphate ($BaSO_4$) from the sides and onto a weighing paper. The weight of the barium sulphate ($BaSO_4$) produced was recorded. The samples were stored in labelled sample envelopes until ready for analysis by the mass spectrometer.

3.1.2.2 PREPARATION OF SO_2 GAS

Because the sulphur dioxide filters were impregnated with a potassium carbonate/glycerol solution, a slightly different method than aerosols was employed to precipitate barium sulphate ($BaSO_4$) for analysis. ***Appendix 3.4*** outlines the procedure.

3.1.3 ANALYSIS OF AEROSOLS AND SO_2 GAS

3.1.3.1 STABLE ISOTOPIC ANALYSIS OF AEROSOLS AND SO_2 GAS

In order for the sulphate aerosol and sulphur dioxide to be analyzed for their stable sulphur isotopic compositions, a portion of the barium sulphate ($BaSO_4$) had to be packed into a 4 mm diameter by 6 mm high tin capsule. The capsule was then sealed and stored in a labelled plastic tray until analysis.

Isotopic analyses of the sulphur dioxide gas and sulphate aerosols were completed using a Carlo Erba NA 1500 Elemental Analyzer (EA) interfaced to a VG Prism II Continuous-Flow Isotope-Ratio Mass Spectrometer (CF-IRMS) at the University of Calgary during the spring of 2003.

As the sample was introduced into the elemental analyzer by an A200S autosampler, a pulse of oxygen gas caused a flash combustion in the quartz reaction tube in the combustion furnace (maintained at a temperature of 1020°C). Ultra High Purity Helium (UHP He) carried the sample gases at a flow rate of 90 mL/min through a water trap, consisting of approximately 10 cm of magnesium perchlorate ($Mg(ClO_4)_2$) and approximately 5 cm of phosphorus pentoxide (P_2O_5), and then into the 6 mm by 800 mm long Gas Chromatograph (GC) column. An open-split interface then diluted other gases in the sample (e.g. nitrogen oxides, NO_x and carbon dioxide, CO_2) before the SO_2 entered the mass spectrometer for stable isotopic analysis.

During analysis, samples were compared to internal and external standards of known concentration and isotopic composition. Internal standards included SW (barium sulphate precipitated from a seawater standard) and STB (barite standard) with $\delta^{34}S_{SO4}$ of +20.8‰ and -2.0‰ respectively. These internal standards have been calibrated to the international reference materials IAEA S-1 and IAEA S-2 with $\delta^{34}S_{SO4}$ of -0.3‰ and +21.0‰ respectively. During the analysis of the SERIES samples, the accuracy was +/- 0.5‰ and the precision was +/- 0.3‰.

3.1.3.2 CHEMICAL ANALYSIS OF AEROSOLS

The concentration of anions (including chloride (Cl), nitrate (NO_3), sulphate (SO_4) and methane sulphonic acid (MSA, CH_3SO_3H)) and cations (including sodium (Na), potassium (K), magnesium (Mg), calcium (Ca) and ammonium (NH_4)) were determined at Memorial University of Newfoundland during the summer and fall of 2003 using a Dionex 100 Ion Chromatograph equipped with version 3.2.1 of the AI-450 Chromatograph Automation Software.

Cation analysis was performed using a Dionex IonPac CS12A 4 mm diameter by 250 mm long analytical column with a Dionex CSRS-ULTRA 4 mm diameter self-regenerating suppressor and a Dionex IonPac CG12A 4 mm diameter x 50 mm long guard column. A 20 mM H_2SO_4 eluent set at a flow rate of 1 mL/min was used for analyses of Na, K, Mg, Ca and NH_4 ranging between 0.2 and 10 ppm.

Anion concentrations were obtained using a Dionex IonPac AS4A-SC 4 mm diameter by 250 mm long analytical column with a Dionex ASRS-ULTRA II 4 mm diameter self-regenerating suppressor and a Dionex IonPac AG 4A-SC 4 mm diameter by 50 mm long guard column. A 1.8 mM Na_2CO_3/1.7 mM $NaHCO_3$ eluent set at a flow rate of 1.0 mL/min was used for analyses of Cl, NO_3 and SO_4 ranging between 0 and 20 ppm while a 3.6 mM Na_2CO_3/3.4 mM $NaHCO_3$ and 1 mM $NaHCO_3$ set at a flow rate of 1.5 mL/min were used for analyses of MSA ranging between 0 and 0.5 ppm (MSA required a special procedure, described in ***Appendix 3.5***).

Each day the ion chromatograph was calibrated using internal standards prepared from National Institute of Standards and Technology (NIST) standard stock solutions and checked with external certified standards (***Table 3.1***). The injecting syringe was rinsed three times with deionized water and 1 mL of air-free deionized water was injected in the sample inlet. A volume of sample to be analyzed was poured from the vial and into a 5 mL beaker so as to avoid contamination of the remaining sample. The syringe was then rinsed once with sample before injecting 1 mL of bubble-less sample solution into the Ion Chromatograph. Analysis lasted approximately 6 minutes per sample for anions (excluding MSA), 30 minutes per sample for MSA (which required a special procedure, described in ***Appendix 3.5***) and 12 minutes per sample for cations.

Table 3.1: External certified standard concentrations for Ion Chromatography (in ppm).

STANDARD:	Cl	NO_3	SO_4	Na	K	Mg	Ca	NH_4
QCP-Rain, W-QCP13036	1.31	3.17	6.71	1.57	0.71	0.40	0.137	0.72
QCP-Rain, W-QCP13035				0.61	0.30	0.15	0.015	0.274
ESD Cation				2.9984	1.4973	1.4983	1.5029	1.4958
ESD Anion	2.9996	1.5029	1.5025					
T171				8.6	2.8	2.78	6.75	

3.1.3.3 BLANK CORRECTION OF AEROSOLS AND SO_2 GAS

Sampling filter blanks, laboratory filter blanks and water blanks were analyzed for this study. Sampling filter blanks were filters inserted into the samplers for less than one minute while the sampler was not running to determine whether sample handling affected the results. Laboratory filter blanks were used to assess contamination during storage in the laboratory. Water blanks were used to assess the cleanliness of the lab ware and lab water during extraction and analysis. Laboratory and water blanks were negligible. Six field sampling blanks were collected, three in/downwind of the patch and three out/upwind of the patch: 1E & 2E, 1I & 2I, 1J & 2J, 3E & 4G, 3L & 4N and 3M & 4O. Once the blanks were analyzed, the results could be used to "blank-correct" the data. In other words, the average concentrations from the blanks were subtracted from the concentrations.

3.1.3.4 UNCERTAINTY ASSOCIATED WITH AEROSOLS AND SO_2 GAS

The percent uncertainty associated with the concentration of each ion is shown in ***Table 3.2***. The percent uncertainty is used when results are plotted in graphs. The mean ± one standard deviation is reported when results are given in the text. Time weighted averages (i.e. average over time) were used where indicated. For calculated values, error propagation was performed with percent uncertainties propagated.

Table 3.2: Percent uncertainty for ion concentrations.

Ion	Cl	SO_4	Na	Mg	MSA
Uncertainty	18	14	9	1	8

3.2 SHIP FUELS

3.2.1 SAMPLE COLLECTION OF SHIP FUELS

Fuel samples from each of the three ships involved in the SERIES cruise were collected in 250 mL Nalgene bottles and double bagged. The Canadian *JP Tully* and Mexican *El Puma* fuel samples were collected during fill-up at Institute of Ocean Sciences, Sidney, B.C. in June and July of 2002 respectively whereas the fuel from the Japanese *Kaiyo Maru* was collected from the ship's tank in August of 2002.

3.2.2 SAMPLE PREPARATION OF SHIP FUELS

Fuels were converted to solid barium sulphate ($BaSO_4$) using a Parr Bomb apparatus in order to analyze fuel samples for sulphate concentration and stable sulphur isotopic composition, (***Figure 3.3***). The Parr bomb method used was developed by Zaback and Pratt (1992). Approximately 0.5 g of fuel was added to the sample combustion capsule of the Parr Bomb and placed in the holder beneath the fuse wire connecting two electrodes. Between 3 to 5 drops of hydrogen peroxide (H_2O_2) were added to 10 mL of deionized water in the bottom of the Parr Bomb. With the oxygen outlet valve open, the lid was then placed on the bottom and sealed tightly by the containment ring. The Parr Bomb was then flushed with oxygen for 3 seconds. Once the outlet valve had been closed, the Parr Bomb was filled with 30 atmospheres of oxygen. The electrode leads from the ignition unit were connected to the Parr Bomb and the Parr Bomb was placed in a cold water bath. Once there were no visible leaks, the ignition unit was detonated. After 15 minutes, the Parr Bomb was removed from the water bath and

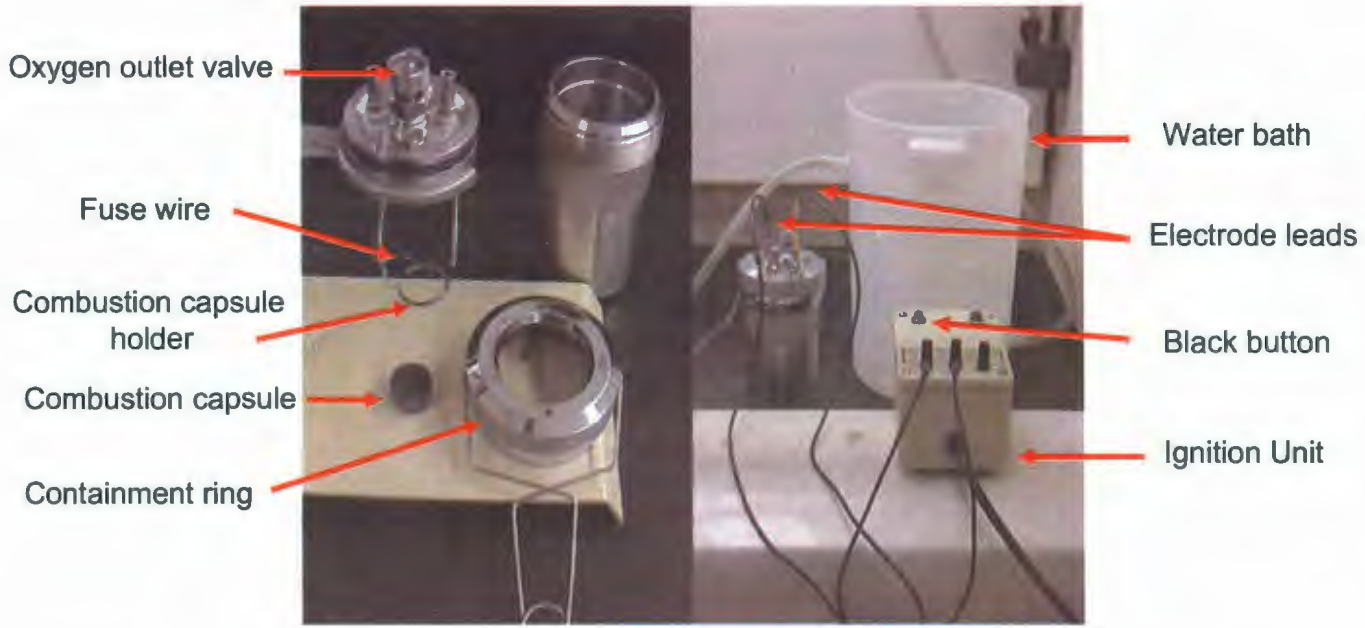

Figure 3.3: A Parr Bomb Apparatus was used to prepare fuel samples for later analysis.

dried off. The pressure inside the bomb was released as the oxygen outlet valve was slowly opened. Once the containment ring was removed, the sulphate solution inside was poured into a 500 mL beaker along with any rinsings from the inner portions of the apparatus (i.e. inside of bomb, electrodes, capsule, underside of lid). The solution was then heated on a hot plate and when it began to boil, the pH was checked. The pH was brought to 4 by adding either hydrochloric acid (HCl) or sodium hydroxide (NaOH) to decrease or increase the pH respectively. Then 10 mL of 0.5 M barium chloride ($BaCl_2$) were added to produce barium sulphate ($BaSO_4$) in solution. The volume was reduced as the solution simmered for 2 to 3 hours. The remaining solution was then vacuum-filtered through a Whatman 47 mm ashless filter and the filter was permitted to dry on a watch glass in an oven set at 80 °C for approximately 30 minutes before igniting it in a Vitrosil crucible with a Bunsen burner. The solid barium sulphate was collected and stored in a clean, labeled 12 mL glass vial until later analysis by the mass spectrometer.

3.2.3 ANALYSIS OF SHIP FUELS

The barium sulphate ($BaSO_4$) produced from the fuel samples were analyzed by EA CF-IRMS at the University of Calgary. The analyzing conditions and standards used for the fuel samples were the same as those used for aerosols and sulphur dioxide.

CHAPTER 4: RESULTS

4.1: SEA SPRAY

4.1.1A: SEA SPRAY INTRODUCTION

Sea spray particles form from bursting bubbles at the ocean–atmosphere interface. Typically bubble bursting is a consequence of wind action such that stronger winds cause more bubble bursting. Sea spray can also be lofted directly into the atmosphere at high wind speeds. Both processes result in sea salt aerosols that are chemically identical to seawater.

Part of the scope of this thesis was to determine the source of marine sulphate aerosols during an iron fertilization experiment, therefore it was important to calculate the amount of:

1) sea spray sulphate (SS SO_4)
2) anthropogenic non sea salt sulphate (Anthro NSS SO_4) and
3) biogenic non sea salt sulphate sources (Bio NSS SO_4).

Sea spray aerosols are composed of compounds found at high abundance in seawater, primarily sodium chloride (NaCl) with trace amounts of magnesium (Mg), sulphates (SO_4), potassium (K), calcium (Ca), carbonates (CO_3), and organics. ***Table 4.1*** shows the molar ratios of common ions in seawater (Lide, 2002; Maidment, 1993). The ratios are preserved during the production of marine aerosols (Keene et al., 1986) and these ratios were used to help determine which ion was more appropriate for calculating SS SO_4 contributions in the sampled aerosols.

Table 4.1: Concentrations and molar ratios for common ions in seawater where the concentration of each ion in seawater is shown in bold. For example, Na/Mg = 470/53.1 = 8.85 mol/L (Lide, 2002; Maidment, 1993)

Ion Y value	X value mol/L (M)	Cl 547	Na 470	Mg 53.1	SO_4 28.1
Cl	**547**	1	1.16	10.3	19.5
Na	**470**	0.859	1	8.85	16.7
Mg	**53.1**	0.0970	0.113	1	1.89
SO_4	**28.1**	0.0514	0.0598	0.530	1

4.1.1B: SEA SPRAY RESULTS

Bulk concentrations of Na, Cl and Mg for each sample are found in ***Appendix 4.1*** and bulk Na, Cl and Mg concentrations with time were plotted in ***Figure 4.1. Figure 4.1*** showed bulk Na, Cl and Mg concentrations had similar trends: bulk Na and Mg outside the patch increased with time (between July 10 to 17 and July 18 to 30, the mean Na concentration outside the patch increased from 1.37 to 2.83 $\mu g/m^3$ and the mean Mg concentration increased from 0.15 to 0.32 $\mu g/m^3$ (t-test $p<0.1$)). Outside the patch, mean Cl concentrations for the same time periods were 2.04 to 2.18 $\mu g/m^3$ and were not significantly different (t-test $p>0.1$). Bulk Na, Cl and Mg concentrations inside the patch peaked twice (July 16 & 17 - Samples 4C and July 22 and 23 - Sample 4H). Concentrations of sea spray ions were undetectable between July 18 and July 24 outside the patch.

Size segregated concentrations of Na, Cl and Mg for each sample are found in ***Appendix 4.2*** and were plotted in ***Figures 4.2a and 4.2b***. The size segregated concentrations had similar trends to the bulk concentrations for both out and in patch. Undetectable to low sea spray concentrations were observed outside the patch from July 18 to July 24. The largest size segregated Na, Cl and Mg concentrations out patch were found in aerosols >3.0 μm (Stage 1 and 2) and it is interesting to note that this was not the same for in patch samples where higher sea spray concentrations were found in aerosols between 1.5 and 7.2 μm (Stage 2 and 3).

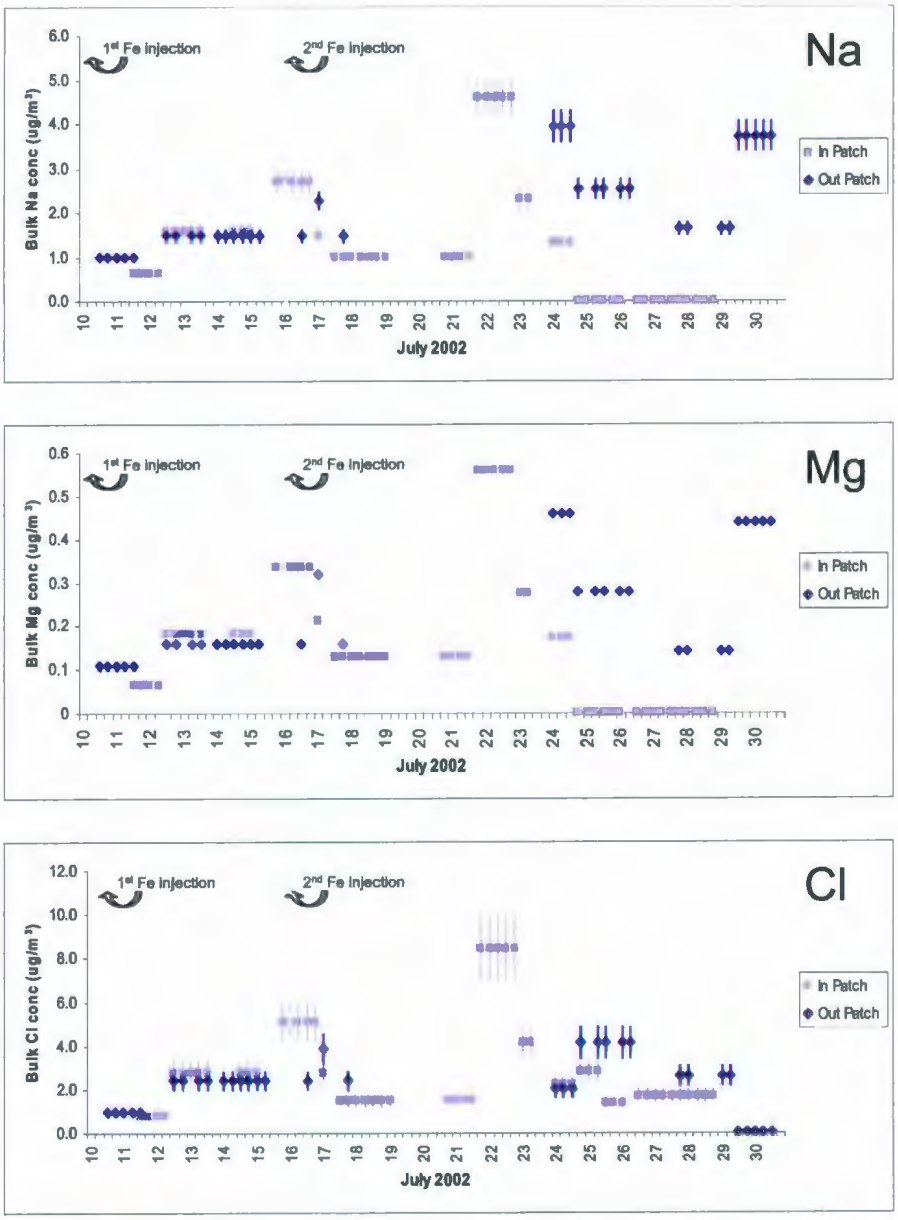

Figure 4.1: Bulk concentrations of Na, Mg and Cl (µg/m³) with time outside and inside the patch.

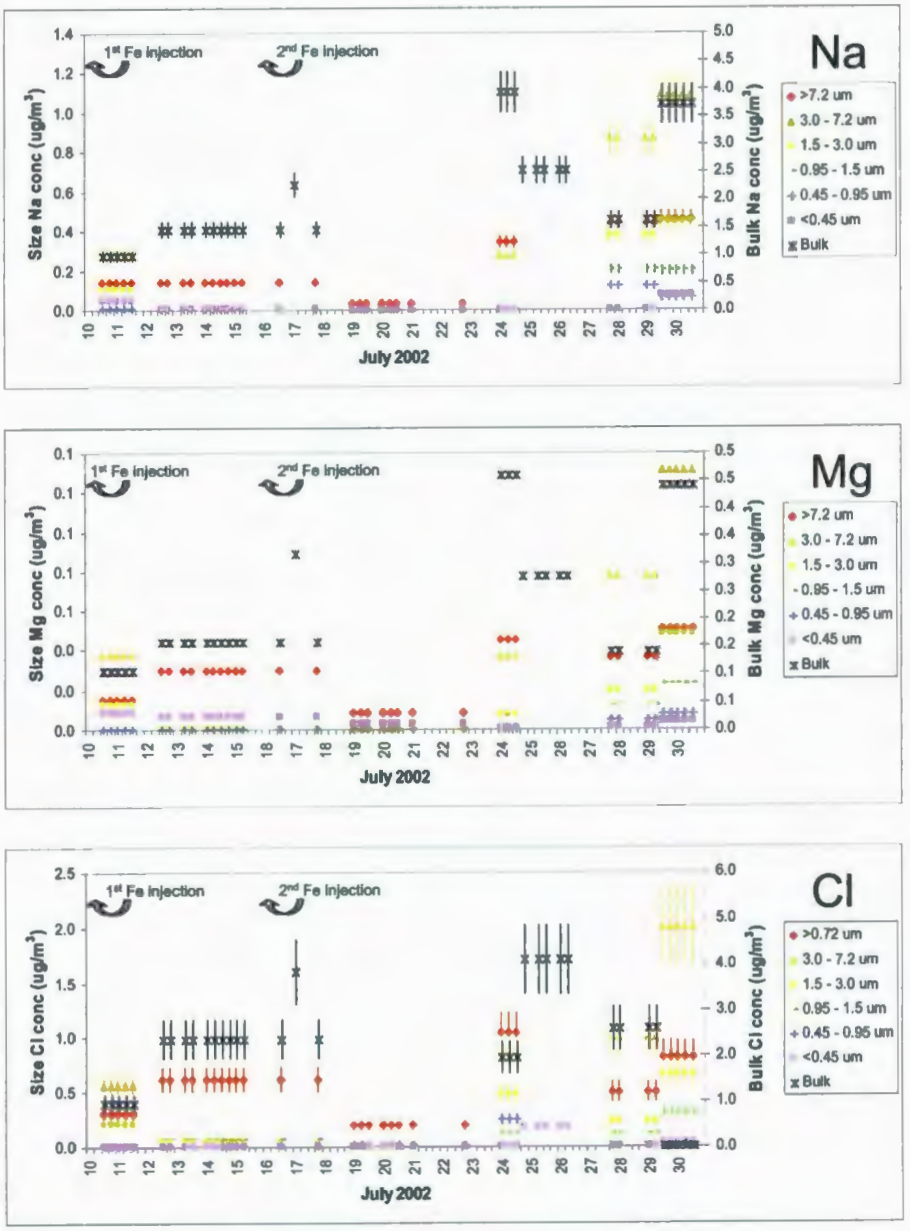

Figure 4.2a: Size segregated concentrations of Na, Mg and Cl (μg/m³) with time outside the patch.

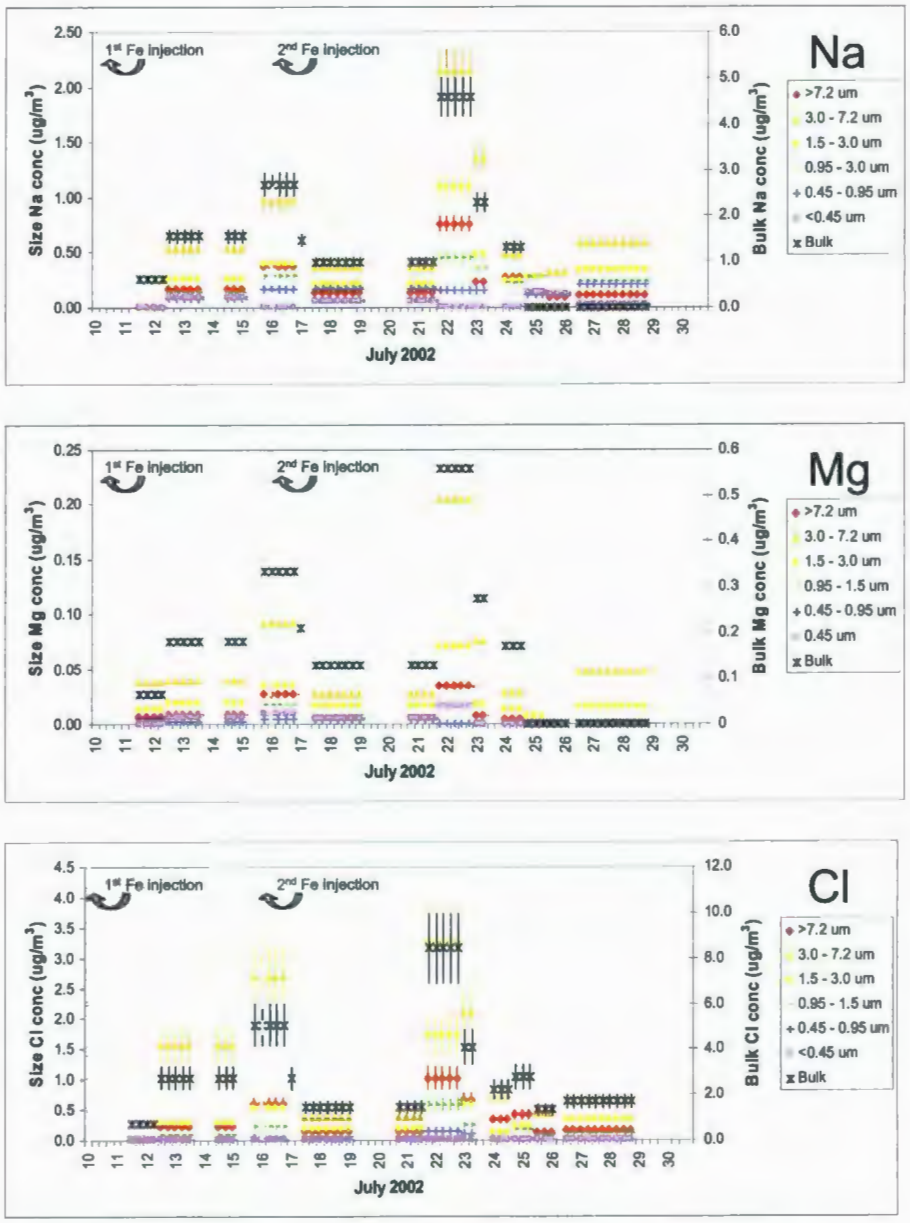

Figure 4.2b: Size segregated concentrations of Na, Mg and Cl (μg/m³) with time inside the patch.

Similar trends were observed when common seawater components such as Mg, Na and Cl as well as wind speed were plotted with time both outside and inside the patch (***Figure 4.3***). Concentrations of Mg, Na and Cl vs wind speed both inside and outside the patch (***Figure 4.4***) showed relationships between wind speed and sea spray components (See ***Table 4.2***): as wind speeds increased, the amount of Mg, Na and Cl concentrations also increased.

In order to determine the most representative ion for sea spray calculations, Cl/Mg, Na/Cl and Mg/Na were plotted in ***Figure 4.5***. The slope of the linear regression lines of the plotted ions were then multiplied by molar masses to get the following molar ratios:

$$Cl/Mg = 4.60$$

$$Na/Cl = 0.575$$

$$Mg/Na = 0.114$$

When compared to the molar ratios of seawater (***Table 4.1***), Cl/Mg was 55% lower, Na/Cl was 34% lower and Mg/Na was 1% higher.

4.1.1C: SEA SPRAY INTERPRETATIONS

The similarity in observed trends for concentrations of Na and Mg, inside and outside the patch, and Cl inside the patch, suggested that these ions were involved in similar production and deposition processes. Concentrations of Na, Cl and Mg were highest

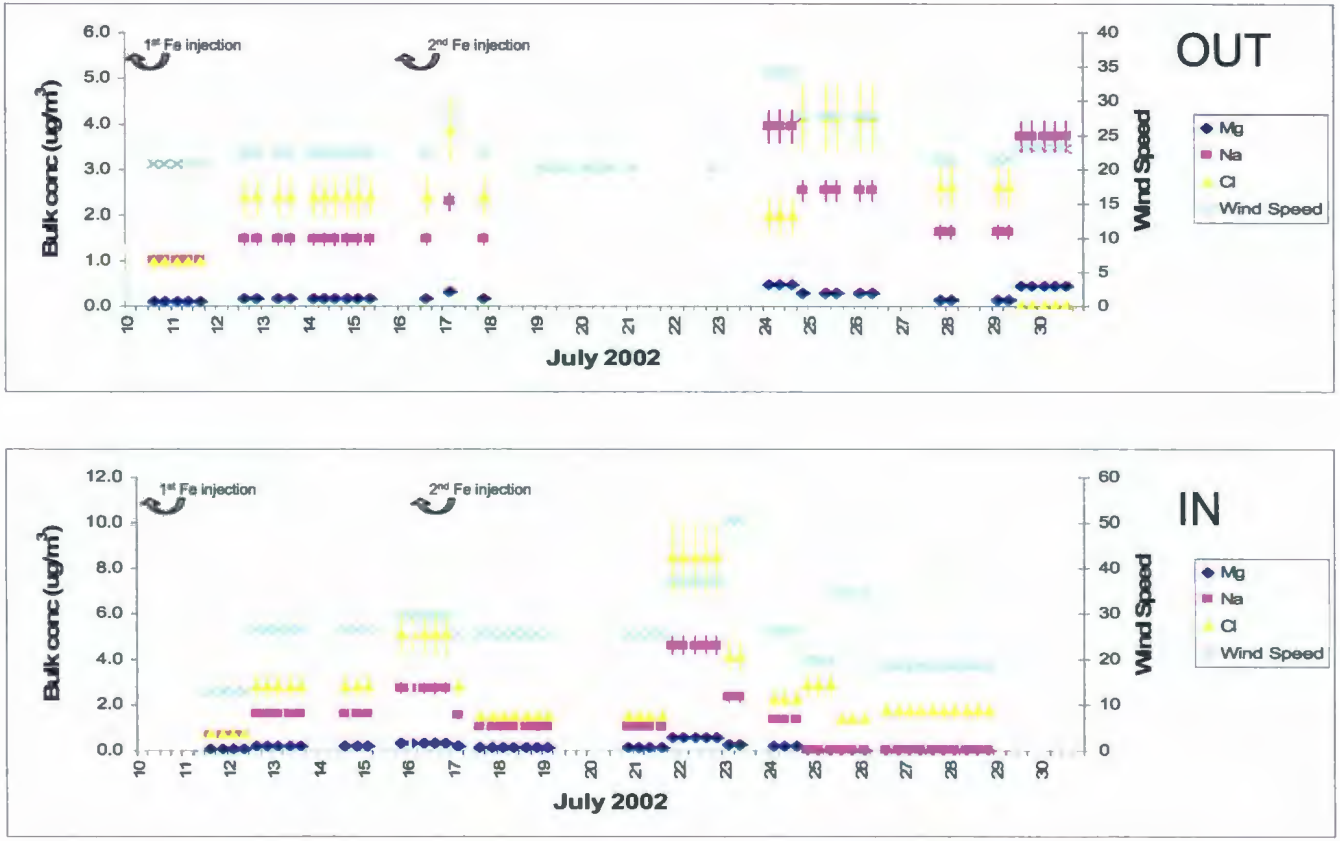

Figure 4.3: Seawater components (Mg, Na and Cl concentrations in $\mu g/m^3$) and wind speed with time outside the patch and inside the patch.

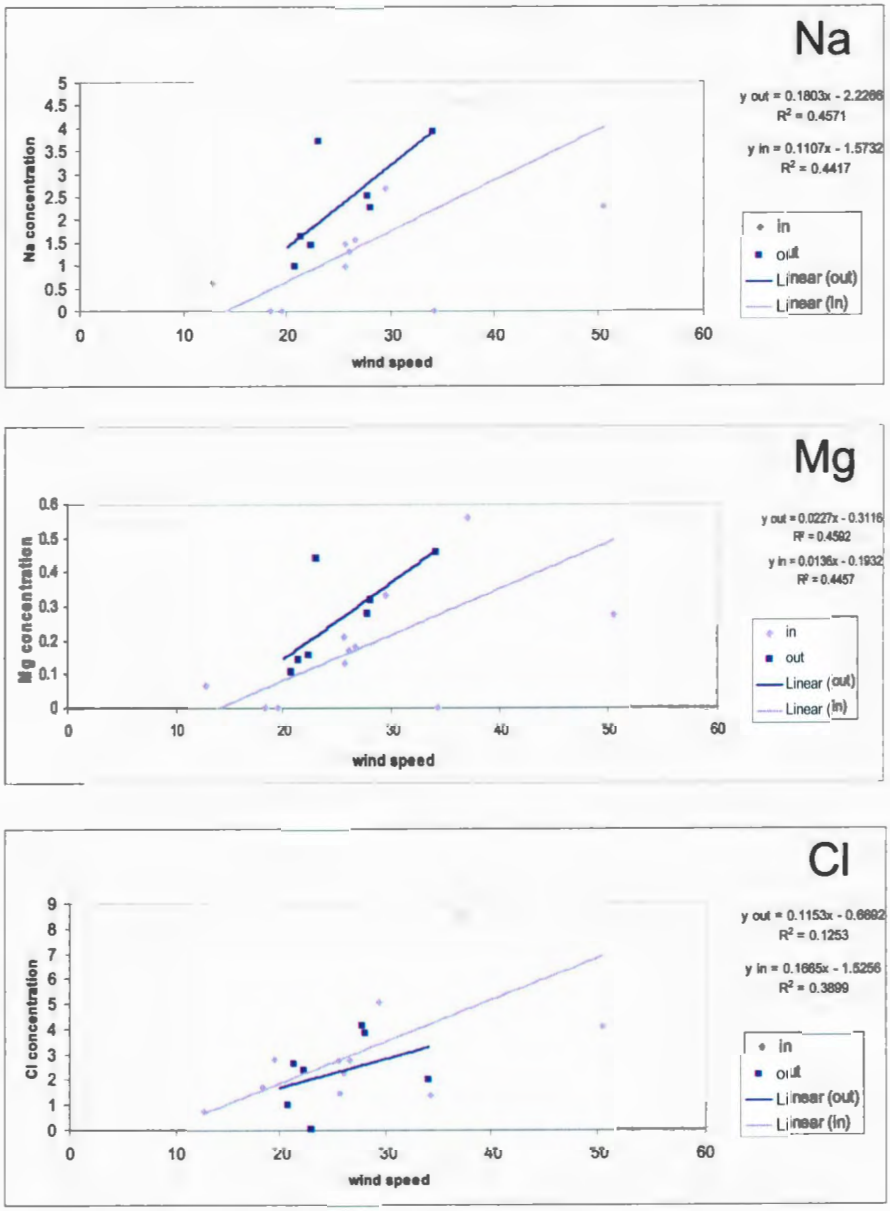

Figure 4.4: Bulk Na, Cl and Mg concentrations (µg/m³) with wind speed (km/hr) outside and inside the patch.

Table 4.2: Wind speed (km/hr) and concentration of Mg, Na and Cl ($\mu g/m^3$) outside and inside the patch. A least squares fit where y = ion concentration, m = slope, x = wind speed, b = y intercept and r is the Pearson Coefficient (r >0.5 is considered a good fit).

Concentration	Equation of line	r
Mg Out Patch	y = 0.227x – 0.3116	0.68
Na Out Patch	y = 0.1803x - 2.2266	0.68
Cl Out Patch	y = 0.1153x - 0.6692	0.35
Mg In Patch	y = 0.0136x - 0.1932	0.67
Na In Patch	y = 0.1107x 1.573	0.67
Cl In Patch	y = 0.1665x – 1.5256	0.62

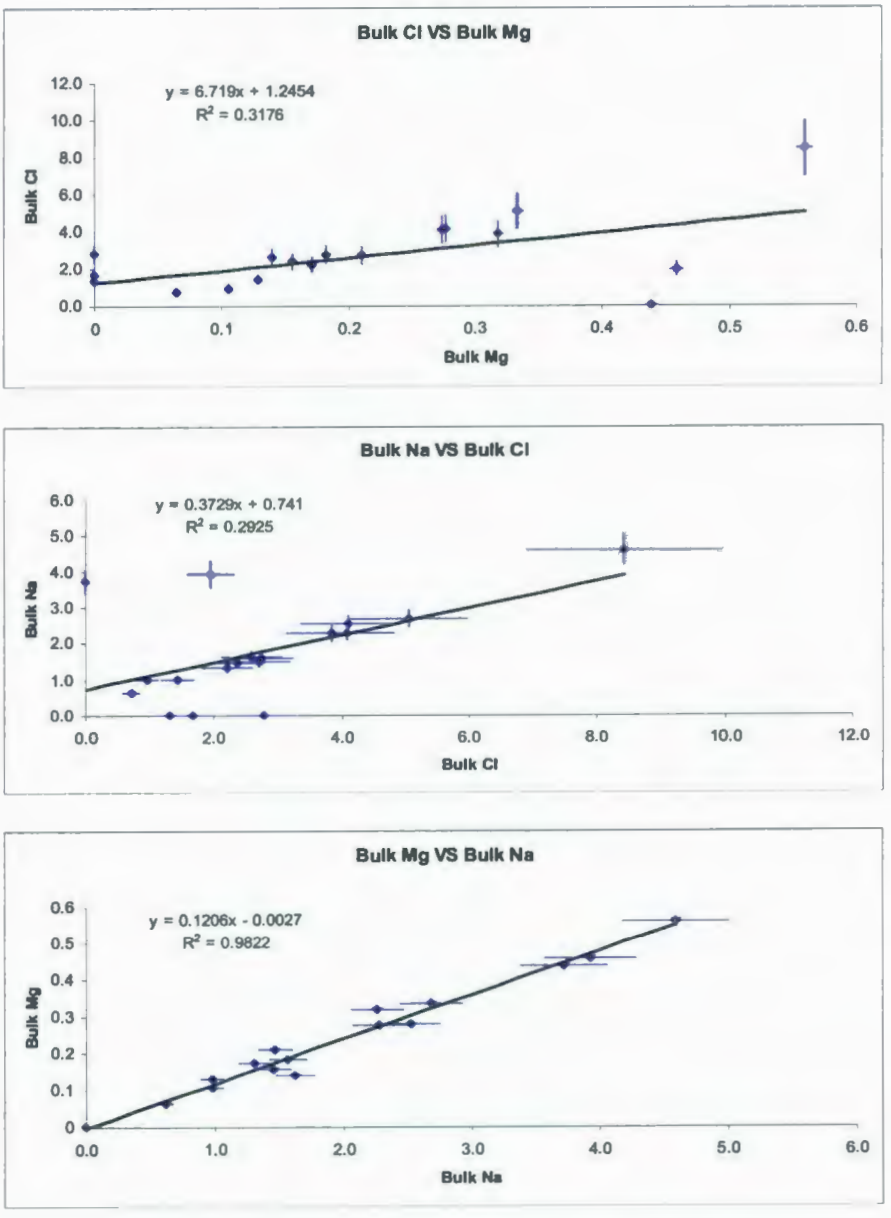

Figure 4.5: Bulk Cl/Mg, Na/Cl and Mg/Na concentrations (in µg/m³).

in aerosols >1.5 μm. The predominance of Na, Cl and Mg in larger aerosols and the similarity of their ratios to that expected in seawater suggested aerosols >1.5 μm were produced by sea spray from the ocean surface (i.e. area source).

The undetectable bulk concentrations and the undetectable to low size segregated concentrations of sea spray components from July 18 to July 24 was explained by washout – aerosols are washed out of the atmosphere by precipitation, causing concentrations to appear low or immeasurable.

Similarities between the wind speed and bulk Na, Cl and Mg concentrations were expected and showed that the wind action directly influenced the production of sea spray aerosols to a large extent. Chloride outside the patch showed the only poor relationship with wind speed ($r = 0.35$) and this may be the result of aged aerosols. Chloride is not a conservative ion; it is volatile and may be depleted as gaseous HCl is produced when exposed to H_2SO_4 or HNO_3 (H_2SO_4 or HNO_3 is present on the surface of aerosols from the oxidation of pollutants such as SO_2 or NO_x) (Singh, 1995). This loss of HCl from the sea salt aerosols encountering polluted air masses advected from Asia as they cross the Pacific may explain why Cl had lower than expected molar ratios. In comparison to Na, Mg had molar ratios that were more similar to molar ratios expected in seawater (Mg/Na was 1% higher than expected in seawater whereas Na/Cl was 34% lower than expected in seawater). Therefore Mg was considered the most appropriate ion for sea salt calculations.

4.2: AEROSOL SO_4

SO_4 aerosols can have a variety of sources in the marine environment: SS SO_4, anthropogenic NSS SO_4 and biogenic NSS SO_4. Each source can contribute different concentrations which may accumulate in particular size fractions. This section will investigate the concentrations and sources of bulk and size segregated SO_4 in aerosols outside and inside the patch.

4.2.1A: AEROSOL SO_4 INTRODUCTION

The total SO_4 concentration includes SS SO_4 plus NSS SO_4. NSS SO_4 is composed of anthropogenic NSS SO_4 plus biogenic NSS SO_4. The total concentration of SO_4 will be used to distinguish sources of the aerosols in combination with stable isotopes of sulphur.

4.2.1B: AEROSOL SO_4 RESULTS

Bulk concentrations of SO_4 for each sample are found in ***Appendix 4.1***. Bulk SO_4 concentrations inside and outside the patch were similar except in the middle of the study when bulk SO_4 had a slight drop in concentration outside the patch and a slight rise in concentration inside the patch as shown in ***Figure 4.6.***

Size segregated concentrations of SO_4 for each sample are found in ***Appendix 4.2*** and are plotted in ***Figures 4.7***. Trends in size segregated SO_4 concentrations show a decrease in SO_4 outside the patch and a rise of SO_4 inside the patch during the middle of the study, much like the bulk SO_4 concentrations. The smallest size fractions (<0.95 μm) had the

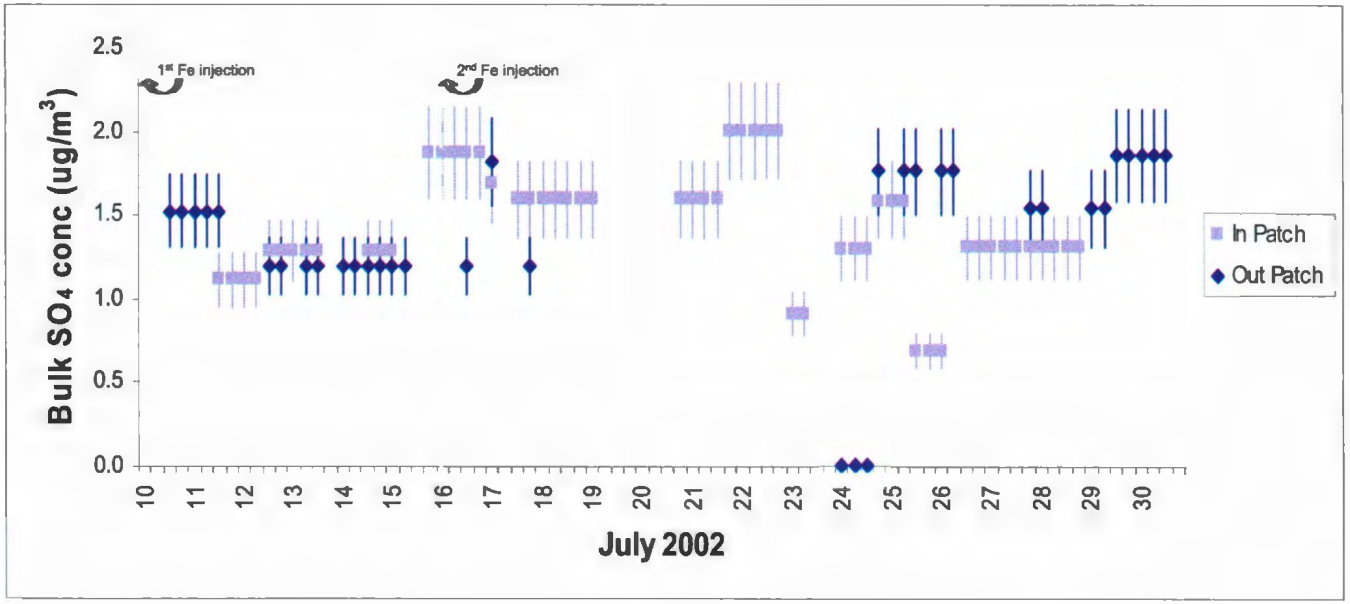

Figure 4.6: Bulk SO_4 concentrations ($\mu g/m^3$) with time outside and inside the patch.

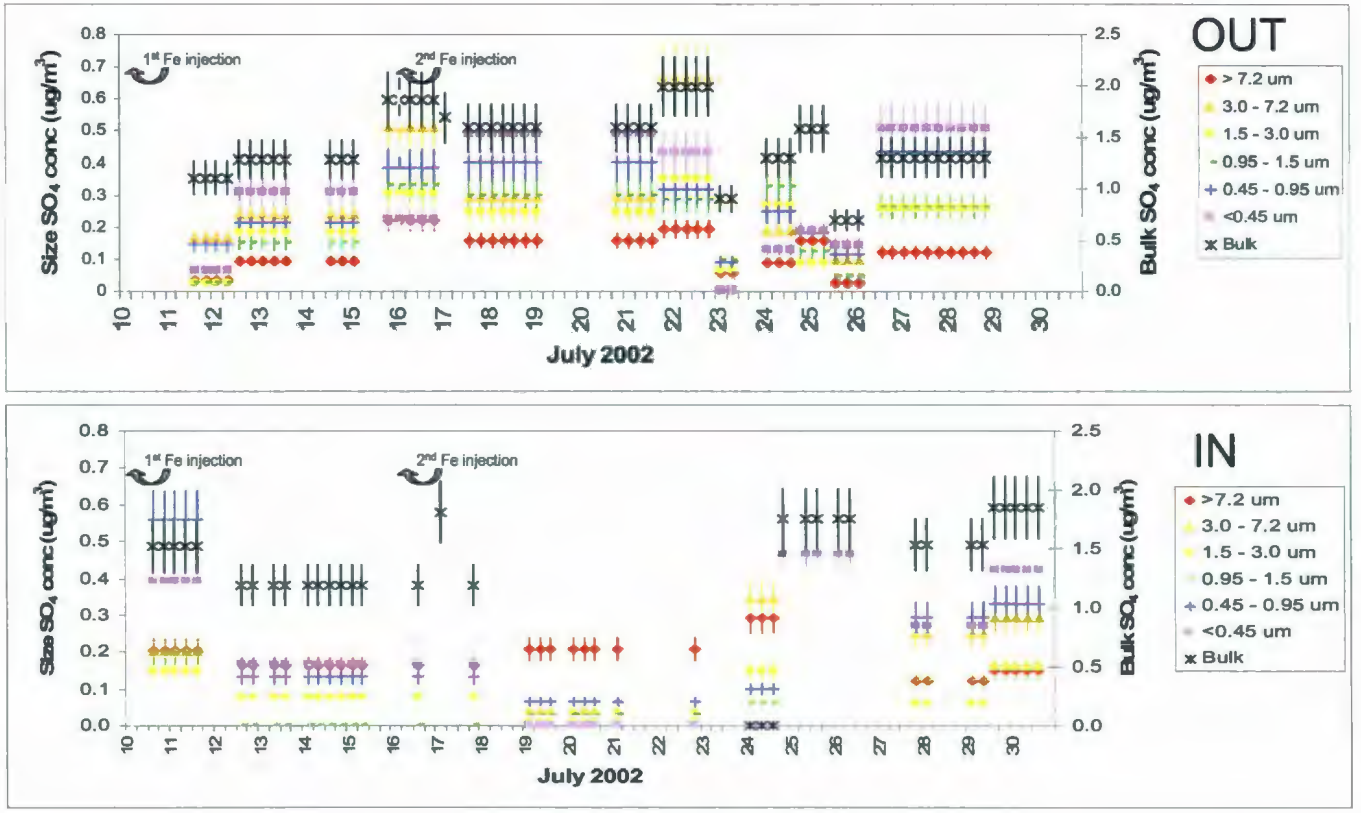

Figure 4.7: Size segregated SO_4 concentrations ($\mu g/m^3$) with time outside and inside the patch.

highest concentrations outside the patch and for the majority of sampling periods inside the patch.

4.2.1C: AEROSOL SO_4 INTERPRETATIONS

The bulk and size segregated concentrations of SO_4 show unique trends outside versus inside the patch. The different trends support the results from Phinney et al., (2009) that suggest SO_4 had different sources contributing outside the patch than inside the patch. Isotopic composition ($\delta^{34}S_{SO4}$) and percent sea salt will be used to determine the sources of the SO_4.

4.2.2A: $\delta^{34}S_{SO4}$ INTRODUCTION

The $\delta^{34}S_{SO4}$ can be an effective method of determining sources of aerosols. For example, SS SO_4 has a uniform $\delta^{34}S_{SS\ SO4}$ in the global oceans of +21 ± 0.2‰ (Rees et al., 1978) while in the Gulf of Alaska anthropogenic SO_4 has a $\delta^{34}S_{Anthro\ NSS\ SO4}$ of +2.0 ± 1.0‰ (based on results from Norman et al., 2004a) and biogenic SO_4 has a $\delta^{34}S_{Bio\ NSS\ SO4}$ of +18.6 ± 0.9‰ (based on results from Patris et al., 2000).

4.2.2B: $\delta^{34}S_{SO4}$ RESULTS

Bulk $\delta^{34}S_{SO4}$ with time (***Figure 4.8***) was constantly near +8‰ for aerosols both outside and inside the patch. One out patch sample had a negative $\delta^{34}S_{SO4}$ (July 24, Sample 1D = -5.6‰). This value was excluded since the SO_4 concentration for this sample was below zero after blank corrections, making the concentration and $\delta^{34}S_{SO4}$ invalid.

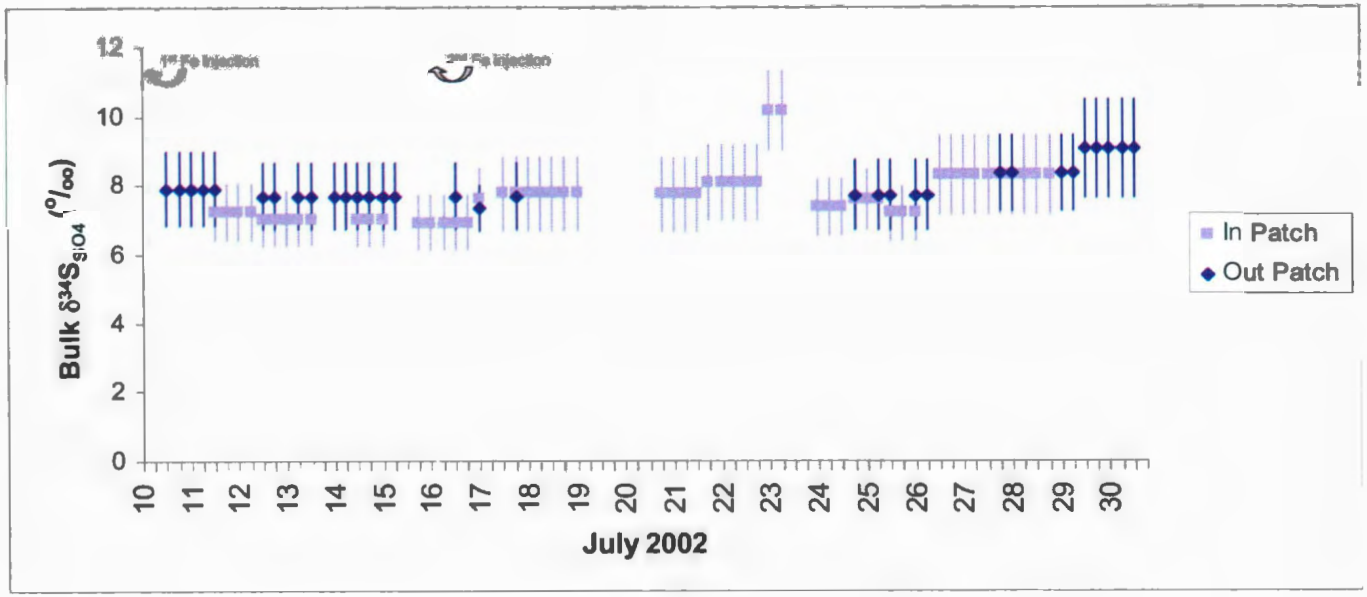

Figure 4.8: Bulk $\delta^{34}S_{SO4}$ (‰) with time outside and inside the patch.

The size segregated $\delta^{34}S_{SO4}$ with time outside the patch (***Figure 4.9***) demonstrated various trends for each size fraction. The $\delta^{34}S_{SO4}$ of aerosols >0.75 μm (Stage 1) increased throughout the study (before and after July 23, t-test $p<0.1$), the $\delta^{34}S_{SO4}$ of aerosols between 3.0 and 7.2 μm (Stage 2) stayed relatively constant throughout the study (before and after July 23, t-test $p>0.1$), the $\delta^{34}S_{SO4}$ of aerosols between 1.5 and 3.0 μm (Stage 3) increased throughout the study (before and after July 23, t-test $p<0.1$), the $\delta^{34}S_{SO4}$ of aerosols between 0.95 and 1.5 μm (Stages 4) decreased in the middle of the study (from July 10 to July 19, July 19 to July 23and July 23 to July 30, t-tests $p<0.1$), the $\delta^{34}S_{SO4}$ of aerosols between 0.45 and 0.95 μm (Stages 5) decreased in the middle of the study (from July 10 to July 19, July 19 to July 23 and July 23 to July 30, t-tests $p<0.1$) and the $\delta^{34}S_{SO4}$ of aerosols <0.45 μm (Stage 6) stayed relatively constant throughout the study (before and after July 23, t-test $p>0.1$).

The size segregated $\delta^{34}S_{SO4}$ with time inside the patch (***Figure 4.9***) showed the $\delta^{34}S_{SO4}$ of all aerosols increased between July 10 and July 17 (t-test, $p<0.1$) and the $\delta^{34}S_{SO4}$ of aerosols less than 0.45 μm (Size 6) stayed constant thereafter (July 17 to July 24 and July 24 to July 30, t-test, $p>0.1$).

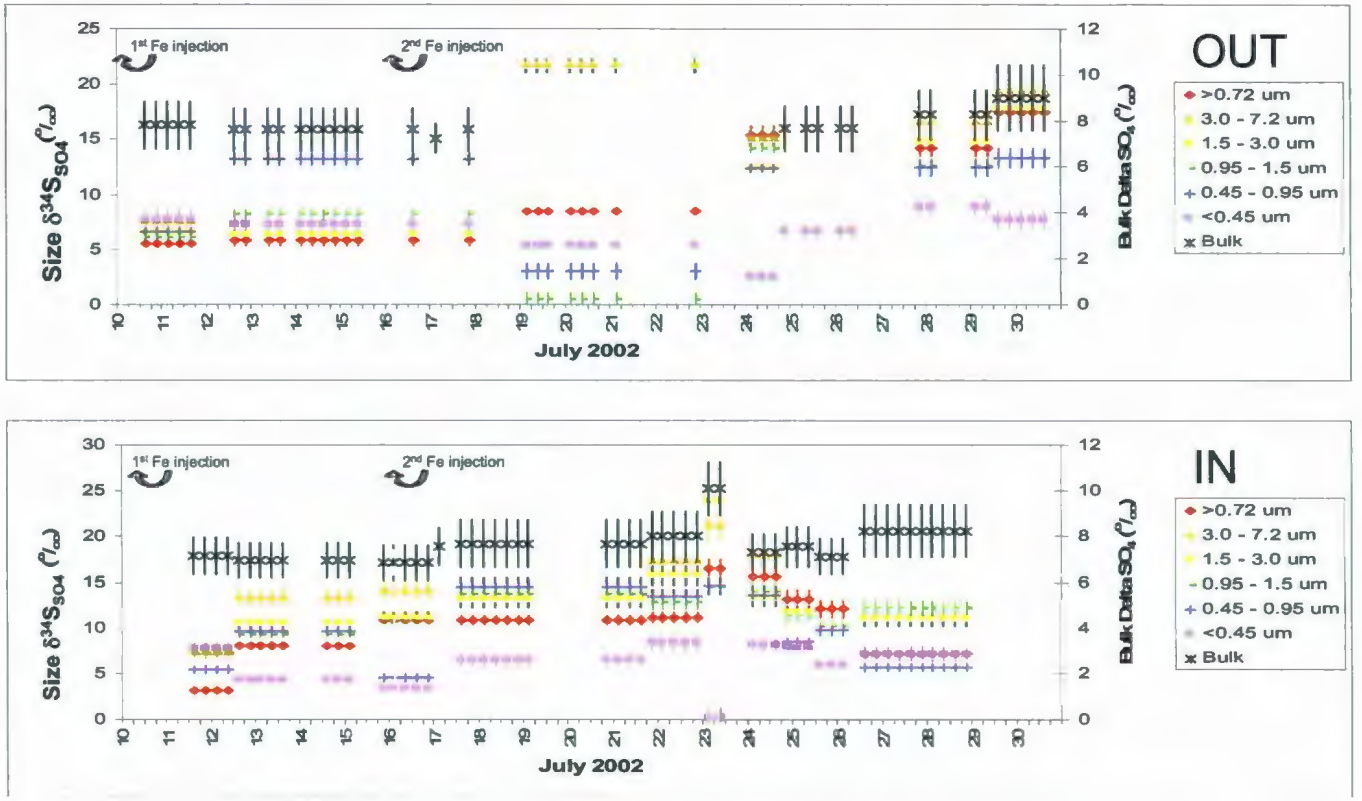

Figure 4.9: Size segregated $\delta^{34}S_{SO4}$ with time outside and inside the patch.

4.2.2C: $\delta^{34}S_{SO4}$ INTERPRETATIONS

Equal bulk $\delta^{34}S_{SO4}$ outside and inside the patch was interpreted as showing that the same sources contributed SO_4 to both areas. A $\delta^{34}S_{SO4}$ of +8‰ likely represented the mixing of anthropogenic and biogenic sources of SO_4 in the study area.

The changing $\delta^{34}S_{SO4}$ trends of size segregated samples showed different sources were contributing to different sizes. An increase in the $\delta^{34}S_{SO4}$ on all aerosol sizes inside the patch after July 17 may show an influence of biogenic sources after that time and that the increase of $\delta^{34}S_{SO4}$ occurred after the second iron fertilization. Outside and inside the patch revealed the same $\delta^{34}S_{SO4}$ for the smallest size fraction (average $\delta^{34}S_{SO4}$ in patch = +6.1, average $\delta^{34}S_{SO4}$ out patch = +6.7, t-test, $p>0.1$). This indicated that the sources contributing and producing new aerosols were likely the same. The smallest size fractions in both areas had a $\delta^{34}S_{SO4}$ much lower than sea spray or biogenic sources and were thus influenced more by anthropogenic sources than other size fractions.

4.2.3A: SOURCE APPORTIONMENT USING SEA SALT AND $\delta^{34}S_{SO4}$

INTRODUCTION

As mentioned above, SO_4 in marine aerosols have three main sources: SS SO_4, anthropogenic NSS SO_4 and biogenic NSS SO_4. Using both the $\delta^{34}S_{SO4}$ and %SS SO_4, a 3-source mixing model can be used to further pinpoint the SO_4 sources (see ***Figure 1.11***). SS SO_4 was 100% SS SO_4 and had a $\delta^{34}S_{SO4}$ of +21 ± 0.2‰ (Rees et al., 1978), biogenic

NSS SO_4 was 0% SS SO_4 and had a $\delta^{34}S_{SO4}$ of +18.6 ± 0.9‰ (based on results from Patris et al., 2000) and anthropogenic SO_4 was 0% SS SO_4 and had a $\delta^{34}S_{SO4}$ of +2.0 ± 1.0‰ (based on results from Norman et al., 2004a).

4.2.3B: SOURCE APPORTIONMENT USING SEA SALT AND $\delta^{34}S_{SO4}$ RESULTS

Appendix 4.1 and ***Appendix 4.2*** show the percent sea salt used in SS SO_4 calculations. As discussed in ***Section 4.1.1C*** (Sea Spray Interpretations), the Mg concentration was determined to be the most appropriate ion for subsequent sea salt calculations. Typically Na concentrations were used if Mg data was unavailable or unreliable and Cl concentrations were used if Mg and Na data was unavailable or unreliable. Samples where seawater ions other than Mg were used for correction are identified in ***Appendix 4.1 and 4.2***. The mass ratios and the concentrations in each sample ($\mu g/m^3$) were used to determine the amount of sea salt for each sample. For example:

Equation 4.1 $\%\ SS\ SO_{4\ (based\ on\ Mg)} = (2.1 \div (SO_{4\ sample} / Mg_{\ sample})) \times 100$

where 2.1 is calculated by converting the SO_4/Mg molar ratio in ***Table 4.1*** to mass ratio using the molar masses.

The $\delta^{34}S_{SO4}$ values of the bulk samples as a function of %SS SO_4 were plotted in the three source mixing model of ***Figure 4.10*** and showed samples contained less than 70% SS SO_4. In addition, most $\delta^{34}S_{SO4}$ plotted approximately halfway between the biogenic

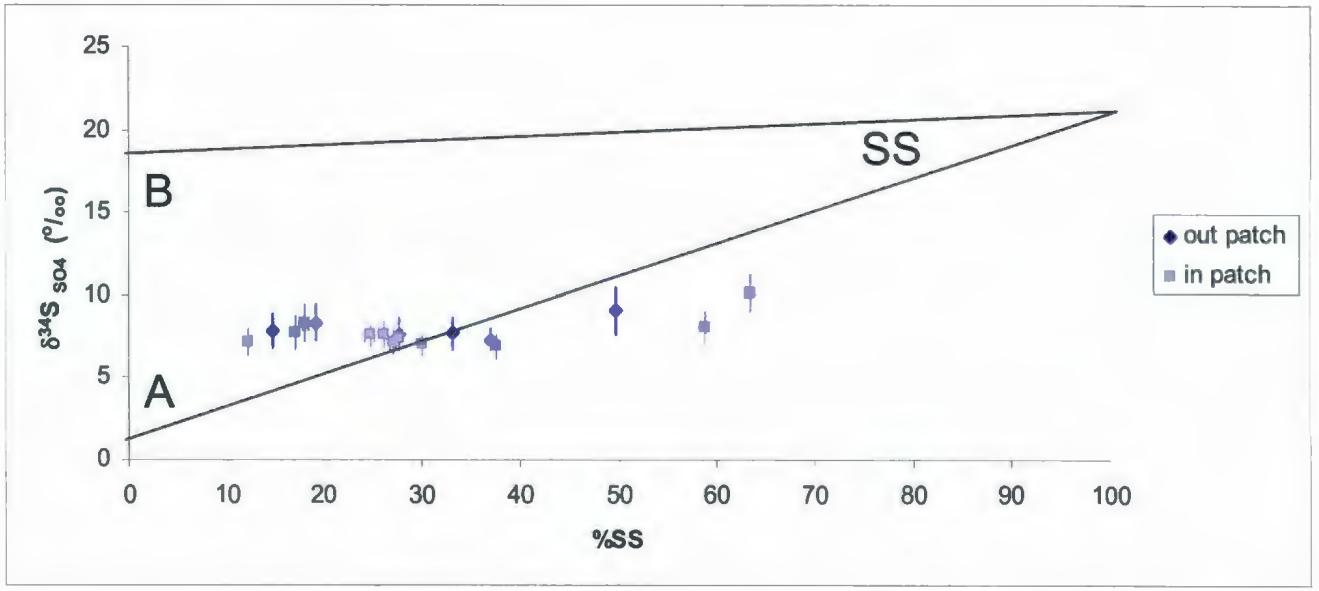

Figure 4.10: **A three source mixing model plotting SERIES bulk $\delta^{34}S_{SO4}$ and %SS outside and inside the patch. A is anthropogenic sulphate (0%SS, +2.0‰), B is biogenic sulphate (0%SS, +18.6‰) and SS is sea spray sulphate (100%SS, +21.0‰). The line between A and B shows mixing of anthropogenic and biogenic sulphate sources, the line between B and SS shows the mixing of biogenic and sea spray sulphate and the line between SS and A shows the mixing of sea spray and anthropogenic sulphate sources.**

and anthropogenic axis (y axis) and surprisingly showed no dependence on %SS SO_4. In patch samples on July 24 & 25 (Sample 4K) and July 25 & 26 (Sample 4L) and July 26, 27 & 28 (Sample 4M) would have plotted along the mixing line for biogenic and anthropogenic sulphate (y axis) but are not shown because they contained an unknown amount of SS SO_4 (Mg and Na data were missing and Cl concentrations were deemed unreliable). As previously discussed in ***Section 4.2.2B***, Sample 1D was excluded. The in patch samples on July 21 & 22 (Sample 4H) and July 23 (Sample 4I) as well as the out patch sample on July 29 & 30 (Sample 1H) contained a high amount of SS SO_4. The concentrations of Na, Cl and Mg on these dates are also high inside and outside the patch.

Size segregated samples showed similar trends as bulk samples when plotted on the three source mixing model (***Figure 4.11***). Most bulk samples contained <70% SS SO_4 while most size segregated samples contained <50% SS SO_4.

The size segregated out patch samples had two main groupings: the majority of the samples had <50% SS SO_4 and moderate $\delta^{34}S_{SO4}$ (average %SS = 19.3%, average $\delta^{34}S_{SO4}$ = +8.1‰) and six samples had >50% SS SO_4 and high $\delta^{34}S_{SO4}$ (average %SS = 73.5%, average $\delta^{34}S_{SO4}$ = +17.1‰). A t-test at the 90% confidence interval showed the average $\delta^{34}S_{SO4}$ were significantly different ($p<0.1$).

The in patch size segregated samples also had two main groupings: the majority of the samples had <50% SS SO_4 and moderate $\delta^{34}S_{SO4}$ (average %SS = 18.8%, average $\delta^{34}S_{SO4}$

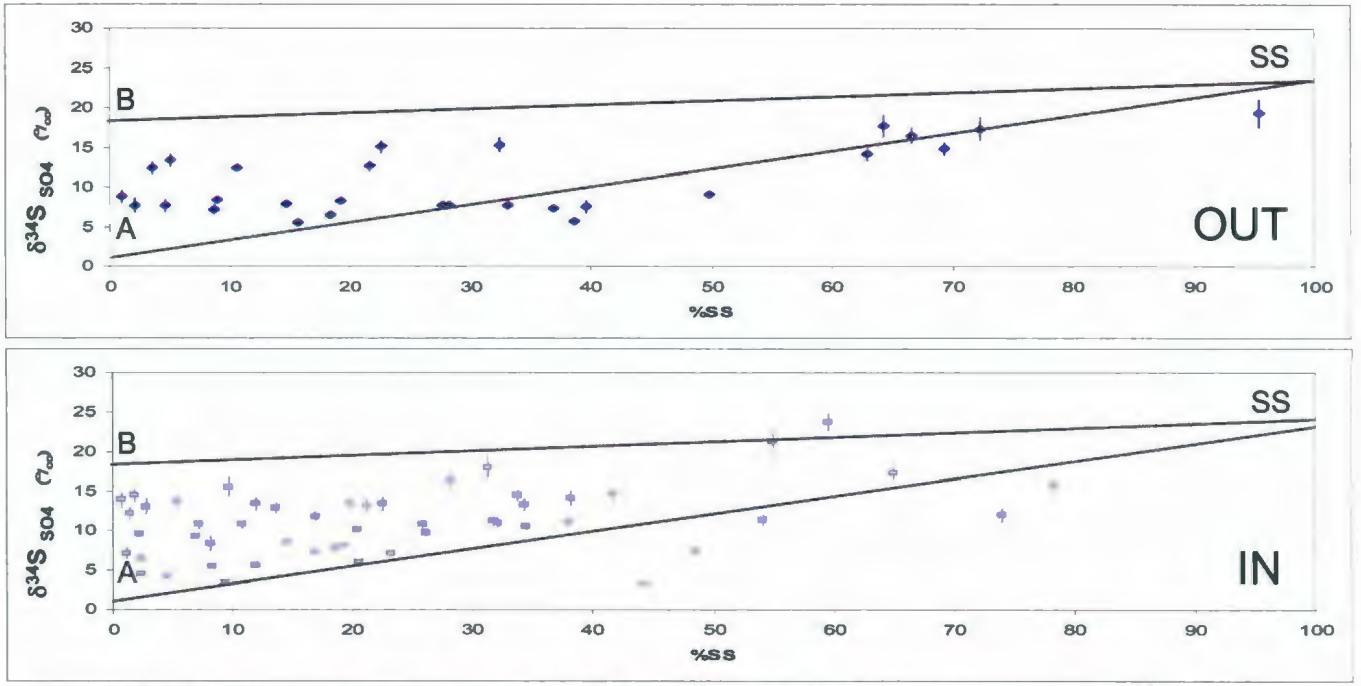

Figure 4.11: **A three source mixing model plotting SERIES size segregated $\delta^{34}S_{SO4}$ and %SS outside and inside the patch. A is anthropogenic sulphate (0%SS, +2.0‰), B is biogenic sulphate (0%SS, +18.6‰) and SS is sea spray sulphate (100%SS, +21.0‰). The line between A and B shows mixing of anthropogenic and biogenic sulphate sources, the line between B and SS shows the mixing of biogenic and sea spray sulphate and the line between SS and A shows the mixing of sea spray and anthropogenic sulphate sources.**

= +10.1‰) and the remaining samples had >50% SS SO_4 and plotted either along the biogenic and sea spray mixing line or below the anthropogenic and sea spray line (average %SS = 64.3%, average $\delta^{34}S_{SO4}$ = +16.8‰). A t-test at the 90% confidence interval showed the average $\delta^{34}S_{SO4}$ were significantly different ($p < 0.1$).

When in patch and out patch samples were compared, the average $\delta^{34}S_{SO4}$ for out patch samples containing <50% SS SO_4 (+8.1‰) was not significantly different than the average $\delta^{34}S_{SO4}$ for in patch samples containing <50% SS SO_4 (+10.1‰) as proven by a t-test at the 90% confidence interval ($p>0.1$). In addition, the average $\delta^{34}S_{SO4}$ for out patch samples containing >50% SS SO_4 (+17.1‰) was not significantly different than the average $\delta^{34}S_{SO4}$ for in patch samples containing >50% SS SO_4 (+16.8‰) as proven by a t-test at the 90% confidence interval ($p>0.1$).

4.2.3C: SOURCE APPORTIONMENT USING SEA SALT AND $\delta^{34}S_{SO4}$ INTERPRETATIONS

The three source mixing model (***Figure 4.10***) showed the bulk samples were influenced mostly by biogenic and anthropogenic sources. In fact, anthropogenic sources may have a slightly stronger influence on the NSS SO_4 fraction, as samples plotted slightly lower than halfway between the biogenic and anthropogenic mixing line (i.e. below +10.3‰).

The size segregated samples outside the patch (***Figure 4.11***) had two main groupings: the group with >50% SS SO_4 and high $\delta^{34}S_{SO4}$ (average %SS = 73.5%, average $\delta^{34}S_{SO4}$ =

+17.1‰) was likely dominated by SS SO_4 and the group with <50% SS SO_4 and moderate $\delta^{34}S_{SO4}$ (average %SS = 19.3%, average $\delta^{34}S_{SO4}$ = +8.1‰) was likely influenced by both biogenic and anthropogenic sources. Like the bulk samples outside the patch, the size segregated samples with <50% SS SO_4 outside the patch plotted approximately halfway between the biogenic and anthropogenic sources. The samples with high SS SO_4 (average %SS = 73.5%) were Sample 2G for aerosols >1.5 μm (out patch, July 27, 28 & 29, Stage 1, 2 and 3) and Sample 2H for aerosols >1.5 μm (out patch, July 29 & 30, Stage 1, 2 and 3). It was interesting to note that the sea salt content was based on Mg and that these six samples contained 57% of the total Mg in all the size segregated samples.

The majority of size segregated samples inside the patch (***Figure 4.11***) had <50% SS SO_4 (average = 18.8%) and moderate $\delta^{34}S_{SO4}$ (average $\delta^{34}S_{SO4}$ = +10.1‰) and plotted on the left side of the three source mixing model, showing that biogenic and anthropogenic sources were the main contributors. The remaining samples had >50% SS SO_4 (average = 64.3%) and therefore were influenced more by SS SO_4. Aerosols between 3.0 and 7.2 μm and 1.5 and 3.0 μm in diameter on July 23 (in patch, Sample 3G, Stage 2 and Stage 3) plotted on the biogenic and sea salt mixing line of the mixing model and thus likely had biogenic NSS SO_4 and SS SO_4 sources. Aerosols between 3.0 and 7.2 μm and 1.5 and 3.0 μm in diameter on July 21 & 22 (in patch, Sample 3F, Stage 2 and Stage 3), between 0.95 and 1.5 μm in diameter on July 24 & 25 (in patch, Sample 3I, Stage 4) and >7.2 μm in diameter on July 25 & 26 (in patch, Sample 3J, Stage 1) plotted below the anthropogenic

and sea salt mixing line of the mixing model and likely had SS SO_4 and anthropogenic NSS SO_4 sources.

The three source mixing model was helpful in distinguishing sources however by removing SS SO_4, the sources of the samples became more evident.

4.2.4A: AEROSOL SS SO_4 INTRODUCTION

The actual concentration of SS SO_4 can be calculated using the %SS SO_4 in a particular sample:

Equation 4.2 $[SS\ SO_4] = (F_{SS\ SO4})\ ([SO_4])$

where

Equation 4.3 $F_{SS\ SO4} = (\%SS\ SO_4) / (100)$

Calculating the amount of SS SO_4 in each sample was the first step in determining the source(s) of SO_4 aerosols.

4.2.4B: AEROSOL SS SO_4 RESULTS

Bulk SS SO_4 concentrations (***Appendix 4.1, Figure 4.12***) had similar patterns to seawater ions (Na, Mg and Cl). Outside the patch, like Mg and Na concentrations, SS SO_4

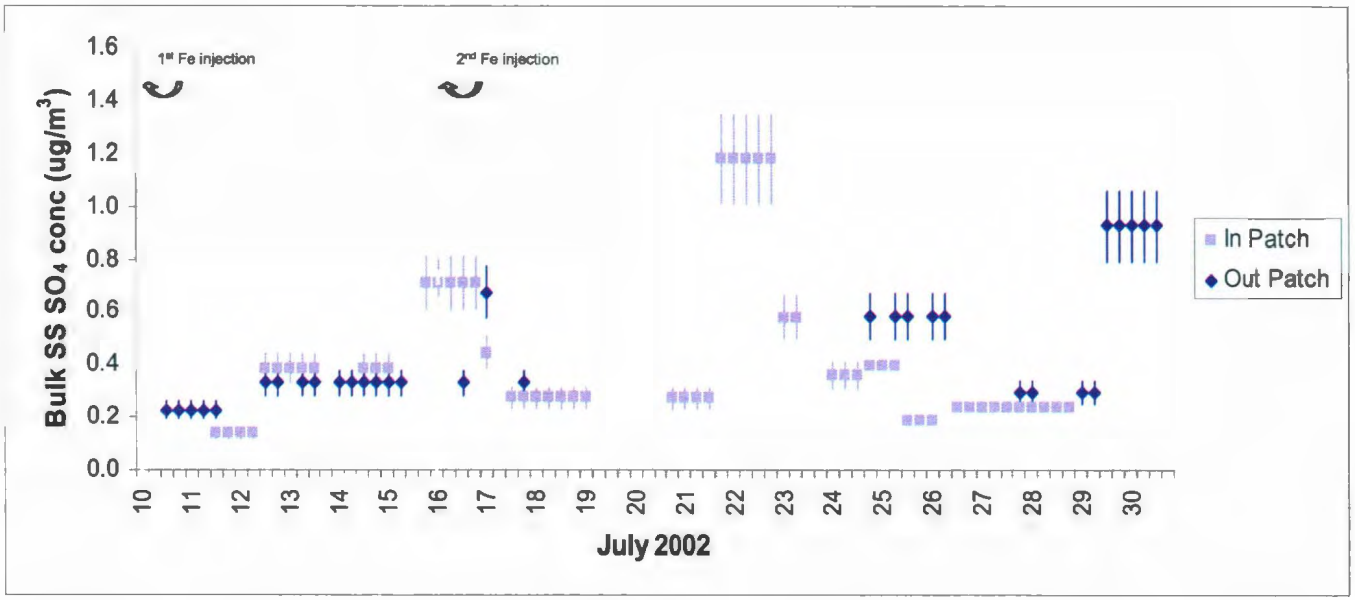

Figure 4.12: Bulk SS SO_4 concentrations with time outside and inside the patch.

concentrations progressively increased in the first three samples and SS SO_4 concentrations on July 28 and 29 were lower than the sample before and after it. Bulk SS SO_4 concentrations inside the patch peaked twice (during Samples 4C, July 15 & 16 and Sample 4H, July 21 and 22).

Size segregated concentrations of SS SO_4 for each sample can be found in ***Appendix 4.2*** and are plotted in ***Figure 4.13***. The size segregated concentrations have similar patterns to the bulk concentrations for both out and in patch. Like Na, Cl and Mg concentrations, the largest size segregated SS SO_4 concentrations out patch were found in aerosols >3.0 μm (Stage 1 and 2 = 78%) and in patch were found in aerosols between 1.5 and 7.2 μm (Stages 2 and 3 = 69%).

The bulk samples contained 31.000 ± 0.003% SS SO_4 outside the patch and 32.00 ± 0.09% SS SO_4 inside the patch. Roughly 5% of the SS SO_4 outside the patch and 13% inside the patch were submicron SS SO_4 (aerosols <0.45 μm, Stage 5 and 6).

4.2.4C: AEROSOL SS SO_4 INTERPRETATIONS

SS SO_4 concentrations had similar patterns to Na, Cl and Mg concentrations which was not surprising considering they were from the same source (sea water) and therefore were interpreted to be involved in the same formation processes (e.g. wind action causing bubble bursting) and depositional processes (e.g. physical deposition near its area source). This may also help explain why SS SO_4 occurred predominately as large

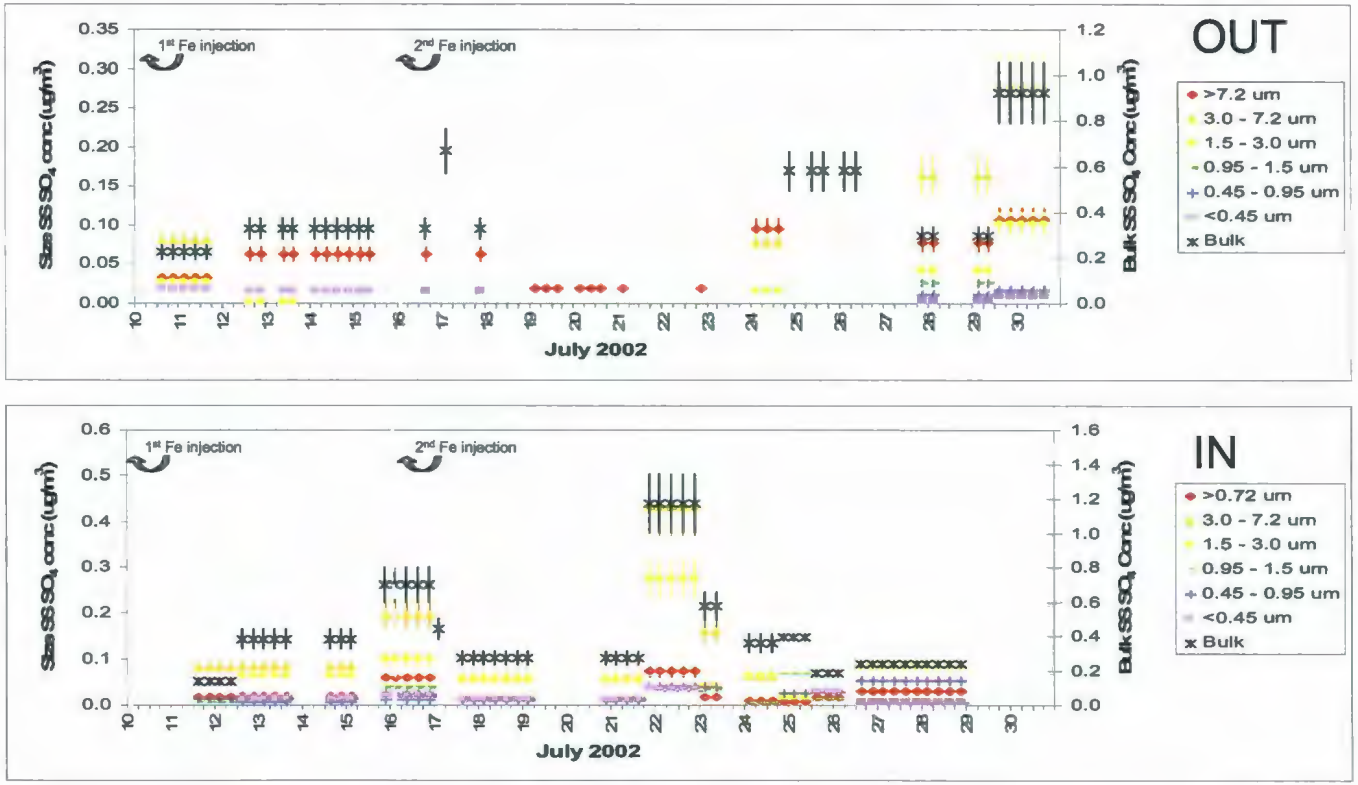

Figure 4.13: Size segregated SS SO_4 concentrations with time outside and inside the patch.

aerosols. The relative amounts of SS SO_4 outside and inside the patch revealed that SS SO_4 contributed approximately 1/3 of the total sulphur in the area.

4.2.5A: AEROSOL NSS SO_4 INTRODUCTION

Calculation of NSS SO_4 is the second step in determining the source(s) of SO_4 aerosols. The NSS SO_4 concentration was calculated similarly to the calculation for SS SO_4 concentration:

Equation 4.4 $[NSS\ SO_4] = (F_{NSS\ SO4})\ ([SO_4])$

where

Equation 4.5 $F_{NSS\ SO4} = 1 - F_{SS\ SO4}$

Equation 4.6 $F_{SS\ SO4} = (\%SS\ SO_4) / (100)$

The $\delta^{34}S_{NSS\ SO4}$ was calculated from

Equation 4.7

$$\delta^{34}S_{NSS\ SO4} = (\ ([SO_4])(\ \delta^{34}S_{SO4}) - ([SS\ SO_4])(\ \delta^{34}S_{SS\ SO4})\ ) / [NSS\ SO_4]$$

where $\delta^{34}S_{SS\ SO4}$ was assumed to be $+21.0 \pm 0.2‰$ (Rees et al., 1978).

The $F_{Anthro\ NSS\ SO4}$ was calculated using

Equation 4.8

$$F_{Anthro\ NSS\ SO4} = (\delta^{34}S_{NSS\ SO4} - \delta^{34}S_{Bio\ NSS\ SO4}) / (\delta^{34}S_{Anthro\ NSS\ SO4} - \delta^{34}S_{Bio\ NSS\ SO4})$$

where it was assumed $\delta^{34}S_{Bio\ NSS\ SO4} = +18.6 \pm 0.9‰$ (based on results from Patris et al., 2000) and $\delta^{34}S_{Anthro\ NSS\ SO4} = +2.0 \pm 1.0‰$ (based on results from Norman et al., 2004a).

The concentration of anthropogenic NSS SO_4 was then calculated from

Equation 4.9 $[Arthro\ NSS\ SO_4] = (F_{Anthro\ NSS\ SO4})\ ([NSS\ SO_4])$

Biogenic NSS SO_4 was calculated using similar equations.

4.2.5B: AEROSOL NSS SO_4 RESULTS

The bulk samples contained 69 ± 0.003% NSS SO_4 outside the patch and 68 ± 0.09% NSS SO_4 inside the patch. Approximately 52% of the sulphur outside the patch and 45% inside the patch was submicron NSS SO_4.

4.2.5C: AEROSOL NSS SO_4 INTERPRETATIONS

Making up approximately 70% of the bulk sulphur, NSS SO_4 was one of the most common forms of sulphur both outside and inside the patch, however, approximately half the NSS SO_4 was found in the submicron aerosols (Stages 5 and 6, <0.95 μm) and suggested the formation of new NSS SO_4 aerosols.

4.2.5.1A: ANTHROPOGENIC NSS SO_4 INTRODUCTION

Anthropogenic NSS SO_4 in the marine environment may include NSS SO_4 from sources such as ship emissions and continental pollution and generally represents "dirty" air. The $\delta^{34}S_{Anthro\ NSS\ SO4}$ is +2.0 ± 1.0‰ (based on results from Norman et al., 2004a).

4.2.5.1B: ANTHROPOGENIC NSS SO_4 RESULTS

The concentration of bulk anthropogenic NSS SO_4 outside the patch remained relatively constant (t-test, $p>0.1$) while the concentration inside the patch had a slight increase in the middle of the study (***Figure 4.14***) (July 10 to 15 = 0.86 μg/m^3, July 16 to 21 = 1.1 μg/m^3 and July 21 to 30 = 0.80 μg/m^3, t-test, $p<0.1$). Bulk anthropogenic NSS SO_4 concentrations are shown in ***Appendix 4.1***. Bulk anthropogenic NSS SO_4 had the same mean time weighted average inside the patch as outside the patch (inside = 0.911 ± 0.20 μg/m^3, outside = 0.962 ± 0.13 μg/m^3; t-test, $p>0.1$).

Size segregated concentrations for anthropogenic NSS SO_4 both outside and inside the patch are listed in ***Appendix 4.2***. The size segregated anthropogenic NSS SO_4 outside the

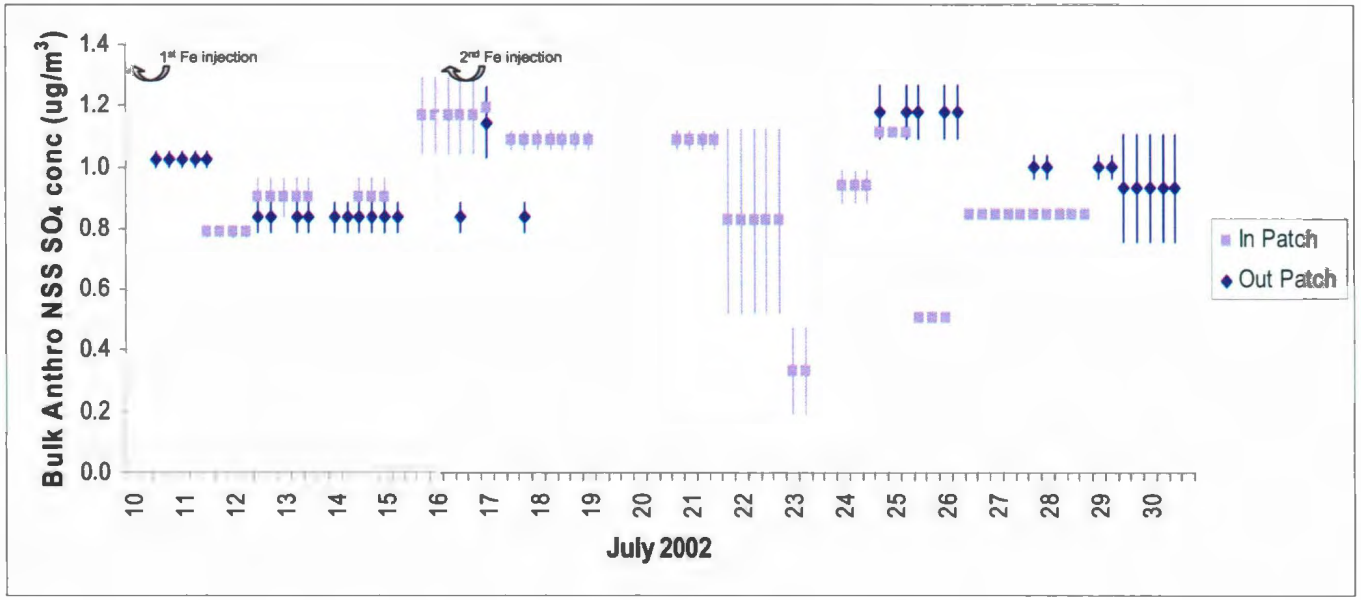

Figure 4.14: Bulk anthropogenic NSS SO_4 concentrations with time outside and inside the patch.

patch (***Figure 4.15***) was dominated by aerosols >7.2 μm (Stage 1) and aerosols <0.45 μm (Stage 6) at the beginning of the study and by aerosols <0.95 μm (Stage 5 and Stage 6) at the end of the study. The anthropogenic NSS SO_4 outside the patch in the larger sizes tended to decrease with time while the anthropogenic NSS SO_4 outside the patch in the smaller sizes tended to stay constant or increase slightly (determined by time weighted averages and t-tests, July 10 to 21 and July 22 to 30). The concentrations of aerosols between 0.45 and 1.5 μm (Stages 4 and 5) outside the patch were immeasurable until the end of the study. The trends for size segregated aerosols outside the patch were considerably different than those inside the patch.

Size segregated anthropogenic NSS SO_4 inside the patch (***Figure 4.15***) was dominated by the smallest size fractions throughout the study. Size segregated anthropogenic samples showed a slight increase in concentration in the middle of the study period (determined by time weighted averages and t-tests, from July 10 to 15, July 16 to 21 and July 22 to 30).

Ninety-two percent of the NSS SO_4 collected in bulk samples both outside and inside the patch was anthropogenic NSS SO_4 and 49% of anthropogenic NSS SO_4 outside the patch and 53% of anthropogenic NSS SO_4 inside the patch were contained within the submicron aerosol fraction.

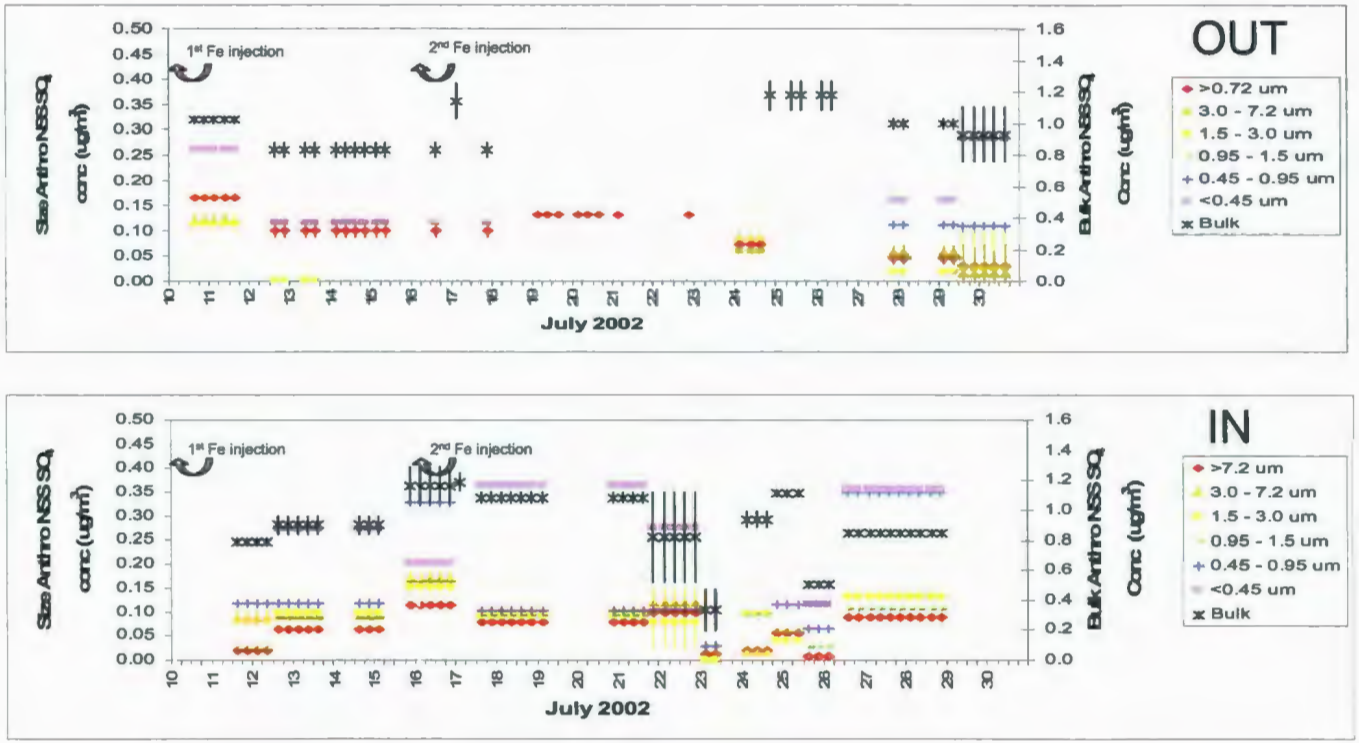

Figure 4.15: Size segregated anthropogenic NSS SO_4 concentrations with time outside and inside the patch.

4.2.5.1C: ANTHROPOGENIC NSS SO_4 INTERPRETATIONS

The relatively constant concentration of anthropogenic NSS SO_4 outside the patch showed that the Station Papa region was constantly being affected by anthropogenic NSS SO_4 sources. The concentration of anthropogenic NSS SO_4 in patch had a slight peak in the middle of the study that revealed additional contributions to anthropogenic NSS SO_4 inside the patch. The presence of ships continuously tracking the patch and constantly emitting ship stack emissions inside the patch was interpreted as the source of the additional anthropogenic SO_4 inside the patch.

Although the bulk anthropogenic NSS SO_4 outside the patch remained relatively constant, the dominant size fractions outside the patch varied. The change in the dominant size of anthropogenic NSS SO_4 outside the patch indicated that different processes were influential. For instance, aerosols >7.2 μm and <0.45 μm (Stage 1 and Stage 6) were most common at the beginning of the study while aerosols <0.95 μm (Stage 5 and Stage 6) were most common at the end of the study. This showed a shift from anthropogenic NSS SO_4 producing new aerosols and forming on pre existing, possibly aged seawater aerosols in the larger size fraction, to anthropogenic NSS SO_4 only forming new aerosols. The decrease in anthropogenic NSS SO_4 concentrations outside the patch in the middle of the study (July 18 to July 24) was explained by the presence of moisture in the air and washout of aerosols during that time.

The size segregated anthropogenic NSS SO_4 samples inside the patch were dominated by the smaller size fractions, indicating that the anthropogenic NSS SO_4 was forming new particles throughout the entire experiment. The increase in concentration of all sizes of NSS SO_4 inside the patch showed the influence of the ship emissions inside the patch as ships tracked the patch.

The percentage of anthropogenic NSS SO_4 collected in bulk samples both outside and inside the patch show that almost all the NSS SO_4 came from polluted air masses. The submicron aerosols showed that both outside and inside the patch approximately half of submicron aerosols were anthropogenic NSS SO_4. Therefore anthropogenic NSS SO_4 aerosols were being produced as new aerosols in both areas.

4.2.5.2A: BIOGENIC NSS SO_4 INTRODUCTION

Biogenic NSS SO_4 in the marine environment may include NSS SO_4 from sources such as oxidation of biogenic SO_2 and generally represents "clean" air. The $\delta^{34}S_{Bio\ NSS\ SO4}$ is approximately $+18.6 \pm 0.9‰$ (Patris et al., 2000).

4.2.5.2B: BIOGENIC NSS SO_4 RESULTS

Bulk biogenic NSS SO_4 ranged from undetectable to 0.28 $\mu g/m^3$ outside the patch and from undetectable to 0.23 $\mu g/m^3$ inside the patch (***Appendix 4.1***). McArdle et al. (1998) found the biogenic NSS SO_4 at Mace Head Ireland was as high as 0.27 $\mu g/m^3$. During SERIES, bulk biogenic NSS SO_4 had a mean time weighted average of 0.17 ± 0.11 $\mu g/m^3$

inside the patch and 0.084 ± 0.11 μg/m^3 outside the patch, therefore biogenic NSS SO_4 concentrations were approximately the same inside and outside the patch. The trend in bulk biogenic NSS SO_4 concentrations inside and outside the patch was undeterminable (***Figure 4.16***). Both outside and inside the patch, less than 10% of the NSS SO_4 collected on bulk samples was biogenic NSS SO_4 (8% biogenic NSS SO_4 in both areas) and corresponded to more anthropogenic influenced bulk $\delta^{34}S_{NSS\ SO4}$.

Appendix 4.2 contains size segregated concentrations outside and inside the patch. Like the bulk NSS SO_4, the size segregated biogenic NSS SO_4 had large error bars making trends difficult to distinguish. The size segregated biogenic NSS SO_4 outside the patch (***Figure 4.17***) was dominated by smaller size fractions at the beginning (<0.45 μm, Stage 6) and at the end (0.45 to 0.95 μm, Stage 5) while in the middle of the study period it appeared to be dominated by the larger size fractions (>3.0 μm, Stage 1 and Stage 2). The mean time weighted average of biogenic NSS SO_4 in submicron aerosols (<0.95 μm, Stage 5 and 6) outside the patch was 0.11 ± 0.06 μg/m^3 and was the same as the time weighted average of submicron aerosols inside the patch (0.10 ± 0.09 μg/m^3, t-test, p>0.1). The biogenic NSS SO_4 concentrations inside the patch (***Figure 4.17***) had an increase in the middle of the study and an increase at the end of the study (determined by time weighted averages and t-tests from July 10 to 17, July 17 to 21, July 21 to 26 and July 26 to 30). For the most part, the biogenic NSS SO_4 inside the patch was dominated by aerosols 0.45 to 0.95 μm and 0.95 to 1.5 μm in diameter (Stage 4 and 5). Outside the

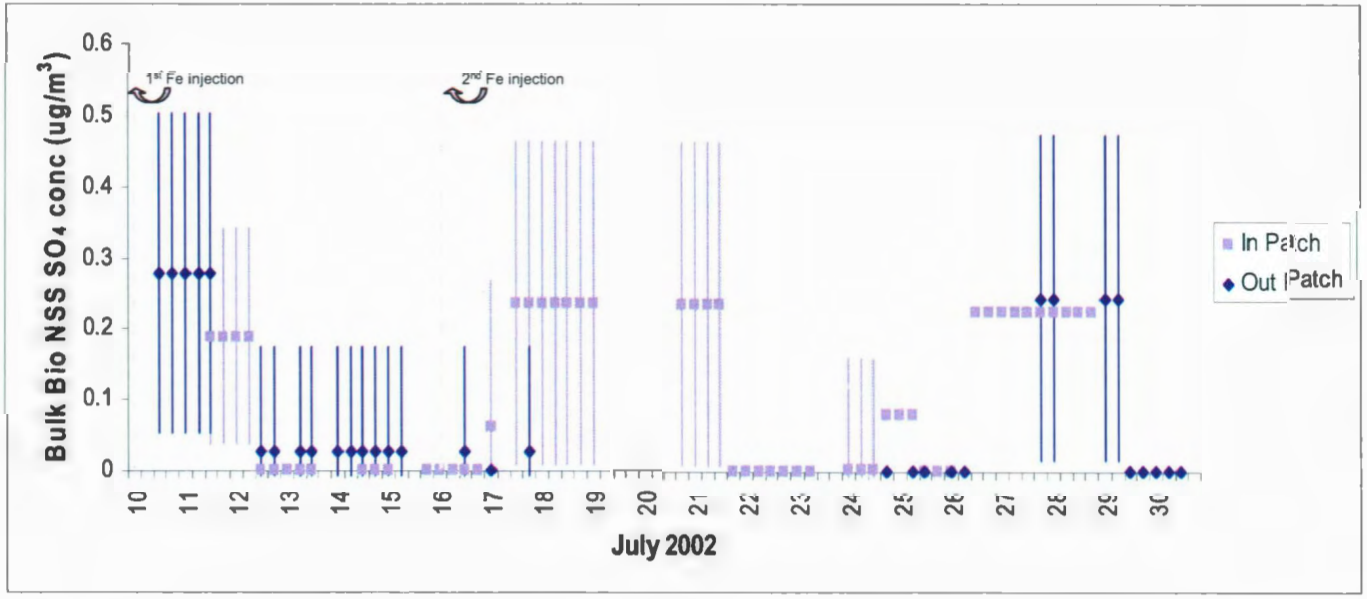

Figure 4.16: Bulk biogenic NSS SO_4 concentrations with time outside and inside the patch.

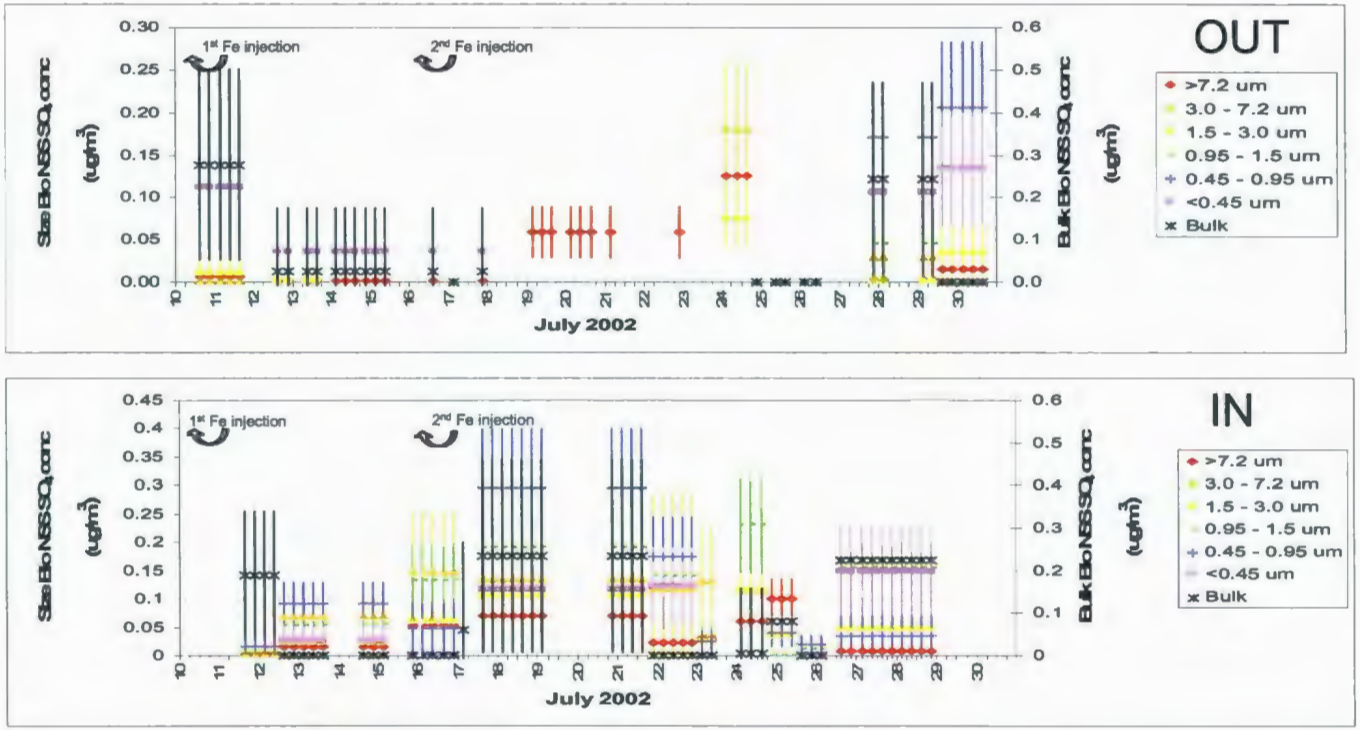

Figure 4.17: Size segregated biogenic NSS SO_4 concentrations with time outside and inside the patch.

patch, 57% of the NSS SO_4 in submicron aerosols was biogenic in origin compared to 32% inside the patch.

The amount of biogenic NSS SO_4 is lower than the amount of anthropogenic NSS SO_4 both inside and outside the patch.

4.2.5.2C: BIOGENIC NSS SO_4 INTERPRETATIONS

The time weighted average concentrations of bulk biogenic NSS SO_4 inside the patch were approximately the same as bulk biogenic NSS SO_4 outside the patch. This result was unexpected since the in patch area was fertilized with iron and a phytoplankton bloom was expected to produce more biogenic NSS SO_4 in the air mass inside or downwind of the patch. The biogenic NSS SO_4 concentrations inside the patch were anticipated to be more pronounced, however the biogenic NSS SO_4 results suggest that the area outside and upwind of the patch was equally productive.

Size segregated out patch biogenic NSS SO_4 showed aerosols <0.95 μm (Stage 5 and 6) were dominant at the beginning and end of the study. It appeared aerosols >3.0 μm (Stages 1 and 2) were dominant for biogenic NSS SO_4 outside the patch between July 18 and July 24 however this corresponded with the same washout event that caused low Na, Mg and Cl concentrations and may explain why other sizes have undetectable concentrations. Inside the patch, the biogenic NSS SO_4 concentrations increased in the middle of the study as well as at the end of the study and were dominated by aerosols

between 0.45 and 1.5 μm (Stages 4 and 5). As mean time weighted average concentrations of submicron biogenic NSS SO_4 aerosols outside the patch were similar to those inside the patch, it indicated that the entire Station Papa area, both inside and outside, was producing new biogenic NSS SO_4 aerosols. Because the out patch area had not been artificially fertilized but was producing biogenic NSS SO_4, the out patch area was being influenced by DMS as well. In fact, approximately 57% of the biogenic NSS SO_4 aerosols outside the patch were submicron and only 32% of the biogenic NSS SO_4 aerosols inside the patch were submicron, evidence that the area outside the patch was indeed producing new biogenic aerosols. Biogenic NSS SO_4 inside the patch was found in slightly larger size fractions than biogenic NSS SO_4 outside the patch and revealed not only did biogenic NSS SO_4 inside the patch form new particles (0.45 to 0.95 μm, Stage 5), it also formed onto or combined with pre existing particles (0.95 to 1.5 μm, Stage 4).

The lower concentration of biogenic NSS SO_4 both inside and outside the patch showed a dominance of anthropogenic sources (92%) over biogenic sources (8%) in both areas.

4.3: MSA

4.3.1A: MSA INTRODUCTION

MSA is biologically produced by phytoplankton in marine environments and is derived from DMS. Because it has no anthropogenic sources, it can be used as an approximation for the biological sulphur contribution to the atmosphere.

4.3.1B: MSA RESULTS

Bulk MSA concentrations outside the patch were up to 1.04 μg/m^3 and inside the patch were up to 0.35 μg/m^3(***Appendix 4.1***), higher than previously recorded in the Pacific (Saltzman et al., 1983 had a maximum of 0.042 μg/m^3; Bates et al., 1992 had a maximum of 0.045 μg/m^3). The time weighted average of bulk MSA outside the patch was 0.14 ± 0.16 μg/m^3, similar to inside the patch which was 0.15 ± 0.07 μg/m^3. As shown in ***Figure 4.18***, the bulk MSA concentration outside the patch had a decrease in concentrations in the middle of the study (i.e. undetectable concentrations) while inside the patch there was an increase in concentrations in the middle of the study (from July 10 to 17 and from July 17 to 26, t-test, $p<0.1$ and from July 17 to 26 and from July 26 to July 30, t-test, $p<0.1$).

The size segregated samples outside the patch (***Figure 4.19, Appendix 4.2***) showed most size fractions decreased at the beginning of the study (exception: aerosols >0.72 μm; determined by time weighted average MSA concentrations and t-tests from July 10 to July 12 and from July 12 to July 18). Between July 18 and July 24 most size segregated MSA concentrations were immeasurable (exception: aerosols >0.72 μm) and continued to be immeasurable between July 24 and July 27 (exceptions: aerosols between 1.5 to 3.0 μm and <0.45 μm). From July 24 to July 30, the MSA concentrations increased and concentrations of all size fractions were again measurable. Outside the patch, aerosols <0.95 μm (stage 5 and 6) had average MSA concentrations that decreased from July 10 to 18 and increased from July 24 to 30 (determined by time weighted averages and t-tests).

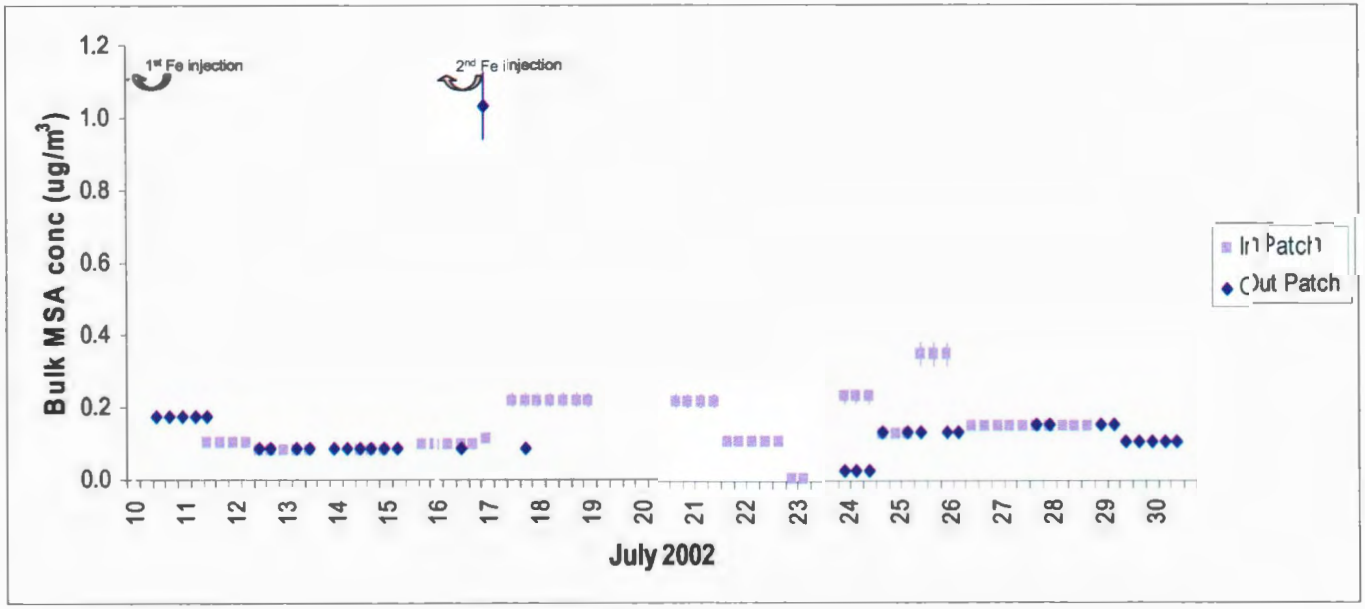

Figure 4.18: Bulk MSA concentrations with time outside and inside the patch.

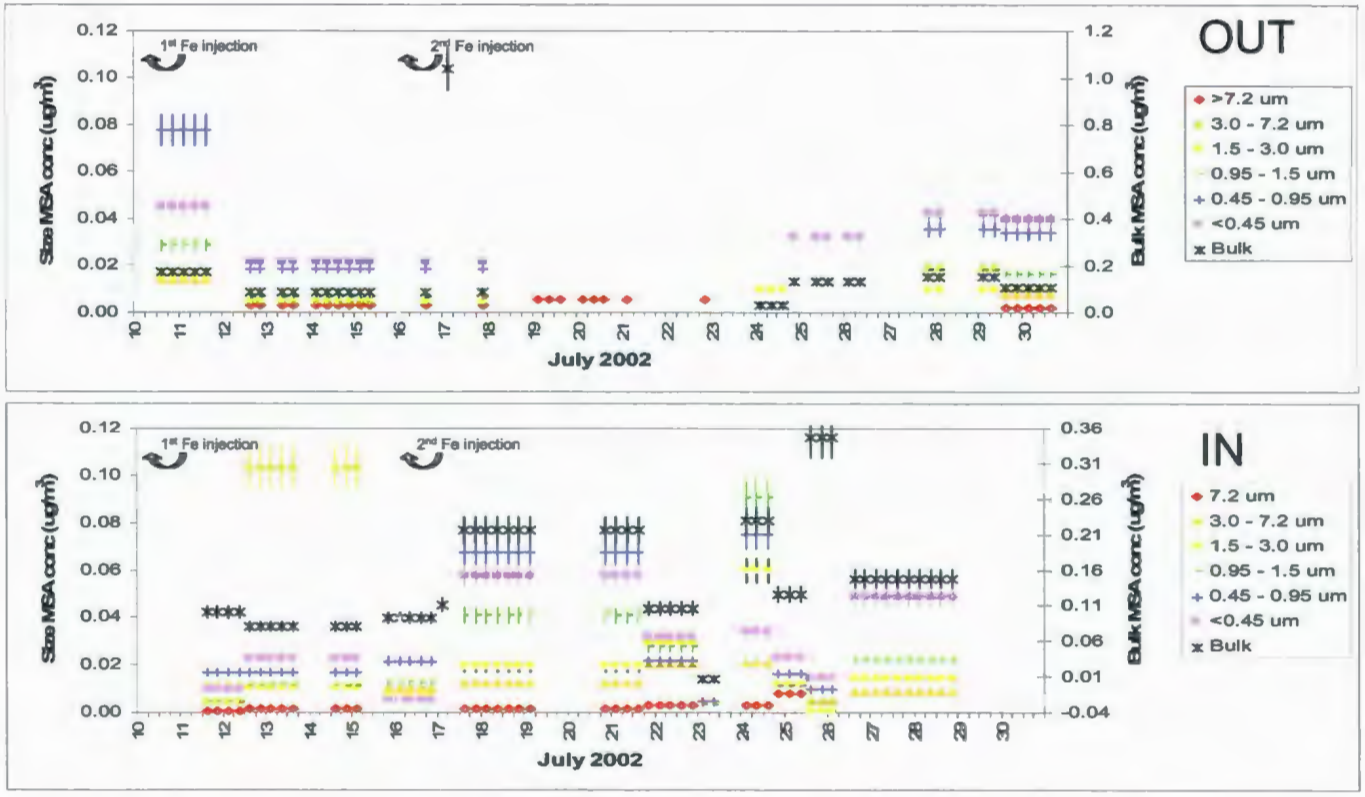

Figure 4.19: Size segregated MSA concentrations with time outside and inside the patch.

All size fractions of MSA aerosols inside the patch increased between July 10 and July 21 and size segregated MSA concentrations thereafter had various trends ***(Figure 4.19)***. Smaller size fractions (≤0.95 μm, Stage 5 and 6) inside the patch increased, decreased and increased throughout the study (determined by time weighted averages and t-tests) Inside the patch, for aerosols less than 1.5 μm, the predominant size of MSA aerosols is smaller than the predominant size of biogenic NSS SO_4 aerosols for corresponding samples. The trend of MSA and biogenic NSS SO_4 concentrations inside the patch were the same. MSA was found to be concentrated in the smaller size fractions with approximately 68% submicron MSA outside the patch and 48% submicron MSA inside the patch.

4.3.1C: MSA INTERPRETATIONS

The concentrations of MSA were approximately 10 times higher than those previously recorded in the Pacific Ocean and indicated that the Pacific Ocean was extremely productive prior to or during the SERIES experiment. As with biogenic NSS SO_4, the time weighted average bulk concentrations of MSA inside the patch (0.15 ± 0.013 μg/m^3) were similar to the concentrations outside the patch (0.14 ± 0.012 μg/m^3) which is expected if inside and outside the patch produced approximately the same proportion and amount of DMS oxidation products.

The size fractions had opposite trends at the beginning of the study: inside the patch the concentrations increased while outside the patch the concentrations decreased and

suggested that there were possibly different processes and/or sources that were affecting the concentration of MSA aerosols in each area. As was determined by bulk biogenic NSS SO_4, size segregated NSS SO_4 and bulk MSA results, another DMS bloom was sampled outside the SERIES fertilized patch, therefore the differences observed were likely due to various sources of newly formed aerosols. Bulk MSA and size segregated MSA concentrations outside the patch between July 18 and July 24 appeared to be affected by a washout event as seen with Mg, Na, Cl, anthropogenic NSS SO_4 and biogenic NSS SO_4 so care must be taken when interpreting MSA concentration trends.

It appeared that MSA was a major contributor of submicron sulphur to both inside and outside the patch.

4.3.2A: MSA TO NSS SO_4 INTRODUCTION

MSA is derived from biogenic sources of sulphur, however, NSS SO_4 can either be anthropogenic or biogenic in nature. The ratio of MSA to NSS SO_4 can help determine the source of NSS SO_4. When a MSA to NSS SO_4 ratio is above 0.5, it suggests that the air mass is not influenced by anthropogenic emissions (i.e. MSA dominates) (Bates et al., 1990; Berresheim et al., 1990). In contrast, a MSA to NSS SO_4 ratio below 0.5 suggests the air mass is influenced by anthropogenic emissions (i.e. NSS SO_4 dominates) (Savoie et al., 1989; Galloway, 1990). Therefore the ratio may be indicative of the preferred pathway for DMS oxidation such that higher ratios suggest the addition pathway and lower ratios suggest the abstraction pathway.

4.3.2B: MSA TO NSS SO_4 RESULTS

The MSA to NSS SO_4 ratios were calculated for the size segregated samples and are shown in ***Appendix 4.2*** (the MSA to NSS SO_4 ratio could be calculated for 59 samples). Only three samples had a MSA to NSS SO_4 ratio above 0.5 (Samples 1H, aerosols between 3.0 and 7.2 μm, Stage 2 = 0.5349, collected July 29 & 30 outside the patch; Sample 4B, aerosols between 3.0 and 7.2 μm, Stage 2 = 0.6638, collected July 12, 13, 14 & 15 inside the patch and Sample 1G, aerosols between 1.5 and 3.0 μm, Stage 3 = 0.1594, collected July 27, 28 & 29 outside the patch).

4.3.2C: MSA TO NSS SO_4 INTERPRETATIONS

MSA to NSS SO_4 ratios were generally below 0.5 so the MSA to NSS SO_4 ratio calculations revealed that the majority of the NSS SO_4 sampled was anthropogenic in nature and agreed with the NSS SO_4 results (92% anthropogenic and 8% biogenic NSS SO_4). The three samples with a MSA to NSS SO_4 ratio above 0.5 were likely biogenic in nature and oxidized via the addition pathway. In this study, isotopic compositions ($\delta^{34}S_{NSS\ SO4}$) were also used to differentiate between anthropogenic and biogenic NSS SO_4 sources. Results from both the MSA to NSS SO_4 ratios and the $\delta^{34}S_{NSS\ SO4}$ point toward anthropogenic influenced NSS SO_4.

4.4: SO_2

4.4.1A: SO_2 INTRODUCTION

Nguyen et al. (1983) reported oceanic background SO_2 concentrations as 100 ng/m^3 and SO_2 concentrations in highly productive areas as 0.3 μg/m^3.

4.4.1B: SO_2 RESULTS

The SERIES SO_2 concentrations (***Appendix 4.1***) were larger than those observed for highly productive areas and were tenfold the background SO_2 concentrations over the ocean: SO_2 concentrations outside the patch were between 0.049 and 1.01 μg/m^3 and inside the patch were between 0.012 and 0.68 μg/m^3. Time weighted average SO_2 concentrations was 0.56 ± 0.38 μg/m^3 outside the patch and 0.37 + 0.21 μg/m^3 inside the patch and both areas showed an increase then decrease with time (***Figure 4.20***).

4.4.1C: SO_2 INTERPRETATIONS

The maximum SO_2 concentrations in each area were well above those recorded previously and pointed toward either high production occurring both in patch and out patch or considerable influence from ship stack emissions. Similar trends in SO_2 concentrations with time indicated that similar sources or similar processes were influencing both in and out patch areas. The trend of the SO_2 concentrations shows that for the first half of the study a source or process was contributing SO_2 to the entire area and for the second half of the study either the production of SO_2 from this source decreased or the loss of SO_2 increased. Similar SO_2 concentrations in both areas was not

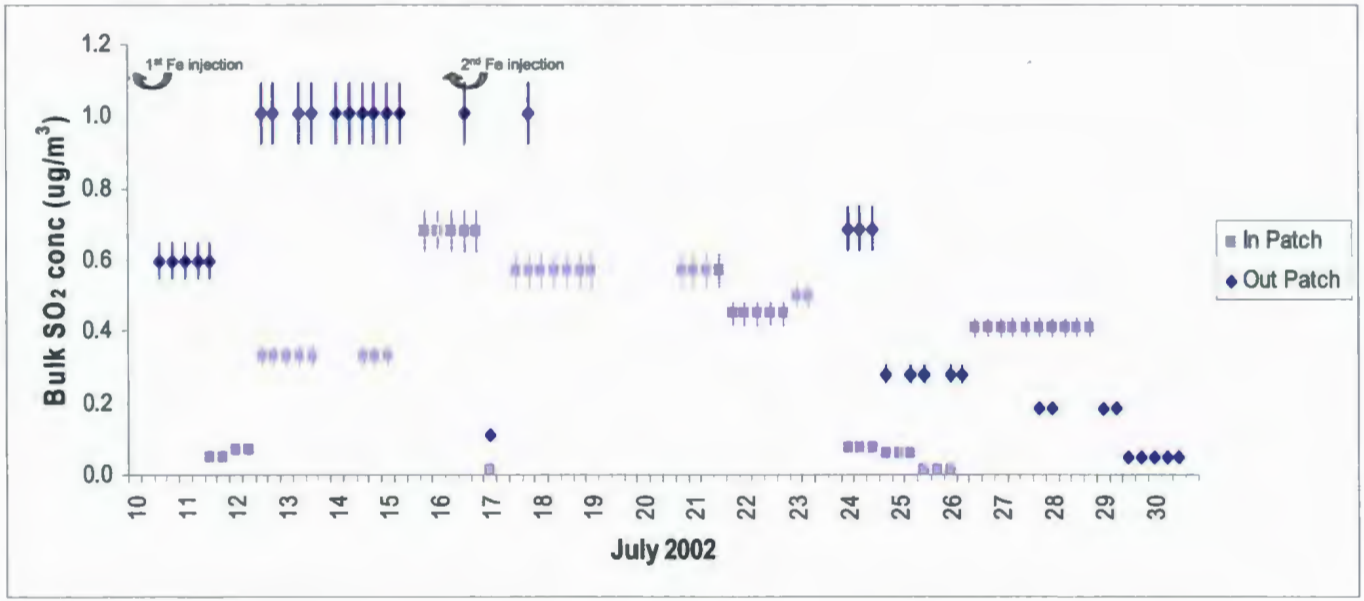

Figure 4.20: Bulk SO_2 concentrations with time outside and inside the patch.

predicted: it was thought that concentrations inside the patch would be higher than outside the patch due to increased SO_2 sources in the vicinity of the patch (local anthropogenic SO_2 sources included patch mapping with ships releasing emissions containing anthropogenic SO_2 and local biogenic sources included the patch releasing DMS that could be oxidized into biogenic SO_2). As discussed in the next section, isotopic compositions ($\delta^{34}S_{SO2}$) can be used to determine sources of SO_2: if the $\delta^{34}S_{SO2}$ shows both areas have SO_2 of a biogenic origin, then another DMS bloom was the main source of SO_2 in the area; if the $\delta^{34}S_{SO2}$ shows both areas have SO_2 of an anthropogenic origin, then emissions from shipping lanes was the main source of SO_2 in the area; if the $\delta^{34}S_{SO2}$ shows one area has SO_2 of a anthropogenic source and one area has SO_2 of a biogenic source, then different sources were affecting SO_2 in each area.

4.4.2A: $\delta^{34}S_{SO2}$ INTRODUCTION

Isotopic compositions ($\delta^{34}S_{SO2}$) can be used to distinguish between SO_2 produced from biogenic or anthropogenic sources since the $\delta^{34}S_{SO2}$ is different: biogenic sources have a $\delta^{34}S_{SO2}$ of approximately $+18.6 \pm 0.9$‰ (based on results from Patris et al., 2000) and anthropogenic sources have a $\delta^{34}S_{SO2}$ of approximately $+2.0 \pm 1.0$‰ (based on results from Norman et al., 2004a). As shown in Norman et al. (2004a), it is reasonable to assume there is no isotope fractionation when SO_2 is produced from DMS or oxidized NSS SO_4.

4.4.2B: $\delta^{34}S_{SO2}$ RESULTS

The $\delta^{34}S_{SO2}$ ranged from +8.9‰ to +14‰ outside the patch and from +1.7‰ to +27‰ inside the patch (***Appendix 4.1, Figure 4.21***) and the $\delta^{34}S_{SO2}$ had a much wider range inside the patch than outside the patch. The $\delta^{34}S_{SO2}$ for samples collected out of the patch had a higher time weighted average than those collected in the patch (out patch = +12 ± ‰, in patch = +7 ± ‰, t-test at 90% confidence interval showed average inside and average outside were different, $p<0.1$). The $\delta^{34}S_{SO2}$ decreased slightly with time as shown in ***Figure 4.21***.

4.4.2C: $\delta^{34}S_{SO2}$ INTERPRETATIONS

The range in $\delta^{34}S_{SO2}$ both outside and inside the patch suggests both areas contained mixtures of biogenic SO_2 sources and anthropogenic SO_2 sources. The higher time weighted average $\delta^{34}S_{SO2}$ outside the patch showed anthropogenic SO_2 sources had a stronger influence inside the patch than outside the patch. This could be explained by ship emissions as research vessels tracked the location of the patch. The decrease in $\delta^{34}S_{SO2}$ inside the patch from approximately +10‰ to +5‰ showed that prior to the study and the presence of research vessels, the area had a $\delta^{34}S_{SO2}$ near +10‰. Thus emissions from research vessels likely reduced the $\delta^{34}S_{SO2}$ by approximately 5‰ in that area.

In addition, the decrease in $\delta^{34}S_{SO2}$ outside the patch from +15‰ to +10‰ suggested that a DMS bloom contributed biogenic SO_2 to the out patch area, out and upwind of the

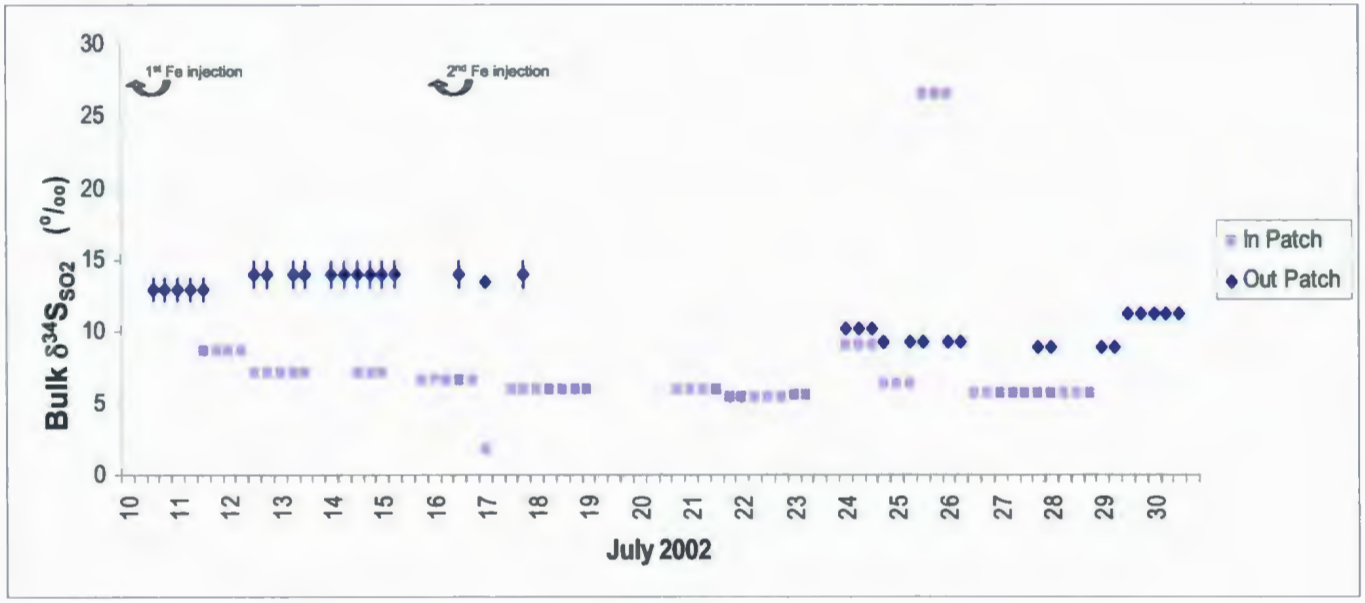

Figure 4.21: Bulk $\delta^{34}S_{SO2}$ with time outside and inside the patch.

SERIES fertilized patch. Eventually this DMS bloom contributed less biogenic SO_2 to the area and the $\delta^{34}S_{SO2}$ of the out patch area stabilized to pre bloom values (approximately +10‰).

Either a SO_2 source depleted in ^{34}S was becoming regionally important, or a source enriched in ^{34}S was becoming regionally less important, as seen by the decrease in $\delta^{34}S_{SO2}$ both inside and outside the patch with time. However, it was interesting to note that the initial $\delta^{34}S_{SO2}$ inside the patch was the same as the final $\delta^{34}S_{SO2}$ outside the patch. This seemed to suggest that the out patch area was affected by a biogenic source that produced less biogenic SO_2 with time and the in patch area was affected by an anthropogenic source that produced more anthropogenic SO_2 with time. A $\delta^{34}S_{SO2}$ between +8‰ and +12‰ was concluded as the background $\delta^{34}S_{SO2}$ for the Station Papa area.

4.4.3A: ANTHROPOGENIC AND BIOGENIC SO_2 INTRODUCTION

As with SO_4, SO_2 concentrations and $\delta^{34}S_{SO2}$ were used to separate the biogenic and anthropogenic fractions. Assuming no isotope fractionation occurred when biogenic SO_2 formed from biogenic SO_4 and when anthropogenic SO_2 formed from anthropogenic SO_4 (Norman et al., 2004a), then it was assumed that the biogenic SO_2 had a $\delta^{34}S_{SO2}$ of +18.6 ± 0.9‰ (Patris et al., 2000) and the anthropogenic SO_2 had a $\delta^{34}S_{SO2}$ of +2 ± 1.0‰ (Norman et al., 2004a).

4.4.3B: ANTHROPOGENIC AND BIOGENIC SO_2 RESULTS

Anthropogenic and biogenic SO_2 concentrations inside and outside the patch were plotted in ***Figure 4.22a*** and ***Figure 4.22b*** respectively. Anthropogenic and biogenic SO_2 concentrations inside and outside patch increased during the first half of the study period (July 10 to July 20) then decreased during the second half of the study period (July 20 to July 31) as proven by t-tests at the 90% confidence interval (anthropogenic SO_2 in patch, $p<0.1$, anthropogenic SO_2 out patch, $p<0.1$; biogenic SO_2 in patch, $p<0.1$; biogenic SO_2 out patch, $p<0.1$). The concentration of anthropogenic SO_2 outside the patch was slightly lower than inside the patch (time weighted average out patch = $0.19 + 0.10$ $\mu g/m^3$, time weighted average in patch = 0.28 ± 0.17 $\mu g/m^3$) while the concentration of biogenic SO_2 outside the patch was higher than inside the patch (time weighted average outside the patch = 0.37 ± 0.29 $\mu g/m^3$, time weighted average inside the patch = 0.06 ± 0.07 $\mu g/m^3$). Of the SO_2 collected in bulk samples, it was calculated that outside the patch 68% was biogenic (i.e. 32% anthropogenic SO_2 outside) and inside the patch 18% was biogenic (i.e. 82% was anthropogenic SO_2 inside).

4.4.3C: ANTHROPOGENIC AND BIOGENIC SO_2 INTERPRETATIONS

Anthropogenic SO_2 concentrations (***Figure 4.22a***) displayed the same trend in both areas. The increase then decrease in SO_2 concentrations inside and outside the patch suggested that there was one regional anthropogenic SO_2 source. Possible regional anthropogenic SO_2 sources included continental derived SO_2 or ship derived SO_2. The anthropogenic SO_2 in the Station Papa region was interpreted to come from shipping lane emissions.

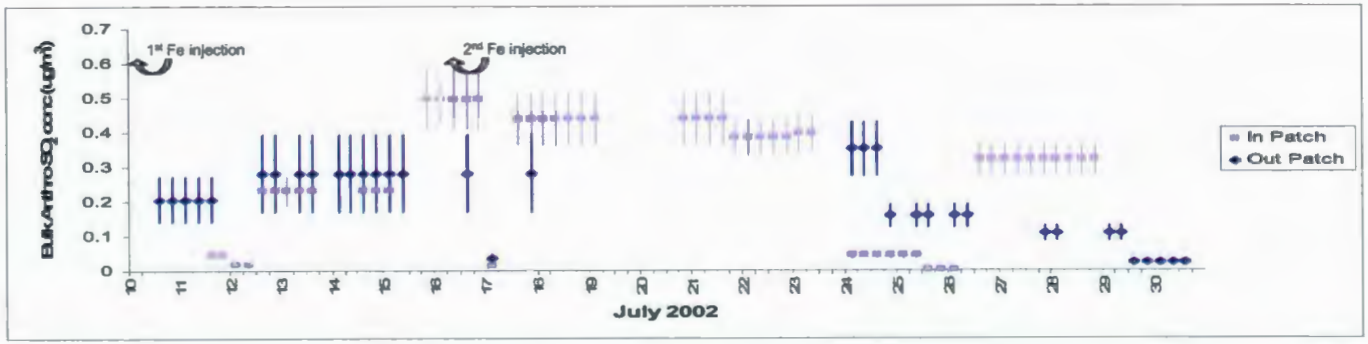

Figure 4.22a: Bulk anthropogenic SO_2 concentrations with time outside and inside the patch.

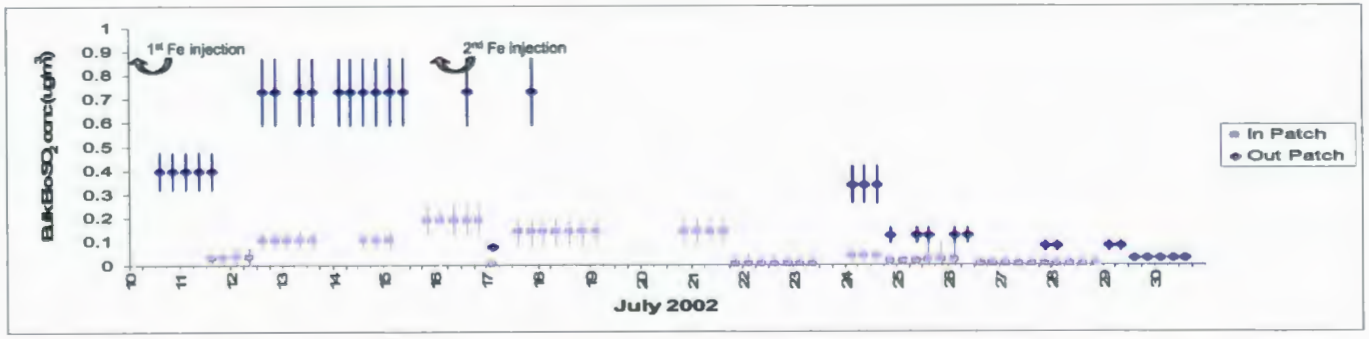

Figure 4.22b: Bulk biogenic SO_2 concentrations with time outside and inside the patch.

The anthropogenic SO_2 was slightly higher inside the patch however there were always ships inside the patch that emitted SO_2 as they tracked the patch. The higher anthropogenic SO_2 concentrations inside the patch, yet similar anthropogenic SO_2 concentrations inside and outside the patch, further supported that ship emissions were the source of anthropogenic SO_2 both inside and outside the patch.

The concentration of biogenic SO_2 (***Figure 4.22b***) had the same trend outside the patch as inside the patch however the concentration of biogenic SO_2 was higher outside the patch (outside the patch = 0.37 ± 0.29 $\mu g/m^3$, inside the patch = 0.06 ± 0.07 $\mu g/m^3$). Therefore it was concluded that the area outside the patch was being affected by a regional DMS bloom, as determined by bulk biogenic NSS SO_4, size segregated NSS SO_4 and bulk MSA results.

4.5 SUMMARY OF SULPHUR SPECIES

4.5.1A: SUMMARY OF SULPHUR SPECIES INTRODUCTION

Part of the aim of this thesis was to apportion sulphur sources throughout SERIES. Source apportionment was completed using physical, chemical and isotopic analysis.

4.5.1B: SUMMARY OF SULPHUR SPECIES RESULTS

Table 4.3 shows the percentages and concentrations of the species found in aerosols and gases collected throughout SERIES while ***Table 4.4*** shows the percentages and

Table 4.3: Percentages and concentrations of bulk aerosols and gases collected throughout SERIES.

Species	Out Patch	In Patch	Out Patch ($\mu g/m^3$)	In Patch ($\mu g/m^3$)
SS SO_4	31%	32%	3.02	4.85
NSS SO_4	69%	68%	6.65	10.46
Total SO_4	100%	100%	9.67	15.31
Biogenic NSS SO_4	8%	8%	0.55	0.79
Anthropogenic NSS SO_4	92%	92%	6.10	9.66
Total NSS SO_4	100%	100%	6.65	10.46
Biogenic SO_2	68%	18%	3.13	0.54
Anthropogenic SO_2	32%	82%	1.47	2.40
Total SO_2	100%	100%	4.61	2.94
Biogenic NSS SO_4	10%	27%	0.55	0.79
Biogenic SO_2	58%	19%	3.13	0.54
MSA	32%	54%	1.71	1.57
Total Biogenic S	100%	100%	5.39	2.89

Table 4.4: Percentages and concentrations of submicron aerosols collected throughout SERIES. The concentration data show a) the amount of submicron aerosols of size segregated aerosols and b) the total amount of aerosol in all size fractions. Percentages are based on values from ***Appendix 4.2.***

Species	Out Patch	In Patch	Out Patch ($\mu g/m^3$)	In Patch ($\mu g/m^3$)
SS	6%	13%	0.07^a of 1.26^b	0.33^a of 2.52^b
NSS	52%	45%	1.80^a of 3.43^b	4.05^a of 8.99^b
Biogenic NSS SO_4	57%	32%	0.76^a of 1.33^b	1.15^a of 3.54^b
Anthropogenic NSS SO_4	50%	53%	1.04^a of 2.10^b	2.90^a of 5.44^b
MSA	67%	48%	0.34^a of 0.51^b	0.54^a of 1.12^b

concentrations of submicron aerosols (<0.95 μm, Stages 5 and 6 of the size-segregated aerosols).

4.5.1C: SUMMARY OF SULPHUR SPECIES INTERPRETATIONS

Both outside and inside the patch, bulk NSS SO_4 was more common than bulk SS SO_4 and bulk anthropogenic NSS SO_4 was more common than bulk biogenic NSS SO_4. This showed that both areas were affected by anthropogenic sources. Of SO_2, bulk biogenic SO_2 was more common outside the patch while bulk anthropogenic SO_2 was more common inside the patch. This has been explained by the presence of ships increasing the amount of anthropogenic sulphur sources during in patch tracking. In terms of the bulk biogenic sulphur species (i.e. biogenic NSS SO_4, biogenic SO_2 and MSA), bulk biogenic SO_2 was most common outside the patch while bulk MSA was most common inside the patch. The preferred DMS oxidation pathway is different in the two areas and may have been affected by the presence of aerosol surfaces due to ship emissions. When focusing on the bulk aerosols, abstraction appears to have been more prevalent outside the patch (i.e. production of biogenic SO_2) whereas addition may have been more important inside the patch (i.e. production of MSA).

As shown in ***Table 4.4***, the concentration of submicron aerosols for each the species was higher inside the patch than outside the patch however the percentage of submicron biogenic NSS SO_4 and MSA outside the patch was higher than inside the patch. With ≥50% of biogenic NSS SO_4 and MSA submicron aerosols, it suggested

that although outside the patch was at a lower concentration, the aerosols that were forming were preferentially forming new, submicron aerosols. There was a low percentage and concentration of SS SO_4 both outside and inside the patch in submicron aerosols however, as discussed in ***Section 4.1.1***, sea salt was forming larger aerosols. This may have also been the case for other species inside the patch (e.g. forming larger aerosols or combining with larger aerosols).

4.6 SAMPLE 4D AND 4E

A bulk sample collected inside the patch on July 16 (Sample 4D collected from 1320 to 1900 hours and another that was collected outside the patch later the same day (Sample 4E collected from 1900 to 2130 hours) may be useful to determine differences outside and inside the patch. As noted in previous sections, these two bulk samples had peculiar results and required further investigation.

The bulk in patch and out patch samples from July 16 (Sample 4D and Sample 4E) must be interpreted with caution. The sampling times were very short and the amount of sample collected onto the sample filters in some instances was low.

Sea spray components inside the patch were between and outside the patch were higher than the sample(s) collected before and after (***Figure 4.1***). The higher concentration of sea spray components out patch can be explained by a higher production of sea spray

aerosols due to higher wind speeds during sample collection (4E = 28.1 km/hr, 2B = 22.41 km/hr) (***Figure 4.31*** and ***Figure 4.3***).

The $\delta^{34}S_{SO4}$ of Sample 4E (outside patch, July 16) was lower than the Sample 2B which was collected before and after it (***Figure 4.8***) suggesting proportionally more anthropogenic sulphur. The lower $\delta^{34}S_{SO4}$ outside the patch (Sample 4E) when compared to inside the patch (Sample 4D) suggested that the out patch was influenced more by anthropogenic sources than inside the patch at that particular time. Ship's emissions were likely the source of the anthropogenic NSS SO_4.

It was interesting to note the very high MSA concentrations in the July 16 out patch sample (Sample 4E, ***Figure 4.18***) which perhaps suggests DMS production upwind. Unfortunately the wind direction during the sampling period was ambiguous. This sample was collected on a sunny day (Sample 4E, outside patch, July 16) when it was expected that distinct oxidation products could be seen. Obviously the addition pathway and hence production of MSA was preferred during the collection of Sample 4E, outside patch on July 16. It was also interesting to note that the sample collected on July 16 inside and downwind of the patch (Sample 4D, ***Figure 4.18***), did not immediately show the high MSA concentrations as outside and upwind of the patch revealed, however MSA concentrations increased thereafter.

The $\delta^{34}S_{SO2}$ inside the patch on July 16 (Sample 4D, $\delta^{34}S_{SO2}$ = +1.67‰) suggested much more anthropogenic influence than the samples collected before and after it (Sample 3C, $\delta^{34}S_{SO2}$ = +6.48‰ and Sample 3D, $\delta^{34}S_{SO2}$ = +5.89‰) while outside the patch on July 16 (Sample 4E, $\delta^{34}S_{SO2}$ = +13.39‰) the anthropogenic influence was only slightly more than the sample collected before and after it (Sample 2B, $\delta^{34}S_{SO2}$ = +13.98‰) (***Figure 4.21***). On July 16, 100% of the SO_2 inside the patch was anthropogenic while 31% of the SO_2 outside the patch was anthropogenic.

Outside and inside the patch the biogenic SO_2 was low (outside = 0.074 $\mu g/m^3$, inside = 0 $\mu g/m^3$, ***Figure 4.22b***). The high MSA concentrations outside the patch (***Figure 4.18***) suggested the addition pathway for DMS oxidation (i.e. MSA produced) was preferred at this particular time outside the patch while high biogenic NSS SO_4 concentrations inside the patch (***Figure 4.16***) suggested the abstraction pathway (i.e. biogenic SO_2 and biogenic NSS SO_4 produced) was preferred at this particular time inside the patch, opposite to the overall percentages of each area shown in ***Table 4.2***.

4.7 FUELS

Fuel from the three ships involved in SERIES was analyzed to determine whether ship emissions influenced the $\delta^{34}S_{SO4}$ or the sulphur concentrations during SERIES air sampling. Data for the fuel samples are shown in ***Table 4.5***.

Table 4.5: Sulphur concentration (mg/g) and $\delta^{34}S_{SO4}$ (‰) of fuels from the three ships involved in SERIES

Ship Name	S Concentration (mg/g)	$\delta^{34}S_{SO4}$ (‰)
JP Tully	0.062	+9.77
El Puma	0.122	+9.33
Kaiyo Maru	4.76	-4.32

The $\delta^{34}S_{SO4}$ of the fuels used by the *El Puma* (+9.33‰) and *JP Tully* (+9.77‰) during SERIES was similar to average $\delta^{34}S_{SO4}$ for diesel fuels across western Canada (+9.9 ± 2.0‰, Norman et al., 2004b). However the $\delta^{34}S$ of the fuel used by the *Kaiyo Maru* was lower (-4.32‰) and can be attributed to the fact that the *Kaiyo Maru* fueled up in Asia while the *JP Tully* and *El Puma* fueled up in Canada. The fuels would likely have different isotopic signatures since they originated from different continents and therefore different sources with different $\delta^{34}S_{SO4}$ (Krouse and Grinenko, 1991).

The sulphur concentrations and $\delta^{34}S_{SO4}$ of the ship emissions may have been affected by sulphur containing oils and lubricants added to the ship fuel. Norman et al. (2004b) showed that these additives can reduce the $\delta^{34}S_{SO4}$ by approximately +4 or +5‰. Therefore while the *JP Tully* and *El Puma* were present at Station Papa, the $\delta^{34}S_{SO4}$ of the ship emissions was approximately +4.5‰ (the average of +9.77‰ and +9.33‰ is +9.55‰, 5‰ lower due to fuel additives makes $\delta^{34}S_{SO4}$ approximately +4.5‰) and when the *Kaiyo Maru* and *El Puma* were present, the $\delta^{34}S_{SO4}$ of the ship emissions was lowered (the average of +9.33‰ and -4.32‰ is +5.01‰, 5‰ lower due to fuel additives makes $\delta^{34}S_{SO4}$ approximately 0‰). A $\delta^{34}S_{SO4}$ of +2.0‰ was used throughout this thesis as an anthropogenic value and was therefore a good approximation. However SERIES research ship emissions contributing sulphur prior to July 23, 2002 (i.e. when the *JP Tully* departed) would result in a slight overestimation of biogenic

contributions and after July 23, 2002 (i.e. when the *Kaiyo Maru* arrived) would result in a slight underestimation of biogenic sulphur. This idea was not discussed in previous results because the effects were minimal. Assuming all three ships combusted fuel at the same rate, the time weighted average of $\delta^{34}S_{SO4}$ from the combined emissions for the three research vessels was calculated as -3.8‰.

CHAPTER 5: CONCLUSIONS AND RECOMMENDATIONS FOR FUTURE WORK

5.1: CONCLUSIONS

The main objectives of this thesis were to determine:

1) The source of SO_2 throughout SERIES

2) The source of NSS SO_4 throughout SERIES

3) The preferred pathway of DMS oxidation during SERIES and

4) Whether SERIES iron fertilization affected atmospheric DMS oxidation products.

5.1A: COMPOSITION OF AEROSOLS AND GASES

Aerosols in the Station Papa area contained sea salt components (e.g. Mg, Na, Cl and SS SO_4). During SERIES, the concentrations of sea salt components were shown to coincide with wind speed. Washout affected the concentrations of sea spray components, as well as the concentrations of other species collected.

Most samples were shown to be mixtures of SS SO_4, anthropogenic NSS SO_4 and biogenic NSS SO_4 using a three source mixing model. The SO_4 isotopic compositions (approximately +8‰) were slightly below what would be expected for a 50:50 mixture of biogenic sources (+18.6‰) and anthropogenic sources (+2.0‰). The anthropogenic sources of NSS SO_4 in patch were determined to be ship emissions from ships in this study continuously mapping the patch.

When NSS SO_4 was separated into biogenic and anthropogenic NSS SO_4, anthropogenic NSS SO_4 concentrations were higher than biogenic NSS SO_4 in the Station Papa area. Biogenic NSS SO_4 concentrations inside and outside the patch were similar however the amount of sulphur in submicron biogenic NSS SO_4 was unexpectedly higher outside the patch.

Bulk MSA concentrations revealed the Station Papa area was producing high concentrations of MSA during SERIES and these MSA concentrations were higher than previously recorded. However MSA to NSS SO_4 ratios revealed that although the area was impacted by biogenic sources, it was influenced by anthropogenic sources as well.

As with MSA, biogenic SO_2 concentrations were higher than previously recorded. A background SO_2 isotopic composition for the area was determined to be between +8‰ and +12‰ and showed both anthropogenic and biogenic SO_2 contributed to the composition of the SO_2. Unexpectedly, the out patch area was influenced more by biogenic SO_2 than the in patch area.

5.1B: PATHWAYS OF DMS OXIDATION

The DMS near the Station Papa area during SERIES was preferentially oxidized via the abstraction pathway; high concentrations of biogenic SO_2 and low bulk MSA to bulk NSS SO_4 ratios were observed. In turn, SO_2 was oxidized to produce NSS SO_4. Biogenic

NSS SO_4 in the Station Papa area produced new aerosols as well as formed on or combined with pre existing aerosols.

5.1C: EFFECTS OF FERTILIZATION

A definite conclusion as to the influence of the SERIES iron fertilization DMS oxidation products cannot be determined given that data presented here. The results of the fertilization experiment were difficult to determine as concurrent DMS blooms, and ship emissions may have affected observations. The data collected during SERIES will prove to be useful however in the scheme of the scientific community.

5.2: RECOMMENDATIONS FOR FUTURE WORK

Future experiments can be informed by SERIES results. Future studies should:

- Develop a better sampling schedule in order to determine whether day time and night time conditions have any effect on oxidation. Requirements such as atmospheric sampling only under ideal conditions and obtaining enough sample for analysis made sample scheduling both inside and outside the patch more random than desired. Sampling aboard two ships may have solved this issue: one ship tracking and sampling inside the patch and the other ship sampling out/upwind of the patch.
- Choose a specific out/upwind patch that can be tracked and compared throughout the experiment rather than randomly cruising to any location out/upwind of the

patch. This will help to determine changes occurring in the area and thus help determine the effects of the iron fertilization experiment better.

REFERENCES:

Andreae, M.O. (1980) **Determination of trace quantities of dimethylsulphide in aqueous solution.** *Anal. Chem.*, 52: 150-153.

Andreae, M.O. (1985) **The emission of sulfur to the remote atmosphere.** In: The biogeochemical cycling of sulfur and nitrogen in the remote atmosphere, J.N. Galloway et al. (Eds.), D Reidel Publishing Co.: 5-25.

Audi, G. and Wapstra, A.H. (1995) **The 1995 update to the atomic mass evaluation.** *Nuclear Physics A*, 595 (4): 409.

Ayers, G.P., Ivey, J.P. and Gillett, R.W. (1991) **Coherence between seasonal cycles of dimethyl sulphide, methanesulphonate and sulphate in marine air.** *Nature*, 349: 404-406.

Barnes, I., Bastian, V., Becker, K.H. and Martin, D. (1989) **Fourier Transform IR studies of the reactions of dimethyl sulfoxide with OH, NO3, and Cl radicals.** In Biogenic Sulfur in the Environment, E.S. Saltzmann and W.J. Cooper (Eds.) ACS Symposium Series 393: 476-489.

Bates, T.S., Johnson, J.E., Quinn, P.K., Goldan, P.D., Kuster, W.C., Covert, D.C. and Hahn, C.J. (1990) **The biogeochemical sulfur cycle in the marine boundary layer over the Northeast Pacific Ocean.** *J. Atmos. Chem.*, 10: 59-81.

Bates, T.S., Calhoun, J.A. and Quinn, P.K. (1992). **Variations in the Methanesulfonate to sulfate molar ratio in submicrometer marine aerosol particles over the south Pacific Ocean.** *Journal of Geophysical Research*, 97, 9859-9865.

Benkovitz, C.M., Schwartz, S.E., Jensen, M.P. and Miller, M.A. (2006) **Attribution of modeled atmospheric sulphate and SO2 in the Northern Hemisphere for June-July 1997.** *Atmos. Chem. Phys. Dicuss.*, 6: 4023-4059.

Berner, E.K. and Berner, R.A. (1996) **Global Environment: water, air and geochemical cycles.** Prentice Hall, New Jersey. 376 pp.

Berresheim, H, Andreae, M.O., Ayers, A.P., Gillett, R.W. Merrill, J.T., Davis, V.J. and Chameides, W.L. (1990) **Airborne measurements of dimethylsulphide, sulphur dioxide and aerosol ions over the Southern Ocean south of Australia.** *Journal of Atmospheric Chemistry*, 10, 341-370.

Berresheim, H. (1987) **Biogenic sulphur emissions from the subantarctic and Antarctic oceans.** *Journal of Geophysical Research*, 92, D11: 13245-13262.

Berresheim, H., Andreae, M.O., Iverson, R.L. and Li, S.M. (1991) **Seasonal variations of dimethylsulphide emissions and atmospheric sulphur emissions and nitrogen species over the western north Atlantic Ocean.** *Tellus*, 43B: 353-372.

Berresheim, H., Andreae, M.O., Ayers, G.P. and Gillett, R.W. (1989) **Distribution of biogenic sulfur compounds in the remote southern hemisphere.** In Biogenic Sulfur in the Environment, Saltzman, E.S. and Cooper, W.J. (Eds.), American Chemical Society, Washington, 393: 352-366.

Bonsang, B., Nguyen, B.C., Gaundry, A. and Lambert, G. (1980) **Sulfate enrichment in marine aerosols owing to biogenic gaseous sulfur compounds.** J. Geophys. 85: 7410-7416.

Boyd, P.W., Watson, A., Law, C.S. Abraham, E., Trull, T., Murdoch, R., Bakker, D.C.E., Bowie, A.R., Buessler, K., Chang, H., Charette, M., Croot, P., Downing, K., FREW< R., Gall, M., Hadfield, M., Hall, J., Harvey, M., Jameson, G., La Roche, J., Liddicoat, M., Ling, R., Maldonado, M., McKay, R.M. Nodder, S., Pickmere, S., Pridmore, R., Rintoul, S., Safi, K., Sutton, P., Strepek, R., Tanneberger, K., Turner, S., Waite, A. and Zeldis, J. (2000) **A mesoscale phytoplankton bloom in the polar Southern Ocean stimulated by iron fertilization of waters.** *Nature*, 407: 695-702.

Boyd, P.W., Law, C.S., Wong, C.S., Nojiri, Y., Tsuda, A., Levasseur, M., Takeda, S., Rivkin, R., Harrison, P., Strzepek, R., Gower, J., McKay, M., Abraham, E., Arychuk, M., Barwell-Clarke, J., Crawford, W., Crawford, D., Hale, M., Harada, K., Johnson, K., Kiyosawa, H., Kudo, I., Marchetti, A., Miller, W., Needoba, J., Nishioka, J., Ogawa, H., Page, J., Robert, M., Saito, H., Sastri, A., Sherry, N., Soutar, T., Sutherland, N., Taira, Y., Whitney, F., Wong, S.E. and Yoshimura, T. (2004) **The decline and fate of an iron-induced subarctic phytoplankton bloom.** *Nature*, 428: 549-553.

Brasseur, G.P., Prinn R.G. and Pszenny, A.A.P. (Eds.) (2003) **The changing atmosphere: an integration and synthesis of a decade of tropospheric chemistry research.** Springer-Verlag, New York. 300 pp.

Bruland, K.W., Donat, J.R. and Hutchins, D.T. (1991) **Interactive influences of bioactive trace metals on biological production in oceanic waters.** *Limnology and Oceanography*, 36: 1555-1577.

Calhoun, J.A. and Bates, T.S. (1989) **Sulfur isotope ratios: tracers of non-sea salt sulphate in the remote atmosphere.** In: biogenic sulfur in the environment, E. Saltzman and W. Cooper (Eds.), pp 368-379.

Calhoun, J.A., Bates, T.S. and Charlson, R.J. (1991) **Sulphur isotope measurements of sub-micrometer sulphate aerosol particles over the Pacific Ocean.** *Geophys. Res. Lett.*, 18: 1877-1880.

Capaldo, K., Corbett, J.J. Kaisbhatla, P., Fischbeck, P. and Pandis, S.N. (1999) **Ship emissions perturb radiation balance over the sea.** *Nature*, 400: 743-746.

Challenger, F. and Simpson, M. I. (1948) **Studies on biological methylation. Part XII. A precursor of the dimethyl sulfide evolved by Polysiphonia fastigiata. Dimethyl-2-carboxyethyl sulphonium hydroxide and its salts.** *J. Chem. Soc.*, 43: 1591-1597.

Charlson, R.J., Lovelock, J.E., Andreae, M.O. and Warren, S.G. (1987) **Oceanic phytoplankton, atmospheric sulfur, cloud albedo and climate.** *Nature*, 326: 655-661.

Charlson, R.J. and Wigley, T.M.L. (1994) **Sulfate aerosol and climate change.** *Scientific American*: 48-55.

Charlson, R.J., Langer, J. and Rodhe, H. (1990) **Sulfate aerosol and climate.** *Nature*, 348: 22.

Charlson, R.J., Schwartz, S.E., Hales, J.M., Cess, R.D. Coakley, J.A., Hansen, J.E. and Hoffman, D.J. (1992) **Climate forcing by anthropogenic aerosols.** *Science,* 255: 423-430.

Chisolm, S. (1995) The iron hypothesis. In: US National Report to IUGG, Rev. Geophys. AGU, Vol 33, www.agu.org/revgeophys/chisho00.html.

Cipriano, R.J. and Blanchard, D.C. (1981) **Bubble and aerosol spectra produced by a laboratory breaking wave.** *Journal of Geophysical Research,* 86: 8085-8092.

Coale, K.H., Johnson, K.S., Fitzwater, S.E. and Gordon, M.E. (1996) **A massive phytoplankton bloom induced by an ecosystem –scale iron fertilization experiment in the equatorial Pacific Ocean.** *Nature*, 383: 496-501.

Cullen, J.J. (1995) **Status of the iron hypothesis after the open ocean enrichment experiment.** *Limnology and Oceanography*, 40, 7: 1336-1343.

Curry, J.A. and Webster, P.J. (1999) **Thermodynamics of Atmospheres and Oceans.** Academic Press, 467 pp.

Davidson, B. and Hewitt, N. (1992) **Natural Sulphur species from the North Atlantic and their contribution to the United Kingdoms sulfur budget.** *Journal of Geophysical Research*, 97, 2475-2488.

Daykin, E.P. and Wine, P.H. (1990) **Rate of reaction of IO radicals with dimethylsulfide.** *Journal of Geophysical Research*, 95, D11: 18547-18553.

Duce, R.A., Arimoto, R., Ray B.J., Unni, C.K., and Harder, P.J. (1983) **Atmospheric trace elements at Enewetak Atoll.** *Journal of Geophysical Research*, 88: 5321-5342.

Dugdale, R.C. and Wilkerson, F.P. (1990) **Iron addition experiments in the Antarctic – a reanalysis.** *Global Biogeochemical Cycles*, 4: 13-19.

Faure, G. (1986) **Principles of Isotope Geology.** John Wiley and Sons, New York.

Fitzgerald, J.W. (1991) **Marine aerosols: a review.** *Atmospheric Environment*, 25: 533-545.

Frost, B.W. (1996) **Phytoplankton bloom on iron rations.** *Nature*, 383: 475-476.

Galloway, J.N. (1990) **Sulfur in the western north Atlantic Ocean atmosphere: results from a summer 1988 ship/aircraft experiment.** *Global Biogeochemical Cycles*, 4: 349-365.

Gran, H.H. (1931) **On the conditions for the production of phytoplankton in the sea.** *Rapp. Proc. Verb. Cons. Int. Explor. Mer* 75: 37-46.

Gravenhorst, G. (1977) **Maritime sulfate over the North Atlantic.** *Atmospheric Environment*, 12, 707-713.

Gong, S.L., Barrie, L.A. and Blanchet, J.P. (1997) **Modeling sea-salt aerosols in the atmosphere.** *Journal of Geophysical Research*, 102: 3805-388.

Gordon, R.M., Coale, K.H. and Johnson, K.S. (1994) **Iron distributions in the equatorial Pacific: Implications for new production.** *EOS*, 75, 114: Abstract.

Hart, T.J. (1934) **On the phytoplankton of the southwest Atlantic and Bellinghausen Sea, 1929-31.** *Discovery Rep.*, 8: 1-268.

Harvey, H.W. (1938) **The supply of iron to diatoms.** *J. Mar. Biol. Assoc. UK*, 22: 205-219.

Hidy, G.M. and Brock, J.R. (1971) **Topics in Current Aerosol Research.** Pergamon Press, New York.

Hynes, A.J., Wine, P.H. and Semmes, D.H. (1986) **Kinetics and mechanisms of OH reactions with organic sulfides.** *Journal of Physical Chemistry*, 90: 4148-4156.

Isotope Sciences Laboratory of the University of Calgary (2003) **Preparation of Sulphur Dioxide (SO_2) Filters.** Personal communication.

Jackson, A.R.W. and Jackson J.M. (1996) Environmental Science: the natural environment and human impact. Longman, Harlow, pp 370.

Jaenicke, R. (1980) **Atmospheric aerosols and the global climate.** *Journal of Aerosol Science*, 11: 577-588.

Jaenicke, R. (1993) **Tropospheric aerosols.** In Aerosol cloud climate interactions. Edited by P.V. Hobbs, Academic Press, San Diego. 235 pp.

Jensen, N.R., Hjorth, J., Lohse, C., Skov, H. and Restelli, G. (1992) **Products and mechanisms of the gas phase reactions of NO3 with CH3SCH3, CD3SCD3, CH3SH, and CH3SSCH3.** *Journal of Atmospheric Chemistry*, 14: 95-108.

Junge, C.E. (1963) **Air chemistry and radioactivity.** Academic Press, New York. 123 pp.

Katz, M. (1977) **The Canadian Sulphur Problem.** In: Sulphur and it inorganic derivatives in the Canadian environment. Ad hoc Panel of Experts Management Subcommittee, NRC Associate Committee on Scientific Criteria for Environmental Quality, national Research Council of Canada, Ottawa: 21-67.

Keene, W.C., Pszenny, A.A.P., Galloway, J.N. and Hawley, M.E. (1986) **Sea salt corrections and interpretation of constituent ratio in marine interpretation.** *Journal of Geophysical Research*, 91: 6647-6658.

Kiene, R.P., Linn, L.J. and Bruton, J.A. (2000) **New and important roles for DMSP in marine microbial communities.** *Journal of Sea Research*, 43, 1-3: 209-224.

Krischke, U., Staubes, R., Brauers, T., Gautrois, M., Burkert, j., Stobener, D. and Jaeschke, W. (2000) **Removal of So2 from the marine boundary layer over the Atlantic Ocean: a case study on the kinetics of the heterogeneous S (IV) oxidation on marine aerosols.** *Journal of Geophysical Research*, 105: 14413-14422.

Krouse, H.R. and Grinenko, V.A. (1991) **Stable Isotopes: Natural and Anthropogenic Sulphur in the Environment Scope 43.** J Wiley and Sons, Chinchester, England. 440 pp.

Leck, C., Bigg, E.K., Covert, D.S., Heintzenberg, J., Maenhaut, W., Nilsson, E.D. and Wiedensohler, A. (1996) **Overview of the atmospheric research program during the International Arctic Ocean Expedition of 1991 (IAOE-91) and its scientific results.** *Tellus*, 48, 2: 136-155.

Lide, D.R. (Ed.) (2002) **CRC Handbook of Chemistry and Physics (83rd ed.).** CRC Press. New York.

Liss, P.S., Watson, A.J., Liddicoat, M.I. Malin, G., Nightingale, P.D., Turner, S.M. and Upstill-Goddard, R.C. (1993) **Trace gases and air-sea exchanges.** *Phil. Trans. R. Soc.* London. 343: 531-541.

Lovelock, J.E. and Margulis, L. (1974) **Atmospheric homeostasis by and for the biosphere: The Gaia Hypothesis.** *Tellus*, Vol. 26, No. 1-2: 2-9.

Lovelock, J.E. and Whitfield, M. (1982) **The life span of the biosphere.** *Nature*, 296, No. 5857: 561-563.

Maidment, D.R. (Ed.) (1993) **Handbook of Hydrogeology.** McGraw-Hill, New York.

Martin, J. (1992) **Iron as a limiting factor in oceanic productivity.** pgs 123-138. In P.G. Falkoski and A. Woodhead (Eds), *Primary productivity and biogeochemical cycles in the sea.*

Martin, J. H., Coale, K. H., Johnson, K. S., Fitzwater, S. E., Gordon, R. M., Tanner, S. J., Hunter, C. N., Elrod, V. A., Nowicki, J. L. Coley, T. L., Barber, R. T., Lindley, S., Watson, A. J., Van Scoy, K., Law, C. S., Liddicoat, M. I., Ling, R., Stanton, T., Stockel, J., Collins, C., Anderson, A., Bidigare, R., Onderusek, M., Latasa, M., Millero, F. J., Lee, K., Yao, W., Zhang, J. Z., Freiderich, G., Sakamoto, C., Chavez, F., Buck, K., Kolber, Z., Greene, R., Falkowski, P., Chisholm, S. W., Hoge, F., Swift, R., Yungel, J., Turner, S., Nightingale, P., Hatton, A., Liss, P. and Tindale, N. W. (1994) **Testing the iron hypothesis in ecosystems of the equatorial Pacific Ocean.** *Nature*, 371:123-129.

Martin, J.H. and Gordon, R.M. (1988) **Northeast Pacific iron distributions in relation to phytoplankton productivity.** *Deep Sea Research*, 35, 177-196.

Martin, J.H., Gordon, R.M. and Fritzwater, S.E. (1988) **Iron deficiency limits phytoplankton growth in the north-east Pacific Subarctic.** *Nature.* 331: 341-343.

McArdle, N.C., Liss, P.S., and Dennis, P. (1998) **An isotopic study of atmospheric sulphur at three sites in Wales and at Mace Head, Eire.** *Journal Geophysical Research*, 103, 31079-31094.

Miller, M.S., Friedlander, S.K. and Hidy, G.M. (1972) **A chemical element balance for the Pasadena aerosol.** *J Colloid Interface Sci.*, 39: 165-172.

Millet, D.B., Goldstein, A.H., Allan, J.D., Bates, T.S., Boudries, H., Bower, K.N., Coe, H., Ma, Y., McKay, M., Quinn, P.K., Sullivan, A., Weber, R.J. and Worsnop, D.R. (2004) **Volatile organic compound measurements at Trinidad Head, California, during ITCT 2K2: Analysis of sources, atmospheric composition and aerosol residence times.** *Journal of Geophysical Research*, 109, 23.

Mizutani, Y. and Rafter, T.A. (1969) **Oxygen isotopic composition of sulphates, Part 5, Isotopic composition of sulphate in rain water, Gracefield, New Zealand.** *N.Z. J. Sci.*, 12: 69-80.

Möller, D. (1984) **Estimation of the global and man-made sulphur emission.** *Atmospheric Environment*, 18, 1: 19-27.

Monroe, J.S. and Wicander, R. (1997) **The Changing Earth.** West Group Publishers. 721 pp.

National Research Council of Canada (1982) **Effects of aerosols on atmospheric processes.** The Council, Ottawa. 208 pp.

Nguyen, B.C., Bonsang, B. & Gaundry, A. (1983) **The role of the ocean in the global atmospheric sulfur cycle.** *J. Geophys. Res.*, 88: 10903-10914.

Nielsen, H. (1979) **Sulphur Isotopes.** In: Lectures in Isotope Geology, E. Jager and J.C. Hunziker (Eds.), Springer, Berlin: 283-312.

Norman, A.L., Belzer, W. and Barrie, L. (2004a) Insights into the biogenic contribution to total sulphate in aerosol and precipitation in the Fraser Valley afforded by isotopes of sulphur and oxygen. Journal of Geophysical Research. 109.

Norman, A.L., Krouse, H.R. and MacLeod, J. (2004b) Apportionment of pollutant S in an urban airshed: Calgary, Canada. In Air Pollution Modeling and Its Application, Berrego, C. and Incecik, S. (Eds), Kluwer/Plenum, New York. 107-125.

Nriagu, J.O., Coker, R.D. and Barrie, L.A. (1991) **Origin of Sulphur in Canadian Arctic haze from isotope measurements.** *Nature*, 349, 142-145.

Patris, N., Mihalopoulos, N., Baboukas, E.D. and Jouzel, J. (2000) **Isotopic composition of sulphur in size-resolved marine aerosols above the Atlantic Ocean.** *Journal of Geophysical Research*, 105, D11, 14449-14457.

Peterson, J.T. and Junge, C. (1971) **Sources of particulate matter in the atmosphere.** In Man's Impact on the Climate. Matthews, W.H., Kellogg, W.W. and Robinson, G.D. (Eds), MIT Press, Cambridge. 594 pp.

Phinney, L., Leaitch, R., Lohmann, U., Shantz, N. and Worsnop, D. R. (2009) **Contributions of DMS and ship emission to CCN observed over summertime North Pacific.** *Atmos. Chem. Phys. Discuss.*, 9, 309-361 on www.atmos chem phys discuss.net 9 309 2009

Plane, J.M.C. (1989) **Gas phase atmospheric oxidation of biogenic sulphur compounds: a review.** In: Biogenic sulphur in the environment, W.J. Cooper and E.S. Saltzmann (Eds.) American Chemical Society, Washington: 404-423.

Price, N.M., Anderson, L.F. and Morel, F.M.M. (1991) **Iron and nitrogen nutrition of equatorial Pacific plankton.** *Deep-Sea Res.*, 38:1361-1378.

Prospero, J.M. (1979) **Mineral and sea salt aerosol concentration in various ocean regions.** *Journal of Geophysical Research*, 84, C2, 725-731.

Prospero, J.M., Savoie, D.L., Saltzman, E.S. and Larson, R. (1991) **Impact of oceanic sources of biogenic sulphur on sulphate aerosol concentrations at Mawson, Antarctica.** *Nature*, 350: 221-223.

Prospero, J.M., Charlson, R.W., Mohnen, V. (1983) **The atmospheric aerosol system: an overview.** *Rev. Geophys. Space Phys.*, 21: 1607-29.

Pszenny, A.A. (1992) **Particle size distributions of methanesulfonate in the tropical Pacific marine boundary layer.** *J. Atm. Chem.*, 14: 273-284.

Pszenny, A.A., Castelle, A.J., Galloway, J.N. and Duce, R.A. (1989) **A study of the sulfur cycle in the Antarctic marine boundary layer.** *J. Geophys. Res.*, 94: 9818-9830.

Quinn, P.K., Bates, T.S., Johnson, J.E., Covert, D.S. and Charlson, R.J. (1990) **Interactions between the sulfur and reduced nitrogen cycles over the Pacific Ocean.** *Journal of Geophysical Research*, 95, 16: 405-416.

Rahn, K.A. (1976) **The chemical composition of the atmospheric aerosol.** Technical report, University of Rhode Island.

Rees, C.E., Jenkins, W.J. and Monster, J. (1978) **Sulphur isotopic composition of ocean water sulfate.** *Geochemica et Cosmochemica Acta.*, 42: 377-381.

Rollinson, H. (1993) Using Geochemical Data: Evaluation, Presentation, Interpretation, Longman Scientific & Technical, Harlow.

Rosman, K.J.R and Taylor, P.D.P. (1998) **Isotopic compositions of the elements 1997**, *J. Phys. Chem. Ref. Data*, 27 (6): 1275.

Saltzman, E.S., Brass, G.W. and Price, D.A. (1983) **The mechanism of sulphate aerosol formation: chemical and sulphur isotopic evidence.** *Geophysical Research Letters*, 10, 7: 513-516.

Saltzman, E.S., Savoie, D.L., Prospero, J.M. and Zika, R.G. (1986) **Methanesulfonic acid and non-sea-salt sulfate in Pacific air: regional and seasonal variations.** *Journal of Atmospheric Chemistry*, 4, 2: 227-240.

Savoie, D.L. and Prospero, J.M. (1982) **Particle size distribution of nitrate and sulfate in the marine atmosphere.** *Geophys. Res. Lett.*, 9: 1207-1210.

Savoie, D.L., Prospero, J.M. and Saltzmann, E.S. (1989) **Non-sea-salt sulphate and nitrate in trade wind aerosols at Barbados: evidence for long range transport.** *Journal of Geophysical Research*, 94, D4: 5069-5080.

Scaire, J., Baboukas, E., Kanakidou, M. Krischke, U., Belviso, S., Bardouki, H and Mihalopoulos, N. (2000) **Spatial and temporal variability of atmospheric sulfur-containing gases and particles during Albatross campaign.** *Journal of Geophysical Research*, 105: 14433-14448.

Seinfeld, J.H. and Pandis, S.N. (2006) In: Atmospheric Chemistry and Physics: from air pollution to climate change, 2nd Ed. John Wiley and Sons, Toronto: 1326.

Shaw, G.E. (1983) **Bio-controlled thermostasis involving the sulfur cycle.** *Climate Change*, 5: 297-303.

Singh, H.B. (1995) **Halogens in the atmospheric environment.** In: Composition, Chemistry and Climate of the Atmosphere, Singh, H.B. (Ed.) Van Nostrand Reinhold, New York: 216-250.

Thode, H.G. (1991) **Sulphur isotopes in nature and the environment: an overview.** In: Stable Isotopes: natural and anthropogenic sulphur in the environment, H.R. Krouse and V.A. Grinenko (Eds.) John Wiley & Sons, New York. SCOPE 43: 1-26.

Thode, H.G., Macnamara, J. and Collins, C.B. (1949) **Natural variations in the isotopic content of sulphur and their significance.** *Can. J. Res.*, 27: 361-373.

Tsuda, A., Takeda, S., Saito, H., Nishioka, J., Nojiri, Y., Kudo, I., Kiyosawa, H., Shiomoto, A., Imai, K., Ono, T., Shimamoto, A., Tsumune, D., Yoshimura, T., Aono, T., Hinuma, A., Kinugasa, M., Suzuki, K., Sohrin, Y., Noiri, Y., Tani, H., Deguchi, Y., Tsurushima, N., Ogawa, H., Fukami, K., Kuma, K., and Saino, T. (2003) **A Mesoscale Iron Enrichment in the Western Subarctic Pacific induces a large centric diatom bloom.** *Science*, 300, No. 5621: 958-961.

Tsuda, A., Takeda, S., Saito, H., Nishioka, J., Kudo, I., Nojiri, Y., Suzuki, K., Uematesu, M., Wells, M., Tsumune, D., Yoshimura, T., Aono, T., Aramaki, T., Cochlan, W., Hayakawa, M., Imai, K., Isada, T., Iwamoto, Y., Johnson, W., Kameyama, S., Kato, S., Kiyosawa, H., Kondo, Y., Levasseur, M., Machida, R., Nagao, I., Nakagawa, F.,

Nakanishi, T., Nakatsuka, S., Narita, A., Noiri, Y., Obata, H., Ogawa, H., Oguma, K., Ono, T., Sakuragi, T., Sasakawa, M., Sato, M., Shimamoto, A., Takata, H., Trick, C., Watanabe, Y., Wong, C. and Yoshie, N. **Evidence for the grazing hypothesis: Grazing reduces phytoplankton responses of the HNLC ecosystem to iron enrichment in the Western SubArctic Pacific (SEEDS II)** (2007) *Journal of Oceanography*, 63: 983-994.

Turekian, V.C., Macko, S.A. and Keen, W.C. (2001) **Application of stable sulfur isotopes to differentiate sources of size-resolved particulate sulfate in polluted marine air at Bermuda during spring.** *Geophysical Research Letters*, 28: 1491-1494.

Turnipseed, A.A. and Ravishankara, A.R. (1993) **The atmospheric oxidation of dimethyl sulfide: elementary steps in a complex mechanism.** In Dimethylsulfide: oceans, atmosphere and climate, G. Restelli and G. Angeletti (Eds.) Kluwer Academic Publishers, Dordrecht: 185-195.

Tyndall, G.S., Burrows, J.P., Schneider, W. and Moorgat, G.K. (1986) **Rate coefficient for the reaction between NO3 radicals and dimethyl sulphide.** Chem. Phys. Lett. 130, 5: 463-466.

von Glasow, R. and Crutzen, P.J. (2004) **Model study of multiphase DMS oxidation with a focus on halogens.** *Atmospheric Chemistry and Physics*, 4: 589-608.

Wagenbach, D., Goerlach, U., Moser, K. and Muennich, K.O. (1988) **Coastal Antarctic aerosol: the seasonal pattern of its chemical composition and radionuclide content.** *Tellus*, 40B: 426-436.

Watson, A.J. and Lovelock, J.E. (1983) **Biological homeostasis of the global environment: the parable of Daisyworld.** *Tellus*, 35B: 284-289.

Weart, S. (2009) **The discovery of global warming.** American Institute of Physics. www.aip.org/history/climate/aerosol.htm#N_75_

Whitby, K.T. (1973) In VIII International Conference on Nucleation. Leningrad. 359 pp.

Wiley, D.J., Harvey, M.J., DeMora, S.J., Boyd, I.S. and Liley, J.B. (1993) **Dimethylsulphide and aerosols measurements at Ross Island, Antarctica.** In: Dimethylsulfide, oceans, atmosphere and climate, G. Restelli and G. Angeletti (Eds.), Kluwer Academic Publishers, Dordrecht.

Woolf, D.K. and Monahan, E.C. (1988) **Laboratory investigations of the influence on marine aerosol production of the interaction of oceanic whitecaps and surface – active material.** In: Aerosols and Climate, Hobbs and McCormick (Eds.) Deepak Publishing, Viginia, USA.

Yin, F., Grosjean, D. and Seinfeld, J.H. (1990) **Photooxidation of dimethyl sulfide and dimethyl disulfide.** *Journal of Atmospheric Chemistry*, 11: 309-364.

Zaback, D.A. and Pratt, L.M. (1992) **Isotopic composition and speciation of sulfur in the Miocene Monterey Formation; reevaluation of sulfur reactions during early diagenesis in marine environments.** *Geochim. Cosmochim. Acta.*, 56 (2) 763-774.

Appendix 3.1: Preparation of Sulphur Dioxide (SO_2) Filters (Method from Isotope Sciences Laboratory of the University of Calgary, 2003)

1. Wear safety glasses, a lab coat and suitable gloves while preparing the SO_2 filter paper. (If organics will be tested, wear PVC gloves. If not, wear latex.)
2. Clean the board and roller thoroughly with distilled water and then with alcohol. Wipe the area with a Kim Wipe. Clean 8 paper clips with deionized water.
3. Set up a stand with a clamp and attach the metal rack. Clip the paper clips onto the metal rack in rows of pairs, with each row five bars apart from each other. This should allow adequate room for the filter papers to not touch each other when being hung to dry.
4. Prepare the oven by lining the bottom with aluminium foil to catch the drippings and setting the temperature to 100°C.
5. Place 6 untreated filter papers on the glass working area, laying half of each sheet on top of another.
6. Cover the untreated filter papers with SO_2 filter mix (Potassium carbonate/ glycerol solution). Use the roller to spread the solution evenly over every filter paper, making sure there are no dry spots. Squeeze out extra solution.
7. Grasp the corners of a filter paper and clip the edges to the rack using the paper clips. Repeat until all filter papers have been clipped.
8. Place the rack with wet filter papers in the oven and heat for 30 minutes or until the filter papers are completely dry.

9. Take the treated filter papers out of the oven and place them in the designated Ziploc bag.
10. Repeat steps 5-9 until enough SO_2 filter papers have been made.

Appendix 3.2: Sampling Details

Sample	Time Sampled (in min)	Dates Sampled	Special Conditions and/or Locations
1A and 2A	1275	July 10 & 11	Steaming toward Station Papa
1B and 2B	885	July 12, 13, 14, 15, 16 & 17	
1C and 2C	705	July 18, 19, 20 & 22	Installed on a sunny day; Filters were wet when removed
1D and 2D	285	July 22 & 23	Portion from western side of patch with low oceanic DMS concentrations
1E and 2E	0	July 23	Blank
1F and 2F	910	July 24, 25 & 26	Western side of front containing low DMS water
1G and 2G	637	July 27, 28 & 29	
1H and 2H	1438	July 29 & 30	Leaving patch
1I and 2I	0	July 30	Blank
1J and 2J	0	July 31	Blank
3A and 4A	1365	July 11 & 12	
3B and 4B	1220 and 810	July 12, 13 & 14	
3C and 4C	915	July 15 & 16	
3D and 4F	2170	July 17, 18, 20 & 21	
4D	340	July 16	50 km downwind
4E	150	July 16	50 km upwind
3E and 4G	0	July 21	Blank
3F and 4H	510	July 21 & 22	
3G and 4I	360	July 22 & 23	Downwind and in patch
3H and 4J	660	July 23 & 24	Patch-mapping
3I and 4K	480	July 24 & 25	
3J and 4L	1205	July 25	Transect through patch
3K and 4M	1198	July 26, 27 & 28	
3L and 4N	0	July 28	Blank
3M and 4O	0	July 30	Blank

Appendix 3.3: Separating sulphate from methane sulphonic acid (MSA) (Method from Isotope Sciences Laboratory of the University of Calgary, 2003)

1. Wear poly vinyl gloves and tear the sample filter into small pieces and place into a clean, labelled 600 mL beaker.
2. Add 200 mL of deionized water to the beaker.
3. Place the beaker in an ultrasonic bath and sonicate for 30 minutes.
4. Rinse a 0.45 μm cellulose nitrate membrane filter paper on a vacuum apparatus. Rinse the vacuum apparatus.
5. Filter the sample to remove any filter paper fibres. Wash the beaker three times with deionized water.
6. Collect the filtrate and washings into a clean, labelled 600 mL beaker. Dispose the filter and filter paper fragments.
7. Obtain 200 mL of solution by decreasing the volume by heating on a hot plate or increasing the volume by adding deoionized water.
8. Fill two 10 mL labelled vials with the sample solution for later analysis by Ion Chromatography.
9. Reduce the sample volume by heating the beaker on a hot plate until <25 mL of solution remained.
10. Check the acidity of the sample solution. pH=6 was obtained by adding sodium hydroxide (NaOH) if the solution was pH<6 or adding hydrochloric acid (HCl) if the solution was pH>6.

11. Heat the sample and 0.5 mL of 10% barium chloride ($BaCl_2$) to precipitate barium sulphate ($BaSO_4$). Mix.
12. Check the acidity of the sample solution and pH<3 was obtained by adding one drop of hydrochloric acid (HCl) at a time. Record the amount of hydrochloric acid (HCl) added.
13. Reheat the sample.
14. Record the weight of a clean 0.45 µm Nuclepore Track-Etch Membrane filter (Note: the diameter of this filter used depended on the amount of precipitate that was visible: if a small amount of precipitate was visible, a 25 mm diameter filter was used but if a large amount of precipitate was visible, a 45 mm diameter filter was used).
15. Rinse the filter on a vacuum apparatus. Clean the vacuum before filtering the sample.
16. Wash the beaker three times with hot deionized water. Filter washing with the sample as well.
17. Scrape the bottom of the beaker with a rubber policeman and rinse the rubber policeman and beaker with hot deionized water. Filtered washings with the sample solution as well. At this point the methane sulphonic acid and sulphate are separated so that the precipitate on the filter contains the sulphate (as barium sulphate ($BaSO_4$)) and the filtrate contains the methane sulphonic acid (MSA). Pour the filtrate containing the methane sulphonic acid into a clean beaker (The methane sulphonic acid procedure and results will not be discussed in this thesis).

<u>Appendix 3.4:</u> Precipitating Sulphate from the Sulphur Dioxide Filters (Method from Isotope Sciences Laboratory of the University of Calgary, 2003)

1. Wear poly vinyl gloves and tear the sample filter into small pieces and place into a clean, labelled 600 mL beaker.
2. Add 200 mL of deionized water to the beaker followed by 2 mL of 30% hydrogen peroxide (H_2O_2).
3. Place the beaker in an ultrasonic bath and sonicate for 30 minutes.
4. Rinse a 0.45 µm cellulose nitrate membrane filter paper on a vacuum apparatus. Rinse the vacuum apparatus.
5. Filter the sample to remove any sample filter paper fibres. Wash the beaker three times with deionized water.
6. Collect the filtrate and washings into a clean, labelled 600 mL beaker. Dispose the filter and filter paper fragments.
7. Add 5 mL of 10% barium chloride ($BaCl_2$) solution.
8. Check the acidity of the sample solution and obtain pH<3 by adding one drop of 3M hydrochloric acid (HCl) at a time. Record the amount of hydrochloric acid (HCl) added.
9. Reduce the sample volume to <50 mL by heating the sample solution on a hot plate.
10. Record the weight a 0.45 µm Nucleopore Track-Etch Membrane filter (Note: the diameter of the filter used depended on the amount of precipitate that was visible:

if a small amount of precipitate was visible, a 25 mm diameter filter was used but if a large amount of precipitate was visible, a 45 mm diameter filter was used).

11. Rinse the filter on a vacuum apparatus and clean the vacuum before filtering the sample.
12. Wash the beaker three times with hot deionized water. Filter the washings with the sample solution as well.
13. Scrape the bottom of the beaker with a rubber policeman and rinse the rubber policeman and the beaker with hot deionized water. Filter the washings with the sample solution as well.
14. Transfer the filter paper from the vacuum apparatus to a clean labelled watch glass.
15. Cover the filter with another watch glass and placed in a 110 °C oven for 60 minutes.
16. Cool the filter paper to room temperature and record the weight (Note: this will be the weight of filter plus barium sulphate, $BaSO_4$, from the sample).
17. Place the filter into a clean labelled crucible and cover with a lid.
18. Put the crucibles in an 800 °C oven for 90 minutes.
19. Cool to room temperature before tapping gently to loosen the barium sulphate from the sides and onto a weighing paper.
20. Record the weight of barium sulphate produced. Store the samples in a labelled sample envelope until ready for packing and analysis by the mass spectrometer.

<u>Appendix 3.5:</u> Analysis of MSA using the Ion Chromatograph (Method taken from Davison and Hewitt (1992))

1. Using degassed deionized water, prepare the two eluents required for this procedure: 1 mM $NaHCO_3$ (used to elute MSA and Cl) and 3.6 mM Na_2CO_3/3.4 mM $NaHCO_3$ (used to flush NO_3 and SO_4 through the column)
2. Prepare standard solutions: 0, 0.1, 0.25 and 0.5 ppm MSA
3. Turn on Ion Chromatograph. Set the high pressure limit to 3600 psi and the range to 1 μS. Adjust flow rate to 1.5 mL/min.
4. Let 1 mM $NaHCO_3$ eluent pump approximately 30 minutes to condition the column
5. To calibrate Ion Chromatograph, insert 1 mL of a freshly prepared standard. After analysis, change the 1 mM $NaHCO_3$ eluent to the 3.6 mM Na_2CO_3/3.4 mM $NaHCO_3$ eluent. To do so, turn off the pump and eluent nitrogen pressure. Loosen the 1 mM $NaHCO_3$ eluent cap slowly to release the pressure. Disconnect tubing from the 1 mM $NaHCO_3$ eluent bottle and connect to the 3.6 mM Na_2CO_3/3.4 mM $NaHCO_3$ eluent bottle. Turn the pump and eluent nitrogen pressure on. Purge bubbles from the tubing and reprime the pump. Change the range to 30 μS and once the background conductivity is between 16 and 19 μS, let it pump for 5 minutes.
6. Switch back to the 1 mM $NaHCO_3$ eluent. To do so, turn off the pump and eluent nitrogen pressure. Loosen the 3.6 mM Na_2CO_3/3.4 mM $NaHCO_3$ eluent cap slowly to release the pressure. Disconnect tubing from the 3.6 mM

Na_2CO_3/3.4 mM $NaHCO_3$ eluent bottle and connect to the 1 mM $NaHCO_3$ eluent bottle. Turn the pump and eluent nitrogen pressure on. Purge bubbles from the tubing and reprime the pump. Change the range to 10 µS and wait approximately 8 minutes until the background conductivity is approximately 6.5 to 6.9 µS.

7. Adjust the range to 1 µS. Analyze the next standard/sample.

APPENDIX 4.1: Bulk results: Mg (µg/m^3), Cl (µg/m^3), Na (µg/m^3), %SS and Ion used for %SS

IN PATCH	Mg	Cl	Na	%SS	Ion used for %SS
4A (In)	0.06422	0.7110	0.6138	12.17	Mg
4A (Down)	0.06422	0.7110	0.6138	12.17	Mg
4B	0.1823	2.748	1.569	29.90	Mg
4C	0.3336	5.064	2.685	37.55	Mg
4D	0.2102	2.719	1.470	26.12	Mg
4F	0.1289	1.427	0.9861	17.03	Mg
4H	0.5597	8.440	4.589	58.87	Mg
4I	0.2739	4.092	2.285	63.47	Mg
4J	0.1714	2.214	1.311	27.71	Mg
4K	0	2.794	0	24.73	Cl
4L	0	1.325	0	26.99	Cl
4M	0	1.678	0	18.02	Cl

OUT PATCH	Mg	Cl	Na	%SS	Ion used For %SS
1A	0.1062	0.9560	0.9853	15	Mg
1B	0.1562	2.370	1.460	28	Mg
1C					
1D	0.4589	1.957	3.929		
1F	0.2768	4.111	2.525	33	Mg
1G	0.1400	2.598	1.628	19	Mg
1H	0.4392	0	3.717	50	Mg
4E	0.3184	3.845	2.266	37	Mg

APPENDIX 4.1: Bulk results: $\delta^{34}S_{SO4}$ (‰), $\delta^{34}S_{NSS\ SO4}$ (‰), $\delta^{34}S_{SO2}$ (‰)

IN PATCH	$\delta^{34}S_{SO4}$	$\delta^{34}S_{NSS\ SO4}$	$\delta^{34}S_{SO2}$
4A (In)	7.138	5.126	8.626
4A (Down)	7.138	5.126	13.56
4B	6.952	0.9613	6.979
4C	6.843	-1.668	6.484
4D	7.553	2.798	1.666
4F	7.683	4.949	5.886
4H	8.005	-10.60	5.343
4I	10.09	-8.874	5.480
4J	7.315	2.069	9.051
4K	7.535	3.113	6.310
4L	7.120	1.990	26.53
4M	8.236	5.503	5.591

OUT PATCH	$\delta^{34}S_{SO4}$	$\delta^{34}S_{NSS\ SO4}$	$\delta^{34}S_{SO2}$
1A	7.810	5.544	12.93
1B	7.607	2.504	13.98
1C			15.47
1D	-5.596		10.11
1F	7.656	1.068	9.298
1G	8.277	5.262	8.905
1H	9.011	-2.876	11.15
4E	7.245	-0.8100	13.39

APPENDIX 4.1: Bulk results: SO_4 ($\mu g/m^3$), SS SO_4 ($\mu g/m^3$), NSS SO_4 ($\mu g/m^3$), Anthropogenic NSS SO_4 ($\mu g/m^3$) and Biogenic NSS SO_4 ($\mu g/m^3$)

IN PATCH	SO_4	SS SO_4	NSS SO_4	Anthropogenic NSS SO_4	Biogenic NSS SO_4
4A (In)	1.108	0.1349	0.9729	0.7844	0.1885
4A (Down)	1.108	0.1349	0.9729	0.7844	0.1885
4B	1.281	0.3829	0.8980	0.8980	0
4C	1.866	0.7005	1.165	1.165	0
4D	1.689	0.4411	1.248	1.188	0.05998
4F	1.589	0.2707	1.319	1.084	0.2343
4H	1.996	1.175	0.8210	0.8210	0
4I	0.9064	0.5752	0.3311	0.3311	0
4J	1.299	0.3598	0.9387	0.9348	0.003898
4K	1.588	0.3911	1.191	1.111	0.07980
4L	0.6872	0.1855	0.5018	0.5018	0
4M	1.304	0.2349	1.069	0.8433	0.2256

OUT PATCH	SO_4	SS SO_4	NSS SO_4	Anthropogenic NSS SO_4	Biogenic NSS SO_4
1A	1.521	0.2231	1.298	1.021	0.2771
1B	1.189	0.3280	0.8610	0.8347	0.02615
1C					
1D	0				
1F	1.758	0.5812	1.177	1.177	0
1G	1.535	0.2940	1.241	0.9969	0.2438
1H	1.852	0.9223	0.9300	0.9301	0
4E	1.810	0.6687	1.142	1.142	0

APPENDIX 4.1: Bulk results: SO_2 ($\mu g/m^3$), Anthropogenic SO_2 ($\mu g/m^3$), Biogenic SO_2 ($\mu g/m^3$), MSA ($\mu g/m^3$) and MSA to NSS SO_4 ratio

IN PATCH	SO_2	Anthropogenic SO_2	Biogenic SO_2	MSA	MSA to NSS SO_4
4A (In)	0.06943	0.04172	0.02771	0.1009	
4A (Down)	0.04593	0.01394	0.03199	0.1009	
4B	0.3280	0.2296	0.09838	0.08109	0.07460
4C	0.6758	0.4932	0.1826	0.09263	0.02296
4D	0.01161	0.01161		0.1111	
4F	0.5685	0.4354	0.1331	0.2163	0.1197
4H	0.3810	0.3810		0.1059	0.07884
4I	0.3936	0.3936		0.006867	
4J	0.07386	0.04249	0.03137	0.2290	
4K	0.05601	0.04147	0.01454	0.1265	
4L	0.01739		0.01739	0.3473	0.1245
4M	0.3178	0.3178		0.1477	0.09624

OUT PATCH	SO_2	Anthropogenic SO_2	Biogenic SO_2	MSA	MSA to NSS SO_4
1A	0.5962	0.2037	0.3925	0.1739	0.1201
1B	1.0070	0.2800	0.7270	0.08595	0.1404
1C	1.7007	0.3202	1.380		
1D	0.6859	0.3508	0.3351	0.02832	
1F	0.2787	0.1562	0.1225	0.1293	
1G	0.1834	0.1071		0.1516	0.15811
1H	0.04880	0.02191		0.1054	0.09472
4E	0.1075	0.03372		1.036	

APPENDIX 4.2: Size segregated results: Mg concentrations ($\mu g/m^3$)

IN PATCH	>7.2 µm	3.0 to 7.2 µm	1.5 to 3.0 µm	0.95 to 1.5 µm	0.49 to 0.95 µm	<0.49 µm
4A	0.00686	0.03777	0.01268	0.00233	0.00569	0
4B	0.00832	0.03835	0.01794	0.00492	0.00232	0.00666
4C	0.02692	0.09166	0.03435	0.01698	0.00425	0.01003
4F	0.00533	0.02726	0.01652	0.00757	0.00334	0.00537
4H	0.03410	0.20430	0.06994	0.01835	0	0.01662
4I	0.00711	0.07504	0.01766	0	0	0
4J	0.00388	0.02782	0.01257	0.00107	0	0
4K	0.00202	0	0.00699	0	0	0
4L	0	0		0	0	0
4M	0	0.04790	0.01562	0.00177	0	0

OUT PATCH	>7.2 µm	3.0 to 7.2 µm	1.5 to 3.0 µm	0.95 to 1.5 µm	0.49 to 0.95 µm	<0.49 µm
1A	0.01498	0.03726	0.01278	0	0	0.00864
1B	0.02929		0	0	0	0.00684
1C	0.00870	0	0	0	0	0.00286
1D	0.04494	0.03649	0.00735	0	0	0.00054
1F						
1G	0.03594	0.07725	0.01913	0.01218	0.00487	0.00122
1H	0.05047	0.13110	0.04831	0.02299	0.00788	0.00421

APPENDIX 4.2: Size segregated results: Cl concentrations ($\mu g/m^3$)

IN PATCH	>7.2 µm	3.0 to 7.2 µm	1.5 to 3.0 µm	0.95 to 1.5 µm	0.49 to 0.95 µm	<0.49 µm
4A	0	0	0	0	0	0
4B	0.2197	1.556	0.2780	0.07461	0	0
4C	0.5731	2.680	0.5212	0.2201	0.02065	0
4F	0.1345	0.3615	0.1653	0.04072	0	0
4H	1.006	3.278	1.725	0.5645	0.1444	0
4I	0.6371	2.101	0.5851	0.2298	0.1055	0
4J	0.3269	0.7230	0.1233	0	0	0
4K	0.4105		0.2100	0.1470	0	0
4L	0.1100	0.4180		0.0678	0.0089	0
4M	0.1608	0.6427	0.3329	0.0882	0	0

OUT PATCH	>7.2 µm	3.0 to 7.2 µm	1.5 to 3.0 µm	0.95 to 1.5 µm	0.49 to 0.95 µm	<0.49 µm
1A	0.2944	0.5588	0.2066	0.0197	0	0
1B	0.6097		0.0479	0.0614	0	0
1C	0.1874	0	0	0	0.01046	0
1D	1.0327	0.8502	0.4736	0.1193	0.2476	0
1F						
1G	0.4940	0.9960	0.2192	0.1080	0.0018	0
1H	0.8155	1.999	0.6552	0.2996	0.01128	0.0299

APPENDIX 4.2: Size segregated results: Na concentrations ($\mu g/m^3$)

IN PATCH	>7.2 µm	3.0 to 7.2 µm	1.5 to 3.0 µm	0.95 to 1.5 µm	0.49 to 0.95 µm	<0.49 µm
4A	0	0	0	0	0	0
4B	0.1567	0.5229	0.2461	0.1242	0.0701	0.0837
4C	0.3625	0.9664	0.3841	0.2778	0.1591	0
4F	0.1288	0.3558	0.2048	0.1702	0.1575	0.0575
4H	0.7556	2.144	1.088	0.4374	0.1504	0
4I	0.2239	1.353	0.4726	0.3401	0.1518	0
4J	0.2703	0.4759	0.2393	0.2158	0	0
4K	0.1440	0	0.2676	0.2658	0.1047	0.1390
4L	0.0896	0.3099		0.1186	0.1166	0.1169
4M	0.1090	0.5775	0.3290	0.2263	0.2072	0.0239

OUT PATCH	>7.2 µm	3.0 to 7.2 µm	1.5 to 3.0 µm	0.95 to 1.5 µm	0.49 to 0.95 µm	<0.49 µm
1A	0.1376	0.2842	0.1025	0	0.0057	0.0493
1B	0.1351		0	0	0	0.0079
1C	0.0300	0	0	0	0	0
1D	0.3426	0.2703	0	0	0	0
1F						
1G	0.4367	0.8690	0.3697	0.2048	0.1183	0
1H	0.4545	1.088	0.4413	0.1965	0.0625	0.0707

APPENDIX 4.2: Size segregated results: %SS

IN PATCH	>7.2 µm	3.0 to 7.2 µm	1.5 to 3.0 µm	0.95 to 1.5 µm	0.49 to 0.95 µm	<0.49 µm
4A	44.43	48.53		16.93	8.332	
4B	19.31	34.23	34.40	6.961	2.273	4.526
4C	25.85	38.12	31.56	10.75	2.322	9.460
4F	7.193	79.86	21.17	5.348	1.739	2.303
4H	38.01	64.95	78.33	13.61	11.87	8.114
4I	28.13	54.95	59.63	33.69	41.71	
4J	9.690	31.17	22.41	0.6893		
4K	2.748		16.98	54.13	14.59	18.59
4L	73.91			20.45	26.01	20.56
4M	23.13	38.48	32.06	1.415	11.94	1.174

OUT PATCH	>7.2 µm	3.0 to 7.2 µm	1.5 to 3.0 µm	0.95 to 1.5 µm	0.49 to 0.95 µm	<0.49 µm
1A	15.63	39.53	18.38			4.64
1B	38.69					8.75
1C	8.95					
1D	32.43	22.56	10.66			
1F						
1G	62.80	66.52	69.26	21.66	3.499	0.96
1H	72.23	95.38	64.28	32.52	5.00	2.09

APPENDIX 4.2: Size segregated results: Ion used for %SS

IN PATCH	>7.2 µm	3.0 to 7.2 µm	1.5 to 3.0 µm	0.95 to 1.5 µm	0.49 to 0.95 µm	<0.49 µm
4A	Mg	Mg		Mg	Mg	
4B	Mg	Mg	Na	Mg	Mg	Mg
4C	Mg	Mg	Na	Mg	Mg	Mg
4F	Mg	Mg	Na	Mg	Mg	Mg
4H	Mg	Mg	Na	Mg	Na	Mg
4I	Mg	Mg	Mg	Cl	Na	
4J	Mg	Mg	Na	Mg		
4K	Mg		Mg	Na	Na	Na
4L	Cl			Cl	Na	Na
4M	Na	Mg	Na	Mg	Na	Na

OUT PATCH	>7.2 µm	3.0 to 7.2 µm	1.5 to 3.0 µm	0.95 to 1.5 µm	0.49 to 0.95 µm	<0.49 µm
1A	Mg	Mg	Mg			Mg
1B	Mg					Mg
1C	Mg					
1D	Mg	Mg	Mg			
1F						
1G	Mg	Mg	Mg	Mg	Mg	Mg
1H	Mg	Mg	Mg	Mg	Mg	Mg

APPENDIX 4.2: Size segregated results: SO_4 concentrations ($\mu g/m^3$)

IN PATCH	>7.2 µm	3.0 to 7.2 µm	1.5 to 3.0 µm	0.95 to 1.5 µm	0.49 to 0.95 µm	<0.49 µm
4A	0.0324	0.1634	0.02432	0.02889	0.1435	0.0642
4B	0.09049	0.2353	0.1789	0.1484	0.214	0.3089
4C	0.2187	0.5050	0.3043	0.3317	0.3839	0.2228
4F	0.1556	0.2882	0.2419	0.2971	0.4029	0.4897
4H	0.1884	0.6605	0.3473	0.2831	0.3170	0.4301
4I	0.05309	0.2868	0.06229	0.09548	0.09098	0
4J	0.08407	0.1875	0.2670	0.3260	0.2497	0.1269
4K	0.1546		0.08644	0.1227	0.1793	0.187
4L	0.02084	0.09623		0.0464	0.112	0.1422
4M	0.1178	0.2614	0.2566	0.2624	0.4337	0.5082

OUT PATCH	>7.2 µm	3.0 to 7.2 µm	1.5 to 3.0 µm	0.95 to 1.5 µm	0.49 to 0.95 µm	<0.49 µm
1A	0.2012	0.1979	0.1461	0.1967	0.5580	0.3911
1B	0.1590		0.07577	0	0.1325	0.1642
1C	0.2042	0.03848	0.006826	0.02987	0.06507	0
1D	0.2910	0.3397	0.1449	0.06028	0.09886	0
1F						0.4637
1G	0.1202	0.2439	0.0580	0.1181	0.2926	0.2677
1H	0.1467	0.2885	0.1578	0.1485	0.3308	0.4236

APPENDIX 4.2: Size segregated results: $\delta^{34}S_{SO4}$ (‰)

IN PATCH	>7.2 µm	3.0 to 7.2 µm	1.5 to 3.0 µm	0.95 to 1.5 µm	0.49 to 0.95 µm	<0.49 µm
4A	3.121	7.262		7.199	5.324	7.704
4B	7.945	13.22	10.46	9.219	9.514	4.176
4C	10.73	14.01	11.17	10.7	4.467	3.369
4F	10.67	13.37	13.09	13.69	14.48	6.378
4H	11.04	17.25	15.66	12.76	13.4	8.247
4I	16.30	21.19	23.69	14.45	14.54	0.1211
4J	15.47	17.93	13.29	13.86	13.51	8.043
4K	12.99		11.74	11.29	8.445	7.732
4L	11.99			10.09	9.693	5.852
4M	7.064		10.92	12.09	5.562	7.060

OUT PATCH	>7.2 µm	3.0 to 7.2 µm	1.5 to 3.0 µm	0.95 to 1.5 µm	0.49 to 0.95 µm	<0.49 µm
1A	5.434	7.504	6.447	6.040	6.576	7.628
1B	5.672		6.223	8.135	13.12	7.175
1C	8.365	21.67	-23.19	0.4450	2.957	5.326
1D	15.26	15.04	12.30	14.08	12.25	2.468
1F						6.533
1G	14.07	16.48	14.73	12.55	12.37	8.752
1H	17.32	19.26	17.69		13.28	7.624

APPENDIX 4.2: Size segregated results: SS SO_4 concentrations ($\mu g/m^3$)

IN PATCH	>7.2 µm	3.0 to 7.2 µm	1.5 to 3.0 µm	0.95 to 1.5 µm	0.49 to 0.95 µm	<0.49 µm
4A	0.0144	0.07932		0.00489	0.01195	
4B	0.01748	0.08054	0.06153	0.01033	0.004863	0.01398
4C	0.05653	0.1925	0.09603	0.03566	0.008915	0.02107
4F	0.01119	0.05724	0.05121	0.01589	0.007006	0.01128
4H	0.07161	0.429	0.272	0.03853	0.03761	0.0349
4I	0.01493	0.1576	0.03708	0.03217	0.037795	
4J	0.008146	0.05843	0.05983	0.002247		
4K	0.004249		0.01468	0.06644	0.02616	
4L	0.01541			0.009488	0.02941	0.02923
4M	0.02725		0.08226	0.003714	0.05179	0.005969

OUT PATCH	>7.2 µm	3.0 to 7.2 µm	1.5 to 3.0 µm	0.95 to 1.5 µm	0.49 to 0.95 µm	<0.49 µm
1A	0.03145	0.07824	0.02685			0.01815
1B	0.06151					0.01437
1C	0.01826					
1D	0.09436	0.07664	0.01544			
1F						
1G	0.07548	0.1622	0.04017	0.02559	0.01024	0.00256
1H	0.1060	0.2752	0.1014		0.01655	0.008841

APPENDIX 4.2: Size segregated results: NSS SO_4 concentrations ($\mu g/m^3$)

IN PATCH	>7.2 µm	3.0 to 7.2 µm	1.5 to 3.0 µm	0.95 to 1.5 µm	0.49 to 0.95 µm	<0.49 µm
4A	0.01801	0.08412		0.024	0.1315	
4B	0.07302	0.1548	0.1174	0.1381	0.2091	0.2949
4C	0.1622	0.3125	0.2083	0.2960	0.3750	0.2017
4F	0.1444	0.2309	0.1907	0.2812	0.3959	0.4784
4H	0.1168	0.2315	0.07526	0.2446	0.2794	0.3952
4I	0.03816	0.1292	0.02521	0.06331	0.05303	
4J	0.07592	0.1290	0.2072	0.3238		
4K	0.1503		0.07177	0.0563	0.1532	
4L	0.005438			0.03691	0.08288	0.113
4M	0.09055		0.1743	0.2587	0.3819	0.5023

OUT PATCH	>7.2 µm	3.0 to 7.2 µm	1.5 to 3.0 µm	0.95 to 1.5 µm	0.49 to 0.95 µm	<0.49 µm
1A	0.1697	0.1197	0.1193			0.3729
1B	0.09749					0.1499
1C	0.1859					
1D	0.1966	0.2631	0.1294			
1F						
1G	0.04472	0.08165	0.01783	0.09252	0.2823	0.2651
1H	0.04075	0.1332	0.05638		0.3143	0.4148

APPENDIX 4.2: Size segregated results: $\delta^{34}S_{NSS\ SO4}$ (‰)

IN PATCH	>7.2 µm	3.0 to 7.2 µm	1.5 to 3.0 µm	0.95 to 1.5 µm	0.49 to 0.95 µm	<0.49 µm
4A	0.01801	0.08412		0.0240	0.1315	
4B	0.07302	0.1548	0.1174	0.1381	0.2091	0.2949
4C	0.1622	0.3125	0.2083	0.2960	0.3750	0.2017
4F	0.1444	0.2309	0.1907	0.2812	0.3959	0.4784
4H	0.1168	0.2315	0.07526	0.2446	0.2794	0.3952
4I	0.03816	0.1292	0.02521	0.06331	0.05303	
4J	0.07592	0.1290	0.2072	0.3238		
4K	0.1503		0.07177	0.0563	0.1523	
4L	0.005438			0.03691	0.08288	0.1130
4M	0.09055		0.1743	0.2587	0.3819	0.5023

OUT PATCH	>7.2 µm	3.0 to 7.2 µm	1.5 to 3.0 µm	0.95 to 1.5 µm	0.49 to 0.95 µm	<0.49 µm
1A	0.1697	0.1197	0.1193			0.3729
1B	0.09749					0.1499
1C	0.1859					
1D	0.1966	0.2631	0.1294			
1F						
1G	0.04472	0.08165	0.01783	0.09252	0.2823	0.2651
1H	0.04075	0.01332	0.05638		0.3143	0.4148

APPENDIX 4.2: **Size segregated results: Anthropogenic NSS SO_4 concentrations ($\mu g/m^3$)**

IN PATCH	>7.2 µm	3.0 to 7.2 µm	1.5 to 3.0 µm	0.95 to 1.5 µm	0.49 to 0.95 µm	<0.49 µm
4A	0.01801	0.08412		0.02055	0.1165	
4B	0.06061	0.08793	0.09667	0.08538	0.1178	0.2704
4C	0.1119	0.1674	0.1502	0.1630	0.3282	0.2017
4F	0.07595	0.09908	0.08766	0.09020	0.1010	0.3622
4H	0.09612	0.1156	0.07526	0.1051	0.1047	0.2733
4I	0.009518	0	0	0.02853	0.02773	
4J	0.01702	0.01596	0.09410	0.09344		
4K	0.05284		0.03782	0.05630	0.1135	
4L	0.005438			0.02516	0.06423	0.1130
4M	0.0858		0.1307	0.1034	0.3481	0.3542

OUT PATCH	>7.2 µm	3.0 to 7.2 µm	1.5 to 3.0 µm	0.95 to 1.5 µm	0.49 to 0.95 µm	<0.49 µm
1A	0.1641	0.1197	0.1108			0.2611
1B	0.09749					0.1151
1C	0.1285					
1D	0.07216	0.08401	0.05725			
1F						
1G	0.04369	0.05457	0.01783	0.04676	0.1112	0.1592
1H	0.02663	0.01332	0.02335		0.1084	0.2814

APPENDIX 4.2: Size segregated results: Biogenic NSS SO_4 concentrations ($\mu g/m^3$)

IN PATCH	>7.2 µm	3.0 to 7.2 µm	1.5 to 3.0 µm	0.95 to 1.5 µm	0.49 to 0.95 µm	<0.49 µm
4A	0	0		0.003452	0.01505	
4B	0.01241	0.06683	0.0207	0.05273	0.09129	0.02449
4C	0.05025	0.1451	0.05813	0.1327	0.04683	0
4F	0.06846	0.1319	0.103	0.191	0.2949	0.1162
4H	0.02069	0.116	0	0.1394	0.1747	0.1219
4I	0.02864	0.1292	0.02521	0.03478	0.0253	
4J	0.0589	0.1131	0.1131	0.2303		
4K	0.0975		0.03394	0	0.03968	
4L	0			0.01175	0.01856	0
4M	0.00475		0.04369	0.1553	0.03379	0.1481

OUT PATCH	>7.2 µm	3.0 to 7.2 µm	1.5 to 3.0 µm	0.95 to 1.5 µm	0.49 to 0.95 µm	<0.49 µm
1A	0.005631	0	0.008408			0.1118
1B	0					0.03475
1C	0.05738					
1D	0.1245	0.1791	0.07219			
1F						
1G	0.001028	0.02708	0	0.04576	0.1711	0.1059
1H	0.01412	0	0.03302		0.2059	0.1334

APPENDIX 4.2: **Size segregated results: MSA concentrations ($\mu g/m^3$)**

IN PATCH	>7.2 µm	3.0 to 7.2 µm	1.5 to 3.0 µm	0.95 to 1.5 µm	0.49 to 0.95 µm	<0.49 µm
4A		0.01034	0.003622	0.004139	0.01682	0.009055
4B	0.001013	0.1028	0009697	0.01085	0.01650	0.02200
4C		0.009649	0.006368	0.01196	0.02123	0.004631
4F	0.000895	0.01164	0.01888	0.04085	0.06737	0.05728
4H	0.002424	0.01973	0.02839	0.02770	0.02147	0.03116
4I				0.002943	0.004414	
4J	0.002675	0.02033	0.05993	0.09042	0.07491	0.03371
4K	0.007725		0.01104	0.01104	0.01619	0.02281
4L		0.003810	0	0.003810	0.009671	0.01407
4M		0.007959	0.01371	0.02167	0.04879	0.04834

OUT PATCH	>7.2 µm	3.0 to 7.2 µm	1.5 to 3.0 µm	0.95 to 1.5 µm	0.49 to 0.95 µm	<0.49 µm
1A		0.01315	0.01485	0.02825	0.07743	0.04480
1B	0.002456		0.003859	0.006314	0.01807	0.02105
1C	0.005284					
1D			0.009259			
1F						0.03173
1G		0.01852	0.009260	0.01803	0.03558	0.04191
1H	0.001511	0.007125	0.008960	0.01641	0.03379	0.03929

APPENDIX 4.2: Size segregated results: MSA to NSS SO_4 ratio

IN PATCH	>7.2 µm	3.0 to 7.2 µm	1.5 to 3.0 µm	0.95 to 1.5 µm	0.49 to 0.95 µm	<0.49 µm
4A		0.12302		0.17247	0.12788	
4B	0.01387	0.66381	0.08260	0.07860	0.07891	0.07460
4C		0.03088	0.03057	0.04042	0.05661	0.02296
4F	0.00620	0.05039	0.09899	0.14526	0.17018	0.11974
4H	0.02075	0.08525	0.37722	0.11323	0.07683	0.07884
4I				0.04648	0.04648	
4J	0.03524	0.15761	0.28922	0.27926		
4K	0.05140		0.15376	0.19601	0.10565	
4L				0.10321	0.11669	0.12449
4M			0.07864	0.08375	0.12774	0.09624

OUT PATCH	>7.2 µm	3.0 to 7.2 µm	1.5 to 3.0 µm	0.95 to 1.5 µm	0.49 to 0.95 µm	<0.49 µm
1A		0.10986	0.12448			0.12014
1B	0.02519					0.14043
1C	0.02842					
1D			0.07156			
1F						
1G			0.51937	0.19491	0.12603	0.15811
1H	0.03709	0.22683	0.15892		0.10751	0.09472